Strain-Based Design Methodology of Large Diameter Grade X80 Linepipe

A Dissertation Presented for the
Doctor of Philosophy
Degree
The University of Tennessee, Knoxville

Mark D. Lower
May 2014

Copyright ® 2014 by Mark D. Lower
All rights reserved

ACKNOWLEDGEMENTS

I am profoundly grateful to my advisor, Dr. John D. Landes, for the many hours of discussion and oversight but especially for the encouragement. I feared the pursuit of an advanced degree at this stage in my life would be overwhelming. It has instead been a richly rewarding experience. I look forward to bragging about being a student of Dr. Landes. I also wish to extend my appreciation to my committee members Dr. J. A. M. Boulet, Dr. David C. Joy, Dr. Randy K. Nanstad, and Dr. S. Andy Sarles. They have all been generous with their time and wisdom.

It is virtually impossible to be successful at an undertaking of this magnitude without having very special people to provide needed support. I have been fortunate to have several.

- There is no way I could have thought about accomplishing this degree without the support of Mr. Claude Robison. He has been my boss, but more importantly, has been a great friend. The thought of fulfilling the potential he saw in me has been a major driver in pressing on when I was drained. He was always ready to clear any roadblock and has been instrumental in making this happen. I cannot say thank you enough!
- I greatly appreciate the time, direction, and encouragement from Mr. Barry Oland. He spent many hours patiently manipulating my many thoughts into a cohesive story. He has taught me well as I have learned many things over the course of writing this dissertation that will benefit me throughout my career.
- Dr. Wally McAfee and Mr. Chris Stevens helped guide me through the pitfalls of material testing. I appreciate you both for answering all of my silly questions and letting me get in the way.
- Special thanks to Ms. Stacy Hubbard and Ms. Kathy Parton for walking beside me, cheering me on, and the many hours of graciously and patiently helping me through.

ABSTRACT

Continuous growth in energy demand is driving oil and natural gas production to areas that are often located far from major markets where the terrain is prone to earthquakes, landslides, and other types of ground motion. Transmission pipelines that cross this type of terrain can experience large longitudinal strains and plastic circumferential elongation as the pipeline experiences alignment changes resulting from differential ground movement. Such displacements can potentially impact pipeline safety by adversely affecting structural capacity and leak tight integrity of the linepipe steel.

Planning for new long-distance transmission pipelines usually involves consideration of higher strength linepipe steels because their use allows pipeline operators to reduce the overall cost of pipeline construction and increase pipeline throughput by increasing the operating pressure. The design trend for new pipelines in areas prone to ground movement has evolved over the last 10 years from a stress-based design approach to a strain-based design (SBD) approach to further realize the cost benefits from using higher strength linepipe steels.

This dissertation presents an overview of SBD for pipelines subjected to large longitudinal strain and high internal pressure with emphasis on the tensile strain capacity of high-strength microalloyed linepipe steel. The technical basis for this dissertation involved engineering analysis and examination of the mechanical behavior of Grade X80 linepipe steel in both the longitudinal and circumferential directions. Testing was conducted to assess effects on material processing including as-rolled, expanded, and heat-treatment processing intended to simulate coating application. Elastic-plastic and low-cycle fatigue analyses were also performed with varying internal pressures. Proposed SBD models discussed in this dissertation are based on classical plasticity theory and account for material anisotropy, triaxial strain, and microstructural damage effects developed from test data. The results are intended to enhance SBD and analysis methods for producing safe and cost effective pipelines capable of accommodating large plastic strains in seismically active arctic areas.

KEY WORDS: anisotropy, strain-based design, tensile-strain capacity, Grade X80 linepipe, low-cycle fatigue, plastic strain, pipeline

TABLE OF CONTENTS

1. INTRODUCTION 1
   1.1 BACKGROUND 1
   1.2 PIPELINE HISTORY 1
   1.3 PIPELINE DESIGN AND CONSTRUCTION ISSUES 2
   1.4 SCOPE AND OBJECTIVES 4
2. PIPELINE DESIGN AND CONSTRUCTION RULES 5
   2.1 STRESS-BASED DESIGN 6
   2.2 STRAIN-BASED DESIGN 8
3. MATERIAL PROPERTIES AND MECHANICAL BEHAVIOR 14
   3.1 MICROSTRUCTURE AND CHEMISTRY 15
   3.2 PHYSICAL PROPERTIES 17
      3.2.1 Forming 17
      3.2.2 Coating 19
   3.3 MECHANICAL PROPERTIES 21
      3.3.1 Monotonic Tensile Testing 21
      3.3.2 Cyclic Fatigue Testing 27
4. ANALYSIS AND LIFE PREDICTION 29
   4.1 STRESS-BASED ANALYSIS METHODS 29
      4.1.1 Isotropic Material Properties 29
      4.1.2 Orthotropic Material Properties 33
   4.2 STRAIN-BASED ANALYSIS METHODS 34
   4.3 LOW-CYCLE FATIGUE ANALYSIS METHODS 37
   4.4 PROTECTION AGAINST FAILURE 40
5. PIPELINE DESIGN AND SAFETY ISSUES 42
   5.1 DESIGN CODE AND MATERIAL STANDARD ISSUES 42
   5.2 LINEPIPE MATERIAL PROPERTY ISSUES 42
6. GRADE X80 LINEPIPE 45
   6.1 CHEMICAL ANALYSIS 45
   6.2 TENSILE PROPERTIES 46
   6.3 TEST SPECIMENS 47
   6.4 MICROSTRUCTURE 48
   6.5 HARDNESS 50
7. MONOTONIC LINEPIPE MATERIAL PROPERTIES AND BEHAVIOR 51
   7.1 TEST SPECIMEN SELECTION CONSIDERATIONS AND ANALYSIS 51
   7.2 CIRCUMFERENTIAL TENSILE TESTING 52
   7.3 LONGITUDINAL TENSILE TESTING 56
      7.3.1 Round Bar Tensile Test Specimens 56
      7.3.2 Rectangular Tensile Specimens 56
   7.4 STRAIN RATIO TESTING 60
   7.5 DISCUSSION AND CONCLUSIONS 66
8. CYCLIC LINEPIPE MATERIAL PROPERTIES AND BEHAVIOR 69
   8.1 TEST SPECIMEN SELECTION CONSIDERATIONS 69
   8.2 FORCE-CONTROLLED FATIGUE TESTING 70
   8.3 STRAIN-CONTROLLED FATIGUE TESTING 72
   8.4 DISCUSSION AND CONCLUSIONS 73
9. PROTECTION AGAINST PLASTIC COLLAPSE 77

9.1 ELASTIC-PLASTIC DESIGN CONSIDERATIONS 77
9.2 ELASTIC-PLASTIC ANALYSIS METHOD 78
9.3 ELASTIC-PLASTIC ASSESSMENT 79
9.4 GRADE X80 ELASTIC-PLASTIC MODEL DEVELOPMENT 82
10. PROTECTION AGAINST FAILURE FROM CYCLIC LOADING 85
10.1 OVERVIEW 85
10.2 FATIGUE ANALYSIS METHOD 85
10.3 FATIGUE ASSESSMENT 86
10.4 GRADE X80 FATIGUE MODEL DEVELOPMENT 89
11. OBSERVATIONS AND CONCLUSIONS 92
12. SUGGESTIONS FOR FUTURE WORK 94
REFERENCES 95
BIBLIOGRAPHY 102
VITA 106

LIST OF TABLES

Table 1. Pipe body dimensions 45
Table 2. Chemical analysis results 46
Table 3. Tensile test data acquired at the pipe mill 46
Table 4. Mechanical property requirements prescribed in API Specification 5L for Grade X80M PSL2 linepipe 47
Table 5. Summary of Circumferential Round Bar Tensile Properties, As-Rolled (* Necking occurred outside limits of clip gage) 53
Table 6. Summary of Circumferential Round Bar Tensile Properties, Expanded 53
Table 7. Summary of Circumferential Round Bar Tensile Properties, Expanded and Strain-Aged, 90° from Weld Seam 54
Table 8. Summary of Circumferential Round Bar Tensile Properties, Expanded and Strain-Aged, 180° from Weld Seam 54
Table 9. Summary of Longitudinal Round Bar Tensile Properties, As-Rolled 57
Table 10. Summary of Longitudinal Round Bar Tensile Properties, Expanded 57
Table 11. Summary of Longitudinal Round Bar Tensile Properties, Expanded and Strain-Aged, 90° from weld seam 58
Table 12. Summary of Longitudinal Round Bar Tensile Properties, Expanded and Strain-Aged, 180° from weld seam 58
Table 13. Summary of Longitudinal Rectangular Specimen Tensile Properties, As-Rolled 61
Table 14. Summary of Longitudinal Rectangular Specimen Tensile Properties, Expanded 61
Table 15. Summary of Longitudinal Rectangular Specimen Tensile Properties, Expanded and Strain-Aged, 90° from weld seam 62
Table 16. Summary of Longitudinal Rectangular Specimen Tensile Properties, Expanded and Strain-Aged, 180° from weld seam 62
Table 17. Summary of Plastic Strain Ratio Specimens 63
Table 18. Summary of Circumferential Round Bar Fatigue Properties 71
Table 19. Summary of Longitudinal Round Bar Fatigue Properties 74
Table 20. Results of elastic-plastic analysis 84
Table 21. Results of Fatigue Analyses 91

LIST OF FIGURES

Fig. 1. Trans-Alaskan Pipeline System (TAPS). 3
Fig. 2. Basis for stress-based design approach [14]. 6
Fig. 3. Basis for SBD approach [14]. 8
Fig. 4. Linepipe loading. 10
Fig. 5. Typical grain boundary. 16
Fig. 6. Mechanical expansion. 19
Fig. 7. Saint-Venant principle. 21
Fig. 8. Mechanical properties. 22
Fig. 9. Stress-strain curve definitions. 23
Fig. 10. Yield strength definitions. 24
Fig. 11. The Bauschinger effect [53]. 26
Fig. 12. Common S-N curve [57]. 28
Fig. 13. Pipe element. 30
Fig. 14. Completely reversed cyclic loading hysteresis loop [36]. 38
Fig. 15. Constant amplitude cyclic stress. 39
Fig. 16. Failure assessment diagram schematic. 41
Fig. 17. Specimen locations and orientations. 47
Fig. 18. Pipe Sample. 48
Fig. 19. Specimen A Circumferential. 48
Fig. 20. Specimen A Longitudinal. 48
Fig. 21. Specimen B Circumferential. 49
Fig. 22. Specimen B Longitudinal. 49
Fig. 23. Specimen C Circumferential. 49
Fig. 24. Specimen C Longitudinal. 49
Fig. 25. Specimen D Circumferential. 49
Fig. 26. Specimen D Longitudinal. 49
Fig. 27. Through-Wall Hardness. 50
Fig. 28. Tensile specimens. 52
Fig. 29. Engineering stress strain curves for circumferential tensile specimens. 55
Fig. 30. True stress strain curves for circumferential tensile specimens. 55
Fig. 31. 0.5% EUL and 0.2% Offset yield points for circumferential tensile specimens. 55
Fig. 32. Fracture surface for as-rolled circumferential tensile test specimen. 55
Fig. 33. Fracture surface for expanded circumferential tensile test specimen. 55
Fig. 34. Fracture surface for expanded and strain-aged circumferential tensile test specimen 90° from weld seam. 56
Fig. 35. Fracture surface for expanded and strain-aged circumferential tensile test specimen 180° from weld seam. 56
Fig. 36. Engineering stress strain curves for longitudinal round bar tensile specimens. 59
Fig. 37. True stress strain curves for longitudinal round bar tensile specimens. 59
Fig. 38. 0.5% EUL and 0.2% Offset yield points for longitudinal round bar tensile specimens. 59
Fig. 39. Fracture surface for as-rolled longitudinal tensile test specimen. 59
Fig. 40. Fracture surface for expanded longitudinal tensile test specimen. 59
Fig. 41. Fracture surface for expanded and strain-aged longitudinal tensile test specimen 90° from weld seam. 60
Fig. 42. Fracture surface for expanded and strain-aged longitudinal tensile test specimen 180° from weld seam. 60
Fig. 43. Engineering stress strain curves for longitudinal rectangular tensile specimens. 63
Fig. 44. True stress strain curves for longitudinal rectangular tensile specimens. 63

Fig. 45. 0.5% EUL and 0.2% Offset yield points for longitudinal rectangular tensile specimens..... 63
Fig. 46. Top view of fracture surface for as-rolled longitudinal tensile test specimen. 64
Fig. 47. Side view of fracture surface for as-rolled longitudinal tensile test specimen. 64
Fig. 48. Top view of fracture surface for expanded longitudinal tensile test specimen..... 64
Fig. 49. Side view of fracture surface for expanded longitudinal tensile test specimen. 64
Fig. 50. Top view of fracture surface for expanded and strain-aged longitudinal tensile test specimen 90° from weld seam..... 64
Fig. 51. Side view of fracture surface for expanded and strain-aged longitudinal tensile test specimen 90° from weld seam..... 64
Fig. 52. Strain Ratio curves for as-rolled material from longitudinal round bar tensile specimens (specimen L-A-3). 65
Fig. 53. Strain Ratio curves for as-rolled material from circumferential round bar tensile specimens (specimen C-A-8). 65
Fig. 54. Strain Ratio curves for expanded material from longitudinal round bar tensile specimens (specimen L-B-2). 65
Fig. 55. Strain Ratio curves for expanded material from circumferential round bar tensile specimens (C-B-8). 65
Fig. 56. Strain Ratio curves for expanded, strain-aged material from longitudinal round bar tensile specimens (specimen L-C-2)..... 65
Fig. 57. Strain Ratio curves for expanded, strain-aged material from circumferential round bar tensile specimens (specimen C-C-9). 65
Fig. 58. Engineering stress strain curves for expanded and strain-aged tensile specimens 90° from weld seam. 67
Fig. 59. Round circumferential tensile specimen from pipe wall. 68
Fig. 60. Fatigue Test Specimens. 70
Fig. 61. Stress versus life curves for round bar test specimens..... 72
Fig. 62. Circumferential force-controlled fatigue specimen stress-strain response for as-rolled linepipe (C-A-2). 72
Fig. 63. Circumferential force-controlled fatigue specimen stress-strain response for expanded linepipe (C-B-2). 72
Fig. 64. Circumferential force-controlled fatigue specimen stress-strain response for expanded and strain-aged linepipe (C-C-5)..... 72
Fig. 65. Strain versus life curves for round bar test specimens, R = -1. 75
Fig. 66. Strain versus life curves for round bar test specimens, R = 0..... 75
Fig. 67. Longitudinal strain-controlled fatigue specimen stress-strain response for as-rolled linepipe (LCF-1)..... 75
Fig. 68. Longitudinal strain-controlled fatigue specimen stress-strain response for as-rolled linepipe (LCF-7)..... 75
Fig. 69. Longitudinal strain-controlled fatigue specimen stress-strain response for expanded linepipe (LCF-11)..... 75
Fig. 70. Longitudinal strain-controlled fatigue specimen stress-strain response for expanded linepipe (LCF-15)..... 75
Fig. 71. Longitudinal strain-controlled fatigue specimen stress-strain response for expanded and strain-aged linepipe (LCF-21). 76
Fig. 72. Longitudinal strain-controlled fatigue specimen stress-strain response for expanded and strain-aged linepipe (LCF-25). 76
Fig. 73. True stress true strain relations at large strains for expanded and strain-aged linepipe..... 80
Fig. 74. Internal pressure vs $\varepsilon L\varepsilon + \varepsilon tf$ based on maximum longitudinal strain. 84
Fig. 75. Crack growth in pure shear and where normal stress enhances crack growth [74]. 89
Fig. 76. Internal pressure vs cycle life based on allowable longitudinal strain amplitude using the triaxiality (T) Parameter and Smith, Watson, Topper (SWT) parameter. 91

NOMENCLATURE

A	cross-sectional area
b	exponent constant for stress-life curve
b_w	exponent constant for a Walker method stress-life fit
c	exponent constant for a plastic strain versus life curve
c_w	exponent constant for a plastic strain versus Walker-equivalent-life curve
D	outer diameter
E_i	Young's elastic modulus in the ith direction
E_i'	Cyclic elastic modulus in the ith direction
G_{ij}	Shear modulus in the jth direction on the plane whose normal is in the ith direction
H_i	Monotonic intercept constant for a stress amplitude versus plastic strain amplitude curve in the ith direction
H_i'	Cyclic intercept constant for a stress amplitude versus plastic strain amplitude curve in the ith direction
l	length
m	work hardening coefficient (Ramberg-Osgood)
m_2	Strain hardening coefficient that is estimated from the ratio of the engineering yield to tensile
n	work hardening coefficient
N_f	fatigue life; cycles to failure
N_w^*	value of N^* from the Walker method; Walker equivalent life
P	internal pressure
R	stress ratio ($R = \sigma_{min}/\sigma_{max}$)
R_f	Final mean pipe radius
R_{fe}	Final mean pipe radius after expansion
R_0	Original mean pipe radius
t	wall thickness
T	Davis-Connelly triaxiality factor
α_{sl}	material constant dependent on metallurgical (crystallographic) structure
$\bar{\varepsilon}$	Effective Strain
$\varepsilon_{ai,k}$	alternating strain in the ith direction for the kth cycle
ε_{app}	applied strain
ε_{all}	allowable strain
ε_d	strain demand
ε_e	elastic strain
ε_f'	intercept constant at ½ cycle for a plastic strain versus life curve
$\bar{\varepsilon}_f$	Effective total forming strain before expansion
ε_L	strain limit
ε_{Lu}	uniaxial strain limit
ε_m	mean strain
ε_p	plastic strain
ε_T	true strain
$\bar{\varepsilon}_{tf}$	Effective total forming strain including expansion
f	safety/design factor
$\sigma_{ai,k}$	alternating stress in the ith direction for the kth cycle

γ	fitting constant for the Walker method
σ_{ar}	stress amplitude for the $\sigma_m = 0$ case; equivalent completely reversed stress
σ_e	effective stress
σ_E	engineering stress
σ_f'	intercept constant at ½ cycle for stress-life curve
$\bar{\sigma}_f$	True fracture strength
σ_{fw}'	intercept constant at ½ cycle for a Walker method stress-life fit
σ_θ	Principle stress in the circumferential (hoop) direction
σ_z	Principle stress in the longitudinal direction
σ_m	mean stress
σ_0	reference stress
σ_r	Principle stress in the radial direction
σ_T	true stress
σ_Y	yield stress
υ_{ije}	Elastic strain ratio that corresponds to a contraction in direction *j* when an extension is applied in direction *i*.
υ_{ijp}	Plastic strain ratio that corresponds to a contraction in direction *j* when an extension is applied in direction *i*.
$\bar{\upsilon}$	Strain ratio weighted average

ACRONYMS

ABS	American Bureau of Shipping
API	American Petroleum Institute
ARO	abrasive resistant overcoat
ASME	American Society of Mechanical Engineers
C	carbon
CE	carbon equivalent
CFR	Code of Federal Regulations
Cr	chromium
CSA	Canadian Standards Association
Cu	copper
DNV	Det Norske Veritas
EUL	extension under load
F/AF	ferrite/acicular ferrite
F/P	ferrite/pearlite
FAD	failure assessment diagram
FBE	fusion-bonded epoxy
FEA	finite element analysis
HRC	Rockwell C Hardness
HTP	high-temperature processing
Mn	manganese
Mo	molybdenum
Nb	niobium
Ni	nickel
NPS	nominal pipe size
P	phosphorus
PHMSA	Pipeline and Hazardous Materials Safety Administration
PSL	product specification level
S	sulfur
SAWL	submerged-arc welding process
SBD	strain-based design
SEM	scanning electron microscope
Si	silicon
SMTS	specified minimum tensile stress
SMYS	specified minimum yield stress
SWT	Smith, Watson, and Topper
TAPS	Trans-Alaska Pipeline System
Ti	Titanium
TMCP	thermo-mechanically controlled process
TSC	tensile strain capacity
UEL	uniform elongation
UTS	ultimate tensile strength

V	vanadium
Y/T	yield strength/tensile strength

1. INTRODUCTION

1.1 BACKGROUND

Oil and natural gas have been important energy resources for over 100 years. Continuous growth in energy demand is estimated to increase total world natural gas consumption from 100 trillion ft^3 in 2004 to 128 trillion ft^3 in 2015 and 163 trillion ft^3 in 2030 [1]. Although the first experiment in hydraulic fracturing (fracking) occurred in Kansas in 1949, fracking boomed after Congress enacted the Energy Policy Act of 2005, exempting fracking from compliance with the Safe Drinking Water Act, the Clean Air Act, and the Clean Water Act, and has enhanced oil and natural gas recovery from deep underground formations, helping to meet the increasing demand for low-cost energy.

Large oil and natural gas reserves are often located far from major markets. Consequently, products recovered from these reserves must be transported long distances, sometimes hundreds of miles, to ports, refineries, and distribution hubs. Improving long-distance transportation economics is a critical factor in determining whether oil and natural gas recovery from remote reserves is cost effective with an acceptable return on investment. Pipelines are generally recognized as the safest and most economical method for transporting oil and natural gas over long distances. However, the cost of pipeline construction can have a significant effect on the final product price paid by the end user.

Development of oil and natural gas resources is highly dependent on the economics and technical feasibility of transporting the recovered resources to the marketplace. This reality is constantly pushing industry towards construction of larger diameter pipelines with higher operating pressures, especially pipelines that transport oil and natural gas from reserves located in remote areas. A key factor in reducing the construction cost of such pipelines requires the use of thinner wall, higher strength linepipe.

Use of higher strength linepipe permits higher allowable operating pressures with increased throughput. A thinner pipe wall minimizes the overall volume of steel needed to construct a pipeline and the volume of weld metal required to connect adjoining linepipe segments. Minimizing the volume of steel and weld metal results in lower material, transportation, and construction costs. To maximize cost savings, the wall thickness is often reduced so that the operating pressure produces a stress state that approaches 80% of the specified minimum yield stress (SMYS) of the linepipe steel. For these reasons, use of high strength steels is considered an economic necessity to supply large volumes of gas at pressures above 1,450 psi over long distances in a competitive manner [1].

From a feasibility viewpoint, lower yield strength thick-wall linepipe cannot be manufactured in a mass production process [2], so producing the required amount of this material needed to construct long pipelines is potentially problematic. Therefore, development of as-rolled steel or thermo-mechanically controlled processed (TMCP) high-strength steel linepipe without heat treatment is essential [2].

1.2 PIPELINE HISTORY

Until the early 1960s, linepipe steels with relatively low yield strengths were used for pipeline construction. Types X52 and X56 linepipe with yield strengths of 52,000 psi and 56,000 psi, respectively, were used almost exclusively. Then, around 1970, Types X65 and X70 linepipe with yield strengths of 65,000 psi and 70,000 psi, respectively, began to gain acceptance but were not widely used because of limitations in welding technology. During the 1970s, linepipe manufacturers began using thermomechanical treatment of steel to improve its mechanical properties. In the 1980s, manufacturers produced Types X60 and X70 linepipe with yield strengths of 60,000 psi and 70,000 psi, respectively, as the dominant steel type.

Around the year 2000, to meet the demand for increased operating pressures in excess of 1,500 psi, and thereby achieve the desired higher throughput, steel manufacturers began producing Type X80 linepipe with a yield strength of 80,000 psi. This steel is produced using thermomechanical processing techniques and is poised to become the next dominant material for new pipeline construction. To date, a number of prominent pipelines have been constructed using Type X80 linepipe, including over 1,000 miles of the Cheyenne Plains natural gas pipeline completed in 2005. Efforts are also under way to develop suitable processing techniques for manufacture of types X100 and X120 linepipe with yield strengths of 100,000 psi and 120,000 psi, respectively. These high-strength steels have been highly recommended for construction of the anticipated Arctic pipelines due to improved transportation efficiency and construction cost savings [3]. However, current manufacturing techniques produce Types X100 and X120 linepipe with insufficient toughness and poor welding ability. Until there are advancements in manufacturing technology that make Types X100 and X120 linepipe more reliable for construction, Type X80 linepipe will continue to be more universally used for new pipeline construction [4].

1.3 PIPELINE DESIGN AND CONSTRUCTION ISSUES

New oil and natural gas reserves tend to be located in northerly regions of North America where the terrain is prone to earthquakes, landslides, and other types of large differential ground movement events. Transmission pipelines that traverse these regions can experience large longitudinal strains and plastic circumferential elongation as the pipeline experiences alignment changes [5]. When these events occur, buried pipelines are subject to a number of loading conditions such as internal pressure changes caused by the fluid action, axial forces induced by thermal effects, and bending caused by differential soil movement that can adversely affect the structural capacity and leak-tight integrity of the transmission pipeline. The Trans-Alaska Pipeline System (TAPS), shown in Fig. 1, was constructed in the arctic region of Alaska in the 1970s. Pipelines are designed to operate based on a location class. Design factors are established by the geographic area along the pipeline based on the expected human concentration and proximity to other structures. Often pipelines that are designed with lower safety margins are allowed to continue to operate as the population encroaches and improvements take place.

Pipelines constructed with relatively low-strength, high-ductility linepipe steel have historically proven to safely accommodate large strains generated by differential ground movement. These linepipe steels are capable of deforming plastically and maintaining their structural capacity and leak-tight integrity [6, 7]. Recently, differential soil movements have been identified as an important consideration in the design and assessment of buried pipelines for the higher strength steels. This concern is supported by the 1964 earthquake in Anchorage, Alaska, that caused a shift in the ground surface of up to 66 ft. According to the United States Geological Survey, as recently as 2002 the Denali fault in Alaska generated a magnitude 7.9 earthquake with horizontal offsets as large as 29 ft. At locations with saturated, low density, or uncompacted sandy soils, seismic events of this magnitude can result in soil liquefaction, a phenomenon whereby a saturated or partially saturated soil loses strength and stiffness and behaves like a liquid.

ORNL 2013-G00903/chj

Fig. 1. Trans-Alaskan Pipeline System (TAPS).

A pipeline is a non-redundant structure (i.e., there is no alternate load carrying path to compensate for failure). Consequentially, there is an increased need for ensuring ductile material behavior during installation and operation. Strain-based design (SBD) is used for many situations for pipelines where the loadings from forces other than the internal pressure can be the largest generators of stress and strain in the pipe wall. Such loadings can be generated by either permanent or transient ground deformation caused by seismic activity, soil subsidence, slope instability, frost heave, thermal expansion and contraction, landslides, pipe reeling, pipe laying, and other types of environmental loading [7]. Deep water pipelines can also experience large lateral displacement in start-up and shutdown operations because of thermal and pressure variations. Traditional allowable stress design methods address scenarios where the global response is mainly elastic and is not sufficient for design of pipelines experiencing large strains in challenging arctic environments and seismic events [8]. For these cases, design methods based on strain have an advantage over design methods based on stress because these loading conditions tend to apply a given displacement rather than a given force to the linepipe. Use of SBD for pipelines began in the 1980s with the use of high-strength (Type X70 and higher) linepipe for pipeline construction in arctic regions [6]. Use of SBD methods is often cost-effective and sometimes necessary when displacement-controlled loading is expected, especially in areas prone to excessive ground movement [6].

SBD of pipelines refers to design methodologies that have a specific goal of maintaining pipeline service and integrity under large longitudinal plastic deformation (often defined as longitudinal strain greater than 0.5%) [9]. Plastic deformation is frequently displacement controlled, although combined displacement- and load-controlled events are possible. In contrast, traditional pipeline design methods are stress-based, where the applied stress must remain below SMYS. As SMYS is typically defined as the yield strength measured at 0.5% total strain, stress-based design limits the longitudinal strain to less than 0.5% [10]. The

ultimate goal of SBD is to prevent plastic instability of the pipe structure undergoing large imposed strains caused by imposed displacements.

In recent years, pipelines have been constructed in discontinuous permafrost areas and earthquake prone regions where the pipeline can experience plastic strains caused by ground settlement or upheaval. Plastic design methods such as SBD are applicable to pipelines in such hostile environments [11, 12]. TransCanada Pipelines Ltd. installed a 1 kilometer trial section of pipeline using Type X100 linepipe in the fall of 2002 and a 2 kilometer section of pipeline using Type X100 linepipe in the winter of 2003-2004. A 5.5 kilometer pipeline section of Type X100 linepipe was constructed in 2006 consistent with SBD requirements [9]. Recently, construction of a pipeline consistent with SBD requirements in an area of discontinuous permafrost has been discussed [11]. Specifications have been developed for construction of a west-to-east natural gas transmission pipeline in China using Type X80 linepipe. However, design compliance problems, such as material anisotropy and strain-aging effects, have been identified regarding the ability of the pipeline to accommodate large deformations [6].

Current planning for transmission pipelines includes the need to design, construct, and operate oil and natural gas pipelines in seismically active and arctic areas where significant ground movements can occur. A multi-disciplinary team of engineers and scientists knowledgeable in seismology, soil mechanics, and soil-pipe interaction is required to establish the design basis for onshore pipelines in these areas. Estimating strain demand for specific design-basis events is necessary to account for postulated ground movement that could occur during an anticipated 50-year service life of a pipeline.

1.4 SCOPE AND OBJECTIVES

This dissertation presents an overview of SBD with emphasis on the strain capacity of pipelines, specifically the tensile strain capacity of high-strength microalloyed steel linepipe governed by low cycle fatigue. This research also summarizes recent experimental and analytical work aimed at refining tensile strain capacity prediction methods. The effects of anisotropy on tensile strain capacity and operating pressures are evaluated under both uniaxial and bi-axial loading conditions.

Evaluation results are intended to produce design and analysis methods for constructing safe and cost-effective pipelines in seismic and arctic areas, where the pipelines must be designed to accommodate large plastic strain. Topics discussed in this research apply to both onshore and offshore pipelines, including buried and above-ground pipelines.

2. PIPELINE DESIGN AND CONSTRUCTION RULES

Rules for design and construction of pipelines are published by the US Department of Transportation's Pipeline and Hazardous Materials Safety Administration (PHMSA) and by industrial organizations including the American Society of Mechanical Engineers (ASME), the American Petroleum Institute (API), and the Canadian Standards Association (CSA). These rules are typically customized for either natural gas or hazardous liquid transmission pipeline applications.

Federal pipeline safety standards that are developed by PHMSA are codified in the Code of Federal Regulations (CFR): 49 CFR 192—*Transportation of Natural and Other Gas by Pipeline: Minimum Federal Safety Standards* and 49 CFR 195—*Transportation of Hazardous Liquids by Pipeline*. These regulations, which reflect years of safe operating experience for pipelines constructed with common linepipe, require operators of transmission and distribution pipeline systems to use linepipe manufactured in accordance with an approved material specification and rules that comply with minimum requirements for design, selection, qualification, and construction of pipelines and components. In addition, federal pipeline safety standards contain both performance-based and prescriptive requirements in all areas of a pipeline life cycle including materials, design, welding, construction, operations, and integrity management. When design considerations extend beyond the fundamental engineering principles used as the technical basis for current rules, supplementary requirements, specifications, and procedures can be authorized by PHMSA through a special permitting process. This process involves ensuring that the design and construction satisfy minimum federal pipeline safety standards.

ASME is a nonprofit professional association that, among many ventures, promotes the development of codes and standards through research, conferences, publications, and government relations. It was founded in 1880 in response to numerous steam boiler pressure vessel failures and is now one of the world's largest technical publishing operations (www.asme.org). The Board on Pressure Technology Codes and Standards is responsible for the B31 series of Pressure Piping Standards and the Boiler and Pressure Vessel Codes. Design rules in ASME B31 codes as well as codes and standards developed by other industrial organizations are incorporated by reference into the federal pipeline safety standards.

Codes and standards that are incorporated by reference into federal pipeline safety standards are the primary vehicles for implementing design, construction, and suggested guidelines developed by industry. In some cases, the entire text of a code or standard is incorporated by reference, but in other cases, only a portion of the text is incorporated. When an entire code or standard is not incorporated by reference, the regulations might contain supplementary rules to address specific safety issues. Sometimes, however, there are no regulations or rules to cover all possible situations. In the absence of specific requirements, industry codes and standards would generally apply, but other methods might also be justified from a technical or safety viewpoint. Current federal pipeline safety standards and industry codes limit internal pressure for natural gas pipelines based on SMYS of the linepipe steel and a design margin based on a prescribed percentage of SMYS that varies depending on pipeline location.

Industry codes and federal pipeline safety standards provide limited guidelines on how to produce safe designs for pipelines in northern climates where ground movement is likely. In addition, they rarely provide explicit design requirements or performance criteria for achieving this objective. Quite often, operators considering construction of pipelines in such areas find it necessary to supplement the guidelines found in existing codes and standards with project-specific design criteria. These criteria must be carefully selected to be consistent with the intent of existing codes and standards while providing designers with more direct guidance on how to achieve the desired performance and safety objectives.

Increased availability of alternative guidance and recommended practices could help simplify the design and qualification process for future pipelines [13]. However, different standards and regulations allow

different design limits and might contain conflicting rules. In addition, they do not always reflect experience with newer types of linepipe steel or advanced design criteria being proposed for future pipeline construction. Rules for design and construction of these future pipelines are beyond the intended scope of those currently published in federal regulations and applicable codes and standards. Consequently, there is a recognized need for advanced design and construction rules for pipelines that use newer types of linepipe steel and alternative design methods.

The state-of-the-art design approach for pipelines, which uses stress-based design methods that are currently reflected in federal pipeline safety standards, is described in Sect. 2.1. Details of SBD methods, which might be required to design pipelines in northern climates, are discussed in Sect. 2.2. Properties for newer linepipe steels needed to design pipelines using SBD methods are discussed in Sect. 3.

2.1 STRESS-BASED DESIGN

Conventional pipeline design methods primarily rely on a stress-based approach. This approach focuses on load-controlled or stress-controlled events where the objective is to ensure that the pipeline is designed to prevent yielding. In a load-controlled event, the magnitude of the load is analyzed completely independently from the deformation or displacement of the structure. Design rules for pipelines typically concentrate on limiting internal pressure to a specified percentage of SMYS of the material. Stress-based design is limited to purely elastic behavior in a material where stress is directly proportional to strain consistent with the principle of Hooke's law:

$$\sigma = E\varepsilon$$

The design margin, or factor of safety, is the difference between the allowable stress and SMYS. The shape and properties of the plastic portion of the material response is not a consideration in stress-based design. Key parameters for the stress-based design approach are illustrated in the stress-strain diagram in Fig. 2.

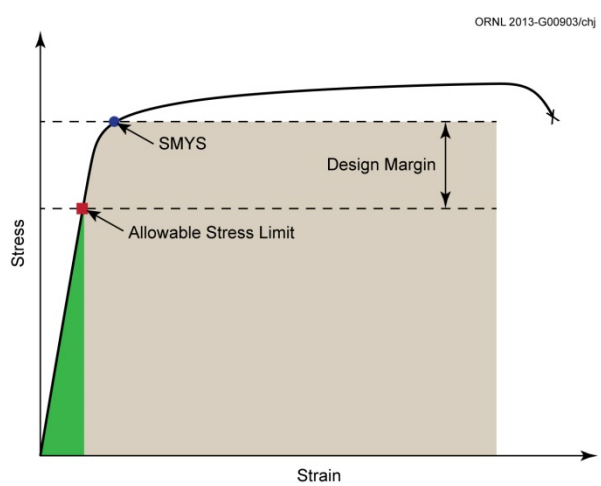

Fig. 2. Basis for stress-based design approach [14].

Almost all codes and regulations provide simplified stress analyses that assume a pipeline to be under plane stress. Plane stress analyses are often assumed for thin, flat plates that are only acted upon by forces that are parallel to the plate. In certain cases, a gently curved thin plate may also be assumed to have plane stress for the purpose of stress analysis. It is important to note that the stress components that are

perpendicular to the cylinder wall are never zero. However, in the case of a large diameter, thin-walled cylinder with fluid under pressure, stress components that are perpendicular to the plate may be considered negligible compared to stresses that are parallel to the cylinder and the embedded safety factor applied to the allowable material stress.

Traditional pipeline design approaches found in most codes and standards are dependent on ductile, isotropic linear elastic linepipe steels with corresponding elastic-plastic stress-strain curves. For isotropic, homogeneous materials, only one set of material properties is required. It is assumed that stresses are distributed uniformly and sufficiently throughout the material in such a way that there is not any material dependence on coordinate rotation or translation. Design life is typically not a consideration and not part of the design calculations. When a pipeline operates in the elastic region and is not subject to cyclic loading, it has been stated that a properly protected and maintained pipeline can provide service indefinitely [15].

The focus of the ASME codes and standards is primarily on stress-based analysis using many of the assumptions listed previously, including plane stress analysis using isotropic, linearly elastic, homogeneous materials where displacements are small and the strains are below the elastic limit. In addition, geometry and loading are axisymmetric, stress and strain are assumed not to vary along the length of the pipeline under consideration, and the pipe is assumed to be straight. Basic design factors limit the circumferential stress to a maximum of 80% of SMYS, which is defined as 0.5% total strain for steel grades up to X80. ASME B31.4 [16] and B31.8 [15] do not list materials with a SMYS greater than 80 ksi but refer the user to the specific pipe specification. Loads that introduce primary stress (i.e., not self-limiting) must satisfy the basic design criteria that can also be based on factors derived from regulatory requirements. Primary stresses that exceed the yield strength will result in distortion or failure and cannot be relieved by local deformation such as stress in the linepipe wall caused by internal pressure. Locally, high circumferential stresses are sometimes disregarded when they are caused by secondary stresses (i.e., self-limiting).

While conventional stress-based design can be used for axial strain less than the yield stress, it cannot account for the effect of larger axial strain on the allowable operating pressure. Effects of axial strain must therefore be considered in determining the limit-load carrying capacity of the pipeline. If the pipeline is restrained in the longitudinal direction (i.e., anchors, soil over-burden, or frozen soil conditions that fully restrain the pipe), the tendency for the pipeline to contract will be limited and will increase the circumferential stress in the linepipe because of the Poisson effect.

Most stress-based pipeline design rules are based on a form of the von Mises yield criterion for an isotropic material under multiaxial loading. The von Mises equivalent tensile stress, used to predict yielding of materials under multiaxial loading conditions using results from uniaxial tensile tests yield criterion based on principle stresses, can be written as follows:

$$\sigma_e = \frac{1}{\sqrt{2}}\sqrt{[(\sigma_1 - \sigma_2)^2 + (\sigma_2 - \sigma_3)^2 + (\sigma_1 - \sigma_3)^2}$$

This is accomplished by mandating a maximum design ratio of allowable stress to SMYS. ASME B31.8 [15] allows a maximum sum of primary and secondary stresses of 90% of the minimum yield strength in the circumferential direction, or by a combined biaxial stress state for restrained pipe. Poisson's ratio is embedded in the stress equations as 0.3. The way the stress equations are presented, a Poisson's ratio of 0.3 would apply to all steel pipeline in all directions based on the ASME B31.4 [16] and B31. 8 [15] analysis rules.

The mechanics of materials approach to stress-based analysis presented in most codes and regulations fails when the previous assumptions are not valid. When pipelines experience large strains and displacements, particularly in the plastic region, the material behavior is no longer linearly elastic. This problem is compounded when material properties vary, such as anisotropic materials where large cyclic plastic displacements are anticipated.

2.2 STRAIN-BASED DESIGN

An SBD approach is a design methodology that focuses on strain limits in conjunction with stress limits as opposed to only stress limits. Expressed another way, an SBD is considered a limit-based design. The theory of strain is based on geometrical concepts of extensions and rotations. To relate the strain at a particular point to stress, material properties are required. The corresponding stress-strain relationship and coefficients can be used to analyze the deformation and displacement of the structure and predict the initiation of the inelastic, or plastic, response of materials.

SBD encompasses both strain demand (applied strain) and strain capacity (strain limit). It also allows a more effective use of the pipeline's longitudinal strain capacity while maintaining the circumferential pressure containment capacity. This is accomplished by ensuring that materials have adequate strain capacity while mitigating strain demand, whenever possible, to ensure an acceptable design or safety margin. The shape and associated properties of the material's plastic stress-strain response are central to SBD. Key parameters for the SBD approach are illustrated on a stress-strain diagram in Fig. 3.

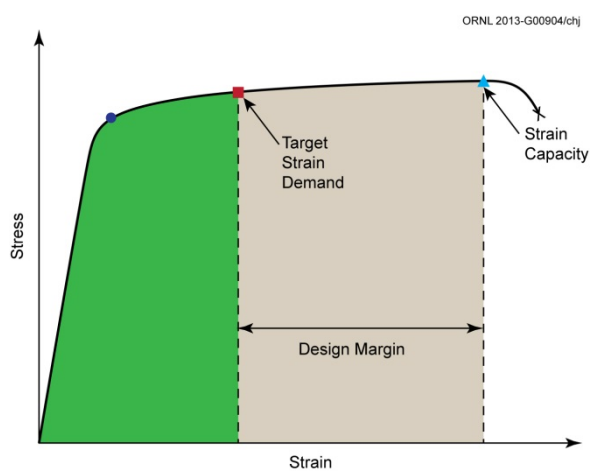

Fig. 3. Basis for SBD approach [14].

The SBD approach was developed as a new technology for supplementing stress-based design for ensuring pipeline operational safety. Research shows that large axial strain can result in a pipeline failure at a critical tensile strain where the operating pressure might be less than its allowed value using conventional stress-based design [17]. Consequently, the SBD approach is under active study because the conventional stress-based design approach cannot be applied in cases where applied strain greatly exceeds the yield strain [18]. The goal of SBD is to maintain pipeline service and integrity under large longitudinal plastic strains generally defined as greater than 0.5% [9] or longitudinal stress over the yield strength.

SBD applies to a subset of the limit states where displacement-controlled loads dominate the pipeline response. Besides operational loadings such as internal pressure, pipelines can also experience large displacements from permanent or transient ground deformation caused by seismic activity, soil subsidence, slope instability, frost heave, thermal expansion and contraction, landslides, pipe reeling, pipe laying, and other types of environmental loading. During construction, pipelines can experience large axial strains as the pipeline is lowered into the trench. These loading conditions apply displacement rather than force to the pipeline and require alternative SBD methods to ensure an acceptable level of safety [5]. Large deformations are typically displacement controlled, although combinations of displacement and load-controlled scenarios are possible. Regulations in 49 CFR 192 Subpart C addresses pipe design. Paragraph 192.103 states:

> *Pipe must be designed with sufficient wall thickness, or must be installed with adequate protection to withstand anticipated external pressures and loads that will be imposed on the pipe after installation.*

The cyclic stress from environmental loading and operational parameters (pressure, temperature, etc.) must also be considered. Paragraph 195.110(a) states:

> *Anticipated external loads (e.g.), earthquakes, vibration, thermal expansion, and contraction must be provided for in designing a pipeline system.*

From a safety viewpoint, pipeline longitudinal strain can be allowed to exceed the specified yield strain under displacement load provided the pipeline can adequately meet the operating requirements without rupture. In these situations, it is possible to supplement the stress-based design method with the SBD method to satisfy stress, strain, and economic concerns [19]. The fundamental criteria equation for SBD is the comparison of the applied strain, or strain demand (ε_d) to the permissible strain, or strain capacity (ε_c) based on the following relationship: [20].

$$(\varepsilon_d) \leq (\varepsilon_c) \quad .$$

There are two ultimate limit states normally associated with SBD: tensile rupture and compressive buckling. A complete design evaluation and analysis requires consideration of both compressive and tensile behavior, although the compressive strain capacity has been extensively investigated and is associated with a limit state that does not involve catastrophic failure or loss of pressure containment as does the tensile limit [21]. Different limit states can exist for specific design criteria such as construction, operation, upset conditions, and maintenance.

The limiting failure mode for a pipeline subjected to axial tension is fracture or plastic collapse. The limiting failure mode for a pipeline subjected to axial compression is buckling. In cases where a pipeline is subjected to global bending, fracture or collapse can occur on the tensile side of the pipe and buckling can occur on the compression side of the pipe. Tensile strain and compressive strain for a pipeline subjected to global bending are illustrated in Fig. 4.

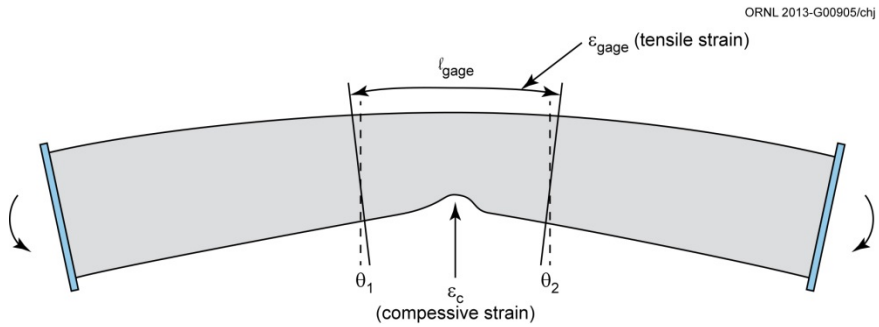

Fig. 4. Linepipe loading.

The objective of an SBD is to ensure a factor of safety comparable to that of existing, state-of-the-art code-based allowable stress designs. To achieve this, there must be adequate separation between the distribution of strain demand expected over the length of the pipeline and the distribution of strain capacity. The overlap between the demand and capacity distributions is related to the probability of failure of the pipeline. Uncertainty in estimates of demand and capacity must be taken into account when determining the probability of failure. In cases where strain demand accumulates slowly, such as for permafrost heave and thaw, the ability to monitor the development of strains and implement corrective measures to reduce the maximum strain demand can have a significant impact on reliability [14]. Allowable strain demand means strain limitation, which includes strain limit and safety factor and can be described as:

$$\varepsilon_d \text{ (strain demand)} < f \text{ (safety factor) } x\ \varepsilon_c \text{(strain capacity)} \ .$$

SBD is currently addressed in a number of regulations and design codes. Some have prescriptive requirements that apply to SBD of pipelines, including:

- DNV-OS-F101, *Submarine Pipeline Systems*,
- CSA-Z662, *Oil and Gas Pipeline Systems*,
- API RP 1111, *Recommended Practice for the Design, Construction, Operation, and Maintenance of Offshore Hydrocarbon Pipelines (Limit State Design)*,
- ASME B31.4, *Pipeline Transportation Systems for Liquids and Slurries*,
- ASME B31.8, *Gas Transmission and Distribution Piping Systems*,
- API 1104, *Welding of Pipelines and Related Facilities*,
- ABS 2001, (American Bureau of Shipping), *Design and Certification of Offshore FRP Piping* Installations, and
- NEN3650, Design of Buried Pipelines.

Some provide a comprehensive overall pipeline standard that includes requirements both for stress and SBD such as Det Norske Veritas (DNV) and Canadian Standards Association (CSA) standards. Others allow for SBD but do not provide much guidance for analysis related to SBD, such as ASME B31.8 and API 1104. Still others provide information on SBD related to a specific subgroup of pipelines such as ABS 2001 or API RP 1111. Several organizations sponsor current research projects that will be released to the public domain after their completion in areas that directly or indirectly impact SBD of pipelines. For instance the Minerals Management Service and the Office of Pipeline Safety cofounded EWi to provide a general guidance on SBD for pipelines in both on- and off-shore environments [19].

The most recognized procedures for tensile strain capacity (TSC) designs have been published by DNV in DNV-OS-F101 and DNV-RP- F108 for offshore pipeline installations. DNV-OS-F101 *Submarine*

Pipeline Systems offshore standard provides design and construction criteria for submarine pipeline systems. In 1982, the DNV proposed the combined use of stress-based and SBD criteria. In 1996, the DNV published a subsea pipelines limit state design criteria in which there are many analytical methods based on a variety of load conditions [19].

DNV-RP-F108 *Fracture Control for Pipeline Installation Methods Introducing Cyclic Plastic Strain* [22] is a recommended practice developed to give detailed guidance for testing and analysis for fracture control of pipelines with large plastic strains. It is intended to complement DNV-OS-F101 and give more detailed guidance for engineering critical assessment procedures and a validation test program. This standard is based on limit state design and recognizes four kinds of limit states: service ability, ultimate, fatigue, and accidental. The appropriate limit state method is applied to the pipeline design, and appropriate design criteria are presented to make the design safety factors less conservative with more flexibility to the designers [19].

In DNV-OS-F101, linepipe subjected to large strains that exceed the actual yield strength in the longitudinal direction are limited to not exceed SMYS by more than 120 MPa nor exceed the specified minimum tensile strength in the longitudinal direction. The yield/tensile (Y/T) ratio in the longitudinal direction shall not exceed the maximum specified value in the circumferential direction by more than 0.02 for standard material [6]. For the base materials whose minimum yield stress is 415 MPa (Grade X60) or more, DNV recommends that Y/T in transverse is a maximum of 0.92; while for less than 415 MPa, DNV recommends a maximum of 0.90. The tensile strain limits may decrease with the increase of Y/T. However, for the base material whose accumulated plastic strain might be more than 2%, DNV recommends that Y/T is lower than 0.85 [19]. Allowable strain values are given up to 5%. Supplemental material testing requirements are given where "the total nominal strain in any direction from a single event is exceeding 1% or accumulated nominal plastic strain is exceeding 2%. The requirements are only applicable when single event strains below 5% are expected."

There are certain limitations to the DNV standard. The referenced procedure, a British Standard BS7910, is a stress-based approach in the form of a failure assessment diagram (FAD). When the material response is in the plastic range, a small change in stress can result in a large change in strain because of the almost perfectly plastic behavior of the material. This is particularly true for modern high-strength linepipe materials, which typically exhibit low strain hardening. A procedure intended to determine stress limits is therefore fundamentally insensitive in determining strain limits when the material response is in the plastic range [10].

DNV requires several additional material tests to account for strain-aging effects on strength, ductility, and toughness on materials where the accumulated plastic strain will exceed 2%. The material must be tested after tension and compression loading has been applied to reach at least the design-accumulated plastic strain and after an artificial age at 250°C for one hour to account for pipe coating temperatures [13]. DNV recommends that pipe expected to encounter accumulated plastic strain of 2% or more have a minimum elongation of 25%. API Specification 5L and DNV-OS-F101 have the requirement of 15.6% minimum elongation for Grade X80 linepipe.

In 1996, the CSA published CSA Z662-96 Annex C, which comprises SBD criteria for submarine pipeline design using a limit state design. It has become the most recognized procedure for TSC design for onshore pipelines [19]. Chapter 11 of CSA Z662-96 allows for a maximum permissible strain in the pipe wall of 2.5%. It is noted that the maximum permitted strain for pipe other than seamless may be less.

The CSA Z662-96 Annex C Limit State Design and SBD criteria are given for rupture (governed by tensile) and local buckling (governed by compressive strain). The proposed generalized complex equations are based on key material and geometric parameters for welded pipelines based on past relevant

test data [10, 23]. For the development of these models, there are no limits on pipe grade and the models are intended to be a one-size-fits-all approach. Tensile properties are represented by the longitudinal uniaxial, monotonic Y/T ratio, which serves as the strain-hardening capacity [9]. Internal pressures can accelerate the crack growth, but its quantitative approach to tensile strain limit has not been found [19]. Based on a generalized parametric study, a generalized tensile strain capacity equation is expressed as a function of several factors [9, 24].

$$\varepsilon_c = f\left(a, C, e, \lambda, t, \frac{Y}{T}, UEL_{pipe}, \delta, \eta, P\right) ,$$

where:

a	=	Flaw depth
C	=	½ flaw length
e	=	Misalignment
λ	=	Weld overmatch
t	=	wall thickness
Y/T	=	Yield strength to tensile strength ratio
UEL	=	Uniform elongation
δn	=	R-curve parameters
P	=	Internal pressure

Other factors not explicitly considered in the Annex C equations were later found to also have a strong impact such as internal pressure [25]. The effects of internal/external pressure on the longitudinal strain capacity are an area of ongoing research [26].

ASME B31.4 and B31.8 provide limited guidance to strain-based applications. ASME guidance limits strain to a maximum of 2% and specifically excludes pipelines that could experience cyclic displacement. ASME B31.4-2012 paragraph 403.3.3 *Strain Criteria for Pipelines* states:

> *When a pipeline may experience a noncyclic displacement of its support (such as fault movement along the pipeline route or differential support settlement or subsidence along the pipeline), the longitudinal and combined stress limits may be replaced with an allowable strain limit, so long as the consequences of yielding do not impair the serviceability of the installed pipeline. The permissible maximum longitudinal strain depends upon the ductility of the material, any previously experienced plastic strain, and the buckling behavior of the pipe. Where plastic strains are anticipated, the pipe eccentricity, pipe out-of-roundness, and the ability of the weld to undergo such strains without detrimental effect should be considered. Maximum strain shall be limited to 2%.*

ASME B31.8-2012 paragraph A842.2.3 *Alternate Design for Strain* states:

> *In situations where the pipeline experiences a predictable noncyclic displacement of its support (e.g., fault movement along the pipeline route or differential subsidence along the line) or pipe sag before support contract, the longitudinal and combined stress limits need not be used as criteria for safety against excessive yielding, so long as the consequences of yielding are not detrimental to the integrity of the pipeline. The permissible maximum longitudinal strain depends on the ductility of the material, any previously experienced plastic strain, and the buckling behavior of the pipe. Where plastic strains are anticipated, the pipe eccentricity, pipe out-of-roundness, and the ability of the weld to undergo such strains without detrimental effect should be*

considered. Similarly, the same criteria may be applied to the pipe during construction (e.g., pull-tube or bending shoe risers).

ASME B31.8-2012 paragraph 833.5(b) *Design for Stress Greater than Yield* states:

The maximum permitted strain is limited to 2%.

There are additional standards that mention SBD, but they add little additional technical insight. The Australian Standard AS2885 *A Modern Standard for Design, Construction, Welding, Operation and Maintenance of High Integrity Petroleum Pipelines* has the status of a "National Standard" for Australia. It allows the use of recognized alternative standards such as American Petroleum Institute (API) 1111 or DNV-OS-F101 for the design of new pipelines but does not contain any additional guidance on large strain design of pipelines. The NEN3650 *Design of Buried Pipelines* is a Dutch pipeline standard introduced in 1992. The stress and strain analyses were based on the ASME codes and a method for defining limit states based on empirical factors only. It has been concluded that a research project is required to define the safety margins more clearly to derive a new stress criterion [27]. The API Recommended Practice 1111-2011 contains an informative design example in Appendix D regarding buckling limit state bending strains. This example derives the limit state equations based on the assumption of small strains and might not be realistic for large strains.

Current research suggests that the SBD approach for pipeline applications is only viable when the linepipe steel is ductile and has high deformability as measured by a low-yield-to-tensile-strength ratio, a high work-hardening rate (n-value), and a high uniform elongation (UEL). The intent is to ensure high material toughness characteristics rather than higher ultimate strength [28], thus the material is more suited to deform plastically before crack initiation or fracture. Low Y/T ratio, adequate uniform elongation, and the shape of the stress-strain curve are of vital importance and are the focus for material development [29].

An SBD evaluation and analysis must address all aspects of the pipeline's life cycle including design, materials, construction, and operations and maintenance such as:

- longitudinal and compressive strain capacity for all parameters in the pipeline's life cycle,
- cyclic stresses and strains from environmental loading and operational parameters such as internal and external pressure, and
- adequate strain capacity to accommodate variations in Y/T ratio, elongation, tensile strength, linepipe chemical composition, microstructures, and steel making practices.

The target anticipated strain demand range for pipeline projects is from 1.0% to one-half of the pipe's UEL. The predictive models have no inherent safety factor, and many of the tensile strain models assume the materials to have uniform and isotropic properties. The potential impact of material anisotropy on the tensile strain capacity is not considered in the models [9]. Most high strength steel linepipe materials exhibit orthogonal anisotropy, meaning the tensile strength is often different between the longitudinal, circumferential, and radial directions [30]. Major model variables not explored in the models are weld joint misalignment, wall thickness, pipe diameter, and effects of cyclic service [9]. This technology is not yet sufficiently validated. Significant further work is required. The prediction models need to be evaluated using anticipated pressure and longitudinal strain ranges to ensure that the model is appropriate for the material, design, construction, and operational and environmental conditions.

3. MATERIAL PROPERTIES AND MECHANICAL BEHAVIOR

Effective use of the SBD approach for pipeline applications compared to the more traditional stress-based design approach requires greater knowledge and understanding of the material properties and mechanical behavior of linepipe steels. In particular, complete stress-strain curves and strain-aging response parameters are needed to implement the SBD approach. As most strains of interest in strain-based analysis are longitudinal, it is critical that both longitudinal and circumferential mechanical properties of the linepipe steel are reliably determined and readily available. Consequently, the field of SBD with the appropriate material characterization is an evolving engineering discipline [9].

Federal pipeline safety regulations in 49 CFR §192.55 (e) for natural gas pipelines state that new steel linepipe, which has been cold expanded, must comply with mandatory provisions in API Specification 5L—*Specification for Line Pipe* [31]. Additional regulations in 49 CFR §192.112 (a)(4) follow for pipelines that are authorized to operate at higher allowable pressures through a special DOT-issued SBD waiver.

> *The pipe must be manufactured using API Specification 5L, product specification level 2 (incorporated by reference, see § 192.7) for maximum operating pressures and minimum and maximum operating temperatures and other requirements under this section.*

Standards committees and task groups within API are comprised of industry experts much like the standards committees in ASME. The API pipeline standards committees charter is to create and maintain standards that facilitate safe operation and maintenance of pipelines. Requirements adopted by API for steel linepipe for use in petroleum and natural gas industries are provided in API Specification 5L. Corresponding requirements adopted by API for pipeline welding are provided in API Standard 1104—*Welding of Pipelines and Related Facilities* [32]. This standard also covers nondestructive examination (NDE) procedures. Both of these API standards are cited references in 49 CFR 192 and 49 CFR 195.

API Specification 5L was initially issued in the 1920s. In 2007, requirements in API Specification 5L and ISO 3183 were combined into a single international standard that includes requirements for higher pipe grades X90, X100, and X120. The current edition of API Specification 5L contains requirements for pipe grades, steel grades, and delivery conditions including chemical composition, strength properties, and NDE procedures for both seamless and welded linepipe intended for transmission pipeline applications. Linepipe grades are designated as either product specification level (PSL) 1 or PSL 2. Requirements for PSL 1 linepipe include minimum yield strength, minimum ultimate tensile strength (UTS), and minimum elongation determined from pipe body test data. Requirements for PSL 2 linepipe include those for PSL 1 linepipe as well as maximum yield strength, maximum UTS, and maximum *Y/T* ratio. Tensile testing of linepipe fabricated to API Specification 5L requirements must be conducted in accordance with ASTM A370—*Standard Test Methods and Definitions for Mechanical Testing of Steel Products* [33] and ASTM E 8—*Standard test Methods for Tension Testing of Metallic Materials* [34].

Most pipeline design codes permit use of mechanical properties specified in API Specification 5L along with a property known as flow stress, which is the average of yield strength and UTS [9]. These mechanical properties are generally used to establish circumferential stress limits in accordance with the stress-based design approach. Design codes for stress-based design applications are not concerned about stresses in the longitudinal direction because the magnitude of pressure-induced circumferential stress is twice the magnitude of the corresponding longitudinal stress. Consequently, the rules in design codes for stress-based design applications, which do not include longitudinal stress limits, cannot be used for SBD applications that are primarily governed by longitudinal strains.

API Specification 5L and the ASME B31 codes provide rules that address the material testing and determination of mechanical properties for use in design. In dealing with the modes of failure from the plastic limit, material mechanical properties must be properly determined and adequately reflected in the design process. As the design margins decrease and allowable pressures in relation to yield stress increase, yield and UTS determinations of the linepipe materials in the final product form are crucial. Most codes and standards list material property specifications based on small-scale, monotonic, uniaxial, smooth bar testing. In almost all cases, the materials are assumed to be isotropic and homogeneous.

3.1 MICROSTRUCTURE AND CHEMISTRY

Numerous alloy designs are used to produce linepipe with higher strength. These designs are categorized by their microstructure as either ferrite/pearlite (F/P) or ferrite/acicular ferrite (F/AF). Each microstructure behaves fundamentally differently depending on the pipe-making process [35]. The approach to alloy designs for linepipe steels that conform to API Specification 5L requirements starts with a basic low carbon-manganese-silicon (C-Mn-Si) base. This alloy design is used for lower strength pipe grades 5LB and X42. Additions of a single microalloy or a dual microalloy in amounts less than 0.065% each, along with low amounts of various solute alloys of copper (Cu), nickel (Ni), and chromium (Cr), depending on plate thickness and rolling mill power, are used to produce pipe grades X52 to X70. When additional strength is required, the main microalloy of choice is niobium (Nb) with vanadium (V) playing a supporting role. The C-Mn-Si base along with microalloy additions produces the F/P microstructure regardless of rolling practice. This alloy-microstructure design combination tends to have the lowest production cost [35].

Alloy designs for higher strength pipe grades X70 and above (or for X65 when compensating for lower plate mill power) start with the C-Mn-Si plus microalloy base and then add small quantities of solute alloys such as Cu, Ni, or Cr, either singly or in combinations to a maximum combined content of about 0.6%, and molybdenum (Mo) to about 0.3%. These additions, particularly Mo, coupled with appropriate rolling and cooling practices result in the F/AF microstructure. Microalloy additions of up to 0.11% Nb, without Mo, can also produce the desired F/AF microstructure. This latter approach is termed high-temperature processing (HTP) because the steel can typically be finish rolled at higher temperatures. Increased additions of the solute alloys (Mn, Cu, Ni, Cr, and Mo) along with boron (B) are used to produce pipe grades X100 and X120. These richer additions produce other forms of bainite along with small quantities of martensite and yield steel with reduced weldability at an increased cost [35].

In general, the F/P microstructure leads to a drop in yield strength between the TMCP skelp (coil or plate) and pipe, while an acicular structure can lead to an apparent yield strength increase. There is generally less scatter in the relationship between pipe tensile strength and skelp tensile strength, with the shift in tensile strength during pipe making being always neutral or positive. As such, the shifts between skelp and pipe yield and tensile strengths can each be in different directions. Toughness also changes during pipe making while behaving somewhat similarly to strength.

In summary, pipe grades up to X70 with an F/P microstructure can be produced using a basic low C-Mn-Si-Nb-V microalloy design, regardless of hot rolling practice. As the strength level or wall thickness increases, additional alloying and more stringent rolling and cooling processing practices must be used to produce steels with an F/AF microstructure [35]. Knowing the reasons for strength change from skelp to pipe is important because F/AF steel is fundamentally different from F/P steel because of yielding behavior, which is largely driven by microstructural composition.

There is a practical significance to grain size and grain boundaries. Grain boundaries are regions between grains where atoms try to accommodate the crystal lattice misalignment between grains (Fig. 5). Therefore, grain size does affect the mechanical properties, and material strength will increase as the

grain size decreases. Grain size will also influence forming properties and fatigue strength. Grain size can be modified by use of mechanical and thermal treatments such as a thermomechanically controlled process or heating to apply a corrosion resisting protective coating.

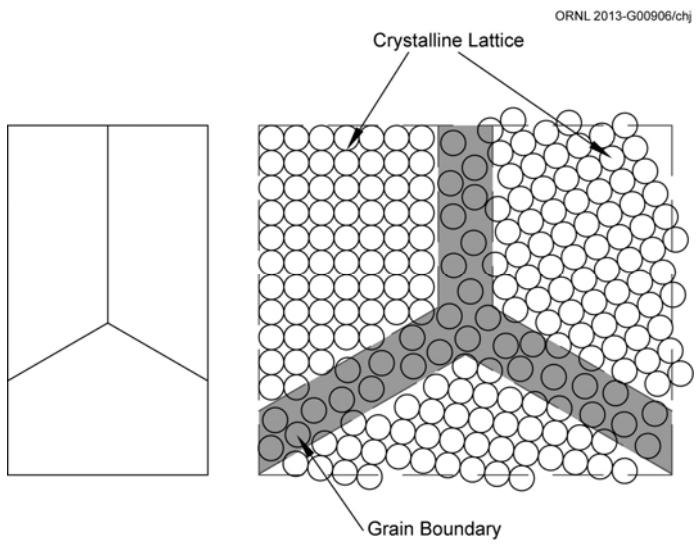

Fig. 5. Typical grain boundary.

Dislocations, or irregularities, within the crystal structure can also strongly influence the mechanical properties of the material. Material strength depends on the ease with which dislocations move through the metal. The stress required for dislocations to move depends on several factors such as grain size, number of dislocations present, and the size and shape of the dislocations. As the material deforms, the number of dislocations increases. Dislocations will generate new dislocations under strain. As the number of dislocations increases, the amount of stress required for deformation increases. At stresses above the yield strength, dislocations start to move. More dislocations are generated as the strain increases. The dislocations interfere with each other's motion, so increased stress is required to continue to yield, or strain the material. This is known as work hardening. There comes a point at which no more dislocations can occur, and the sample begins to thin with potentially catastrophic results. This is referred to as the ultimate strength of the material. For strains greater than the strain required to reach the ultimate strength, there is a decrease in the stress required to continue the deformation.

It is well known that the phase constituents in a microstructure have a strong effect on the shape of the stress-strain curve and therefore on the determination of the yield strength of the steel [3]. This strain-aging effect can result in an increase in the yield strength as much as 60 MPa. In a worst case scenario, this can change the shape of the stress-strain curve from continuous yielding to discontinuous yielding. The processes for steel making and pipe forming should be optimized to minimize the strain aging effect [1]. Recent research seems to suggest that while strain aging has an effect on the yield strength, it does not have much effect on the ultimate strength [21].

Changes to microstructure can also have an impact on fatigue strength. Fatigue resistance is generally enhanced by reducing voids in the material, decreased grain size, and a dense network of dislocations. Processing improvements aimed at changing the microstructure might not be successful unless it can be accomplished without substantially decreasing the ductility [36].

Requirements for chemical composition and tensile test results are given in API Specification 5L. The minimum uniform elongation requirement is 18% for steels with SMYS ≥ 415 MPa and 20 to 22% for steels of lower strength. A common specification limit is 0.92 for Y/T. API Specification 5L restricts the Y/T of cold-expanded steel pipe to 0.93 [13]. These limits are intended to ensure a ductile rather than brittle response to overpressure events.

3.2 PHYSICAL PROPERTIES

The physical properties of microalloyed high-strength linepipe are affected by plate and pipe forming operations and the coating application process.

3.2.1 Forming

Steelmaking facilities that produce slabs for API Specification 5L [31] pipe grades typically consist of a starting metallic process (blast furnace—pig iron, direct reduced iron, or scrap), melting furnaces, ladle metallurgy furnaces or stations, vacuum degassing (might or might not be used depending on desired end characteristics), and continuous casters. The main goals in producing slabs of suitable quality for natural gas transmission pipeline applications are to:

- Maintain tight chemistry control to promote consistent microstructure and mechanical properties.
- Maintain good internal cleanliness to promote high toughness, good weldability, hydrogen-induced cracking (HIC) resistance, and formability.
- Minimize centerline conditions to promote consistent thru-thickness properties and microstructure, HIC resistance, and internal lamination issues.
- Maintain good surface quality to minimize pipe surface defects.
- Maintain dimensional control to enhance downstream processing efficiencies.

Conventional rolling involves either hot rolling or controlled rolling operations. In hot rolling, the product finishes at its prescribed final thickness with no regard to the final reduction temperature, that is, it finishes naturally based on the mill's capability (number of passes, draft/pass, etc.) to make the final thickness. Controlled rolling involves setting a desired finish temperature or invoking a mild (two times the final thickness) intermediate hold temperature along with a desired finish temperature. Thermomechanical rolling involves either TMCP or HTP. These rolling process routes are used for both coil and plate. After hot rolling, the steel is air or water cooled to achieve the desired microstructure, hence strength.

Thermomechanical processing or rolling is commonly performed in two rolling processes. Steel billets are heated to over 2000°F and then are progressively rolled to reduce the billets to the final plate thickness. The plate is shifted back and forth on the roller table, gradually leading to a finer microstructure, until the final forming temperature is achieved. Final forming begins in a temperature range between 800 and 900°C. The homogenously heated slab from the heating furnace will produce a course-grained microstructure that integrates work hardening and heat-treatment into the forming process by controlling temperatures and rolling reductions during the hot rolling and the control of cooling after rolling. Final forming below these temperatures will lead to higher ultimate strength and low toughness levels. The final plate produced using the thermomechanical rolling process will achieve mechanical properties that cannot be achieved or repeated through heat treatment alone. Steels produced using this process are characterized by excellent combinations of strength, toughness, and weldability. The lower carbon

equivalent of TMCP steels compared with conventional normalized grades of equivalent strength means easier welding with increased strength, as well as an increased safety margin against hydrogen cracking and lower preheat temperatures. Also, the low carbon and impurity content means that they are well suited to cold forming [37]. API Specification 5L cautions that subsequent heating above 580°C (1075°F) can lower the strength.

A limitation to TMCP steels of practical importance is that they cannot be normalized [37], and there is a variation in mechanical properties [38]. If TMCP steels behaved in the same way as conventional steels, they would be unusable in high-strain applications. However, previous experience has shown that TMCP steels can meet relevant strength and toughness requirements in pressure vessel applications. The surface layer will be strong and tough, while the center will exhibit more ductile properties. TMCP plate for high-strength linepipe will often display high anisotropy with different behaviors in the longitudinal and circumferential directions [39]. The fiber texture produced in the steel plate manufacturing process can cause significant plastic property anisotropy, as does the tensile property in whole wall thickness [40].

Grade X80 welded pipe is produced by forming plates in several steps until the required geometrical and mechanical properties discussed above are achieved. The pipe fabrication process begins with adding welding run-off tabs to the four corners of the plate material. The longitudinal edges are crimped to the desired pipe radius to allow for a round geometry in the vicinity of the longitudinal weld. The pipe is formed using a variety of methods including UOE/JCOE (U/JC forming, O-pressing, expansion), pyramid forming, and 3-roll bending. The deformation is applied to the plates in a compression and superposed bending mode that is dependent on the geometry, namely diameter and wall thickness. The strains in the outer fibers can be approximated by the wall thickness to diameter ratio. Whereas the intrados is deformed in compression, the extrados is exposed to tensile strains [1]. In general, the yield strength of the plate material increases as the pipe forming ratio (D/t) increases. In the typical forming range of large-diameter pipe, a plate-to-pipe strength increase of about 13 MPa per 0.2% forming ratio has been observed [35]. The inside and outside seam welding is typically performed using the submerged arc process.

The last forming step consists of the mechanical expansion that improves the geometry of the pipe and corrects deformations such as out-of-roundness or bending that might have occurred during the welding process (Fig. 6). As the pipe is expanded from the inside, uniform diameter, straightness of the pipe, and homogeneous mechanical properties through reduction of residual stresses can be obtained. Expansion leads to circumferential tensile strains throughout the pipe wall, typically in the range of 1% plastic deformation. Cold expansion up to 1.5% might be necessary to ensure the roundness and proper outer diameter (D) of pipe [41]. By the time the process of pipe production is completed, different fibers have been exposed to different load cycles. Although cold expansion up to about 1.5% is typically used to improve the pipe's diametrical dimensional conformance and increase yield strength, a high rate of cold deformation is also considered to be detrimental to the ageing resistance of the steel [1].

ORNL 2013-G00907/chj

Fig. 6. Mechanical expansion.

After expansion, the finished linepipe is subjected to a hydrostatic test. Depending on the actual pressure applied, the pipe under testing could experience a moderate cold expansion. This could consequently change the tensile properties of the pipe. A test pressure equivalent to 100% SMYS can be used depending on the final design pressure, which could boost the transverse pipe axis yield strength slightly [1]. Typically, all strength levels of linepipe in diameters up to nominal pipe size (NPS)72 and thicknesses up to 2 in. can be produced by one or more of these pipe-making processes. However, production of spiral pipe from coil with strengths higher than pipe grade X80 could be challenging or alloy additions undesirably costly [35].

Work hardening of the pipe material is a consequence of a combination of elastic and plastic deformation. Work hardening leads to an increase in the yield strength with a corresponding decrease in ductility. The strain history incurred at each point in the pipe forming can significantly alter the yield strength of the pipe relative to the steel plate. This implies that it is necessary to understand the work hardening, which governs the changes of strength from plates to pipes [42]. A greater work hardening rate provides greater resistance to strain localization but can also lead to anisotropic properties and residual stresses [41]. Pipeline steel strain hardening capacity has historically been controlled by placing a minimum requirement on the elongation to failure of the pipe material and of the weld material and by requiring a minimum difference between the yield and ultimate strength of the pipe steel [13].

3.2.2 Coating

Regulations in 49 CFR §192.112 (f)(1) state that:

> *The pipe must be protected against external corrosion by a non-shielding coating.*

Subsequent to pipe making, most pipe is coated with a fusion bond epoxy (FBE) coating before shipment to the installation site. This coating is typically a one-part, heat curable, thermosetting, powdered epoxy-based coating widely used to protect pipelines from corrosion. It comes in a powder form and will remain in a powder form under normal storage conditions. These coatings can be used to protect both external and internal surfaces of the pipe to provide corrosion protection. Abrasive resistant overcoating (ARO) is a hard top coat intended to protect the underlying FBE coating from damage during installation and operation. This coating is typically used for bores, directional drills, and rocky terrain where additional protection for the coating is required. The application or ARO is performed while the FBE is still in the gelatinous stage. Field application of coating is performed after girth welds are made.

A typical heat-curable coating process involves heating the pipe to temperatures of 200 to 250°C for several minutes. The powder is then "flocked" (sprayed) on the hot pipe. As the powder contacts the pipe, it liquefies and flows onto the surface. The residual heat in the pipe will work to cure the coating within just a few minutes with air cooling. This process is known as "fusion-bonding." Because it is a thermoset polymer, the coating cannot be remelted with the application of additional heat. The pipe girth welds are typically coated at the installation site using a variety of methods involving reheating of the local area that is then flocked.

The strain accumulated during the pipe-forming process combined with the thermal process of applying corrosion-resistant coating causes aging effects in the formed pipe. Both plastic straining and temperature exposure lead to changes in the material that affect the final mechanical properties of the pipe [1, 6]. Diffusion of free interstitial carbon and nitrogen atoms is activated by these processes. These atoms tend to move into dislocation cores forming what are called Cottrell atmospheres. The dislocations are pinned, and their mobility is much reduced.

Strain aging results in the reduction of ductility and toughness that can occur after plastic deformation has been applied in carbon-manganese steels. The change in pipe tensile properties associated with coating application is the result of strain age embrittlement where free nitrogen and free carbon in the steel diffuse to new dislocation sites formed during the plastic strain cycle of the pipe expansion process. Changes in material properties in the longitudinal direction are of particular interest [43, 44, 45].

Strain aging is particularly noted in steels that exhibit discontinuous yielding with an upper yield point, a lower yield point, and a yield plateau before strain hardening begins. As a result, yielding and work hardening behavior of the pipe body is modified [41]. The mechanical properties such as yield strength, tensile strength, Y/T ratio, and the stress-strain curve shape also change due to thermal aging [13, 46, 47]. The coating process has been shown to alter the yield strength by as much as 8% [48]. The uniform elongation decreases with the increase of the aging temperature. This decrease is caused by the decrease of the work-hardening rate [12]. Strain age embrittlement often leads to [14, 49]:

- Changes in yield behavior (from continuous to discontinuous yielding),
- Increase in yield strength,
- Increase in Y/T ratio,
- Increase in tensile strength,
- Decrease in ductility, and
- Decrease in toughness.

Aging effects on tensile properties during the coating process must be minimized and fully characterized. It is important to understand the effect of the coating conditions on the thermal aging phenomenon [30]. Thus, there is a strong demand for a high strength, high deformability linepipe with resistance to strain-aged hardening for high-strain applications [47]. The strain-aging resistance of the coated linepipe decreases as the increase of tensile pre-strain induced during pipe making. Also, it was found that strain aging behavior of pipe was different along the through thickness direction [50].

Since it is rare for linepipe to not be coated before installation and operation, it is important to consider the effects of thermal aging on the pipe properties to ensure that the properties remain acceptable after coating. Uniform elongation has been shown to decrease by thermal ageing at temperatures of 200°C and higher. Obvious Luders elongation has been observed at an aging temperature of 160°C and higher in the circumferential direction [12]. After having been exposed to elevated temperatures as usual for coating applications cold formed material changes the shape of the stress-strain curve and could result in a yield plateau [1, 32].

3.3 MECHANICAL PROPERTIES

Mechanical properties of linepipe steel needed as input for the SBD approach involve monotonic tensile testing and cyclic fatigue testing.

3.3.1 Monotonic Tensile Testing

The tensile test is the most fundamental test method used to determine mechanical properties. The standard tension tensile test is based on the Saint-Venant Principle (after Barre de Saint-Venant, 1864), which states that localized stress concentrations disappear a short distance from the concentration. This means that the stress is uniform in a uniaxial loaded bar away from the ends. Figure 7 illustrates the stress distribution at various locations along the length of a square bar that is pulled using friction grips at both ends. The grips introduce the tensile load on the surface of the bar, but in a very short distance the stress is evenly distributed through the bar. The relationship of uniform tensile stress (force per unit area) is only valid away from boundary conditions that introduce stress concentrations.

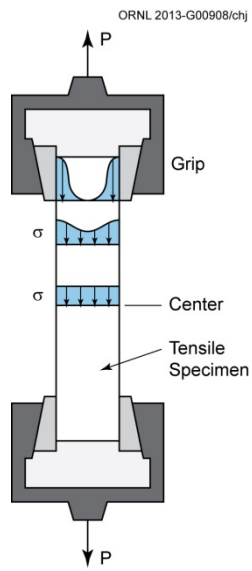

Fig. 7. Saint-Venant principle.

Standard tensile tests for linepipe mechanical properties are straightforward. The monotonic stress-strain diagram and mechanical properties are obtained by recording the stress-strain relationship during the tensile testing to characterize material properties including the elastic limit, yield strength, and ultimate strength. It is important to understand the elastic region where the strain disappears when the loading is removed, and the plastic region where permanent deformation occurs. The tensile, or ultimate, strength of the material is typically defined as maximum load divided by the original cross-sectional area. The Y/T ratio is an indicator of the work hardening capacity of a material. Materials with a high work hardening capacity (low Y/T) will have higher uniform elongation and are therefore better able to dissipate strain, avoid local strain accumulation, and avoid localized thinning.

The measured value of Y/T is critically dependent on the direction of testing and the procedures for extracting a tensile specimen [13].The measurement of tensile properties in pipe material using small

scale testing is usually performed at room temperature for production testing but is often influenced by specimen geometry and test method. Monotonic, uniaxial stress-strain curves up to the minimum uniform elongation limit provide a characterization of yield and ultimate strength to demonstrate the ability to meet the specified requirements. The following properties can be obtained from tensile testing:

- engineering and true stress-strain curves,
- yield strength,
- ultimate strength,
- maximum uniform elongation,
- total elongation,
- true fracture strength, and
- reduction of area.

Key parameters for the determination of mechanical properties are illustrated in the stress-strain diagram in Fig. 8.

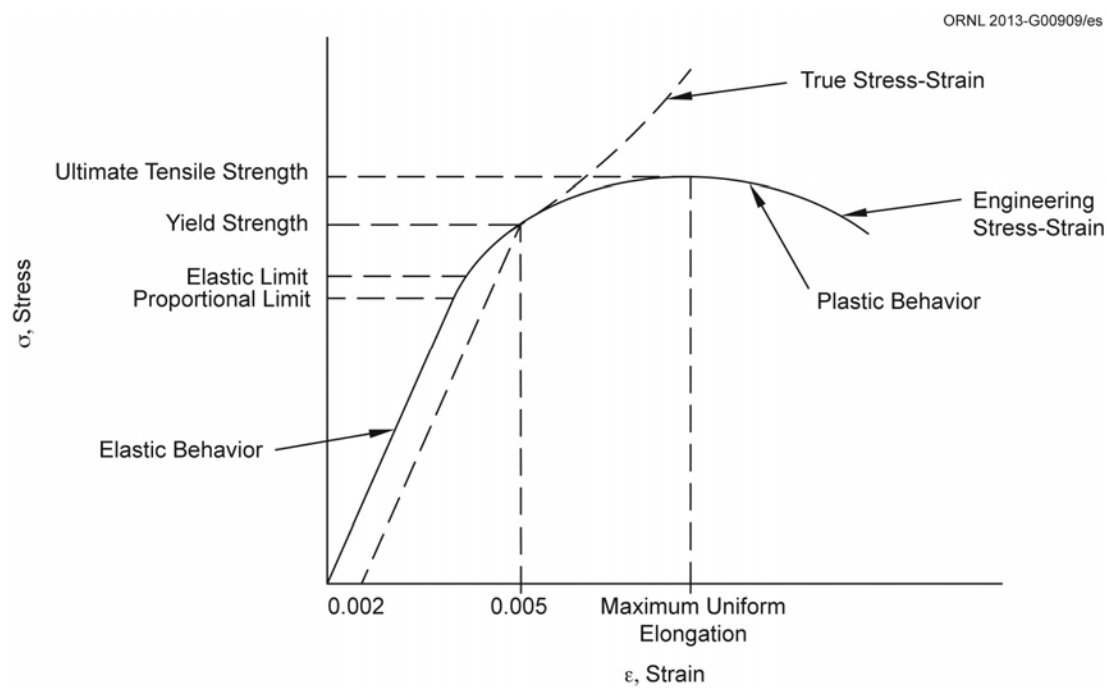

Fig. 8. Mechanical properties.

Stress-strain curves can exhibit different yield point characteristics (Fig. 9). A roundhouse-type stress-strain curve exhibits a smooth, continuous yielding of the material. A knee-type stress-strain curve displays a very sharp transition at the proportional limit when the material begins to deform plastically. The yield type exhibits discontinuous yielding behavior, and might even drop slightly after reaching a maximum yield point.

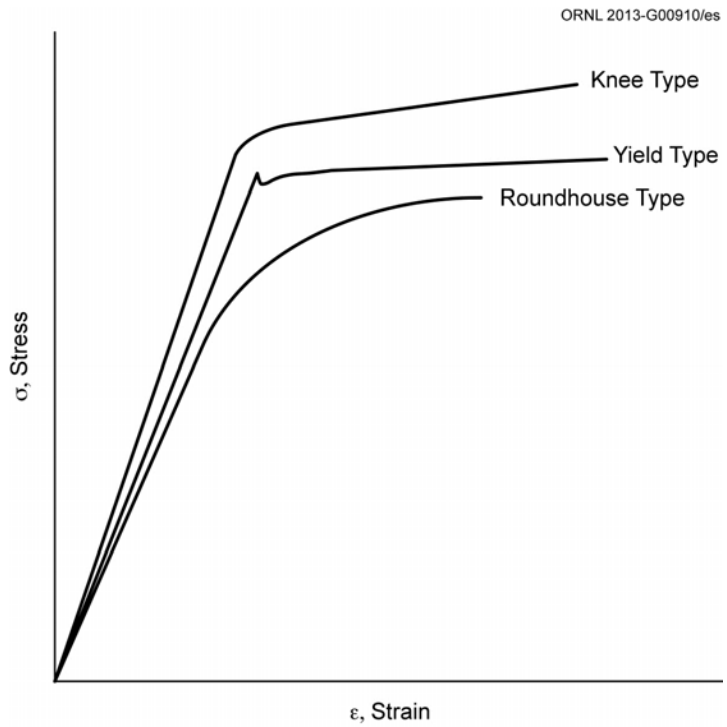

Fig. 9. Stress-strain curve definitions.

W. Lüders first reported noticing localized bands of plastic deformation in certain materials before fracture. These bands resulted in a drop below the initial yield strength. The overall range might show a slight decrease or flat yield in the stress-strain curve. The yield-type stress-strain curve exhibits clear Lüders elongation, an uneven yielding phenomenon where areas of yielding originate in segregated areas and sweep to adjacent material. This usually creates a sharp yield point, and could even cause a drop in stress immediately following the proportional limit. Full stress-strain curves are needed for SBD, particularly in light of the problem with yield strength definition and different shapes of stress strain curves between linepipe material and weld metal [10]. The shape of the stress-strain curves are typically very different for higher grade linepipe materials, especially those produced using the TMCP process.

The initial portion of the stress-strain curve is primarily elastic, meaning that if the stress is removed the strain will essentially return to zero. The proportional limit is defined as the point where stress is no longer proportional to the strain. The point at which deformation becomes permanent is the elastic limit of the material. When the yield strength is not easily defined from the stress-strain curve, the yield point is arbitrarily defined. The 0.5% extension under load method (UEL, often abbreviated in European publications as $R_{t0.5}$) is typically used for linepipe steel grades less than Grade 555 (X80). The 0.2% offset method (abbreviated in European publications as $R_{p0.2}$) is widely used for defining the yield strength of many steels but is not a standard method for linepipe steels (Fig. 10). Studies have shown that the 0.5% extension under load method used for a lower grade might not be the best method to determine the yield point for grades greater than Grade 555 [3, 1]. API Specification 5L uses the 0.2% offset method for linepipe grades greater than Grade 625 (X90) (Fig. 10).

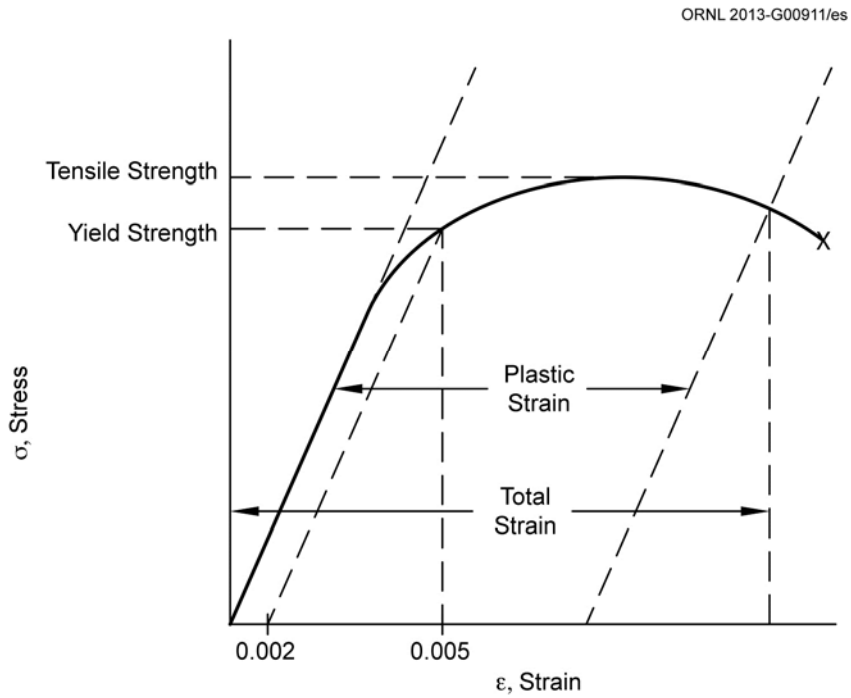

Fig. 10. Yield strength definitions.

Determination of the yield stress is sensitive to specimen preparation and measurement techniques. Tensile testing operations allow the test to be controlled in terms of stress rate (load control) or strain rate (displacement control). In the case where the operation is controlling the stress rate, the strain rate will increase as the specimen begins to yield and will continue to increase when the specimen no longer elongates uniformly (i.e., strain becomes localized along the gage length). In the case of high-strength, low work hardening materials, controlling the stress rate will produce very high strain rates beyond yield, which results in dynamic tensile strength elevation and a low Y/T ratio [21]. Therefore, tensile specimens for high-strength linepipe materials should be tested based on strain rate (displacement) control [21].

Although some codes specify a specific standard to be followed for small-scale testing, API Specification 5L permits the use of many specimen geometries including round bar, flattened strap, or ring expansion. Circumferential test specimens must be rectangular and represent the full wall thickness of the linepipe. Round bar test specimens are allowed for circumferential tensile tests with varying requirements for the gage diameter of the test specimens within the gage length. The gage diameter of test specimens is given as a function of pipe diameter and wall thickness in API Specification 5L. The ring expansion test is another method for determining the tensile strength of linepipe steel. In this test method, yield strength in the circumferential direction is determined using the relationship between internal pressure and circumferential expansion as the ring expands radially. Although the ring expansion test is allowed by API Specification 5L "if agreed," no testing specifications are given. A standard test method for performing ring expansion tests is presented in ASTM A370—*Standard Test Methods and Definitions for Mechanical Testing of Steel Products* or ISO 6892 *Metallic Materials—Tensile Testing*. For pipe grades above X70, the longitudinal tensile test requirements would be outside the scope of API Specification 5L. Table 7 (e) states:

> *For pipe requiring longitudinal testing, the maximum yield strength shall be ≤ 495 MPa (71, 800 psi).*

Requirements stated in API Specification 5L paragraph 10.2.3.2 follow.

> *Rectangular test pieces, representing the full wall thickness of the pipe, shall be taken in accordance with ISO 6892 or ASTM A 370 and … transverse test pieces shall be flattened.*
>
> *Longitudinal tensile tests of pipe with t ≥ 19.0 mm (0.748 in), such test pieces shall be 12.7 mm (0.500 in) in diameter.*

Round bar test specimens are allowed for transverse tensile tests with varying requirements for the diameter of the test specimens within the gage length depending on the wall thickness of the linepipe. Flattened straps are by far the most common and most economical when testing is done in production. API Specification 5L paragraph 10.2.3.2 states:

> *[T]ransverse test pieces shall either have a rectangular or round cross-section. Rectangular cross-section test pieces shall be from flattened samples, while round cross-section test shall be from non-flattened samples.*
>
> *Flattening of test pieces shall be carried out according to documented procedures.*

Alloys with a smaller Y/T ratio seem to produce a smaller Bauschinger effect [51]. For X80 linepipe steels, the Bauschinger effect increases as the deformation increases. When axial loading is applied, X80 steel has the characteristics of elastic, perfectly plastic within the range of 2.5% deformation and work-hardening characteristics exceeding 2.5% deformation [52].

Procedures for flattening vary widely and can have a significant effect on the measured yielding behavior. The final yield strength through the pipe wall after pipe forming can be different from the measured yield strength after flattened specimen preparation. Flattened strap samples will permit the full pipe wall thickness to be tested but the plastic deformation required to flatten the specimen will introduce reversed strain resulting in the potential for lower measured yield strength known as the Bauschinger effect. The Bauschinger effect, named after Johann Bauschinger, describes the phenomena where the yield strength decreases when the direction of the strain is changed and materials are strained into the nonlinear stress-strain area in one direction followed by straining in the opposite direction (Fig. 11). The effect of such cycling is that the reversed yield strength is decreased [53] and is more notable in the high strength pipe grades (i.e., greater than X70) [48]. For linepipe materials, work hardening is dominant on the inner surface of the pipe while the Bauschinger effect is dominant on the outer surface. The final yield strength is an interaction between work hardening and the Bauschinger effect. Because of this interaction, hoop yield strength for high-strength linepipe (specifically pipe grades X70 through X120) cannot be accurately measured using full thickness tensile test specimens because the curvature of the linepipe must be removed before testing. The flattening process alters the material's strength by introducing additional strain history [54].

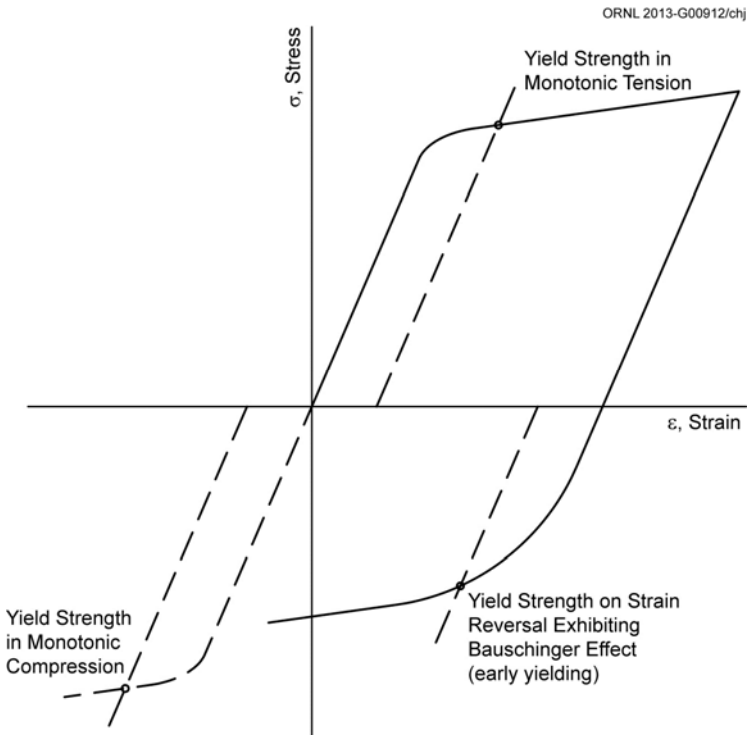

Fig. 11. The Bauschinger effect [53].

Machined round bar test specimens do not add a plastic deformation step inherent in flattening, but the entire cross-section cannot be tested. Round bar specimens have their own issues in preparation and testing because of pipe curvature, especially for small diameters, and thin wall linepipe. They also tend to be more expensive than flattened straps. A round bar specimen is exposed to the same strain history as that of the ring expansion specimen but has a reduced residual stress because of machining. The change in shape of the stress-strain curve and apparent modulus can be attributed to the removal of material. A small-sized round bar specimen measures a lower strength because of some fine-grained surface material being machined off during sample preparation [1]. Round bar specimens tend to be expensive and time consuming when used as a material and production qualification tool. Because of the setup restriction, the strain in the ring expansion test is limited to a maximum of 2%, thus limiting the stress-strain curve for a ring expansion test to stress associated with approximately 2% strain [55]. Ring expansion tests are usually restricted to 0.6% strain because of the limitations of the test specimen and equipment.

There is currently a joint industry project among material and pipe suppliers regarding tensile testing. Twenty-two companies are involved in a round robin study of material characterization of the various methods. However, in the past few years, the round bar specimen has been recommended for the transverse pipe axis tensile testing, and the strap specimen has been recommended for the longitudinal pipe axis testing [1]. Although research is under way to develop suitable alternatives, pressurized full-scale tension testing remains the only fully validated method to confirm tensile strain capacity. The goal is to confirm that the design meets the strain demand requirement when the key parameters are at the extremes of the acceptable construction envelope [56].

Total elongation at failure (i.e., the total extension of the specimen at plastic collapse) is the sum of both uniform and nonuniform elongation. Uniform elongation is the strain at the ultimate engineering stress. Uniform elongation is associated with uniaxial stress, whereas the nonuniform elongation occurs during

localized strain (i.e., necking) and is associated with triaxial stress. Uniform elongation is determined by evaluation based on a large strain. This material property will provide insight into the ability to undergo a large strain demand without discrete cross-sectional changes and while avoiding strain localization.

The nonuniform elongation is highly dependent on geometry, particularly the ratio of gage length to cross-sectional area. ASTM E8/E8M and ASTM A370 provide geometry dimensions for various specimen types. Both elongation and reduction of area are typically expressed as a percentage.

Uniform elongation, as well as the Y/T ratio, is a measure for the ductility of materials. Plastic deformation depends on the work hardening behavior of the steel. Higher strength material typically has lower uniform elongation. which means lower deformability before failure [28]. It is to be expected that the ductility is diminished in response to plastic straining during the forming process. Although both parameters are used to characterize the ductility, they do not respond uniformly to cold forming [1]. Also, the appearance of expressed Lüders plateaus leads to an increase in uniform elongation [1]. Experimental data show that the uniform elongation can be affected by both ultimate tensile strength and Y/T for materials with yield strength in the 56 to 70 ksi range. In general, the uniform elongation decreases as the Y/T and yield strength increase.

Requirements for the number of specimen tests are prescribed in ASME B31.4 [16] and B31.8 [15]. The minimum frequency for testing in ASME B31.8 is one per 50 lengths of pipe at random. Because tensile strain limits usually have much larger natural variations than stress limits, the lack of multiple tests under the same test condition makes it difficult to determine the natural variation [10].

3.3.2 Cyclic Fatigue Testing

Cyclic strains often affect the material's mechanical properties when a material is placed in service where displacement enters the plastic region. Under conditions of cyclic loading, pipelines can suffer the effects of ratcheting, which is the process of accumulating additional deformation because of a combination of static and cyclic loading [4]. The material properties can be vastly different from those obtained at the material qualification phase using monotonic, uniaxial testing. Evolution of the material property as a function of cyclic strain should be considered for SBD [9]. Large plastic deformation can impair the usefulness of the material by introducing residual stress that remains after unloading. Residual stresses can either increase (work hardening) or decrease (work softening) after unloading. Cyclic strain hardening/softening is the effect seen if a material is strained in one direction followed by unloading before the material is strained in the same direction once more. The effect of such cycling is that the yield stress is increased and the strain-hardening is decreased [53]. Improved understanding and analysis of permanent deflections, residual stress, and yielding during cyclic loading is made possible through a study of plastic deformation using cyclic fatigue testing.

High-cycle fatigue usually refers to fatigue when peak stresses are well below the yield strength of the material. However, low-cycle fatigue deals primarily with the effects of plastic deformation associated with SBD. Low-cycle fatigue discussed in many standards is typically below 10,000 load cycles [57]. Low-cycle fatigue in pipelines is normally understood to be less than 1000 with stress/strain ranges in the elastic-plastic region [53]. There are few methods for assessing tensile failure resistance of pipelines when the plastic strain exceeds 0.005 (0.5%). More validation trials are needed in the open literature to support the use of the existing methods assessing high axial strains (Fig. 12) [13]. Therefore, a well-defined, validated, and generally accepted procedure for assessing low-cycle fatigue in pipelines does not currently exist, especially when strains exceed 2%.

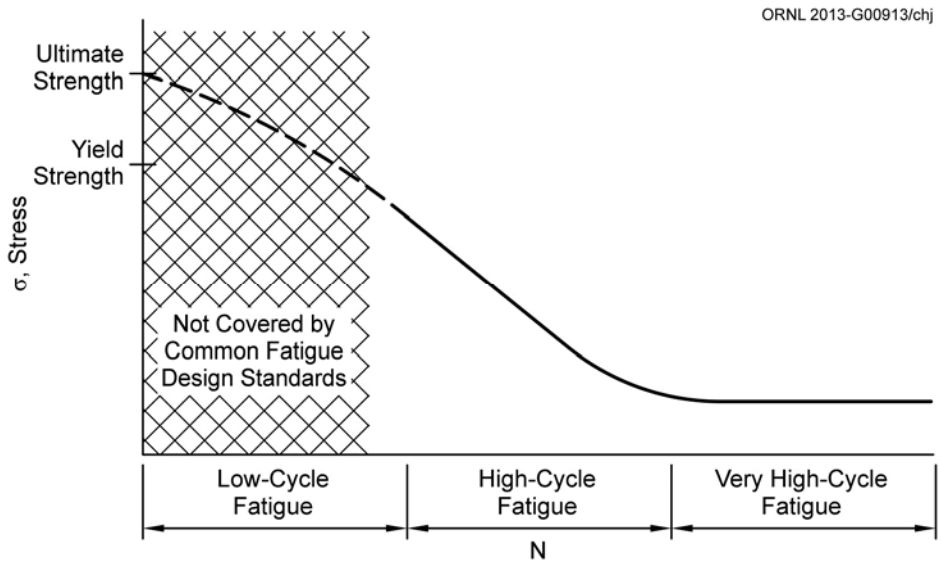

Fig. 12. Common S-N curve [57].

Ideally, fatigue tests are conducted on full-scale structural components under conditions that closely approximate the actual loading conditions. However, full-scale testing of large-diameter, high-strength linepipe is costly, time-consuming, and difficult to conduct. To predict the effects of fatigue behavior, the stress-life and strain-life approaches using smooth bar specimens under load-controlled or strain-controlled conditions are used. Data obtained from these tests can be used to evaluate the fatigue resistance of materials, plot stress vs the number of cycles to failure (S-N curves), quantify the cyclic yield strength, and determine strain-hardening.

It is useful to know and understand the fatigue life including fatigue crack initiation and growth to the point of fracture to predict failure. However, it is beneficial to quantify the cycles required to initiate a fatigue crack and propagate a crack from subcritical dimensions to a critical size that can be detected using post-construction inspection equipment. This is also an active area of research to detect smaller flaws to better determine fitness for service.

The ASME codes and standards caution that low-cycle, high-strain fatigue must be considered in the life-cycle design and construction assessment, including the determination of accumulated damage (ratcheting). To achieve the overall design safety objective, it is prudent to consider the use of a life-cycle engineering approach that includes operational controls, strain-based limit state design, site-specific design, construction mitigation, and operational monitoring and intervention [56]. A special laboratory test methodology described in the ASTM Standard E606/E606M—*Standard Test Method for Strain-Controlled Fatigue Testing* [58] has been developed for characterizing cyclic stress-strain behavior during low-cycle fatigue testing. Additional standards for fatigue testing include ASTM E466—*Conducting Force Controlled Constant Amplitude Axial Fatigue Tests for Metallic Materials* and ASTM E468—*Presentation of Constant Amplitude Fatigue Test Results for Metallic Materials*.

4. ANALYSIS AND LIFE PREDICTION

To predict the structural integrity and safety of a pipeline against ductile rupture caused by large plastic deformation it is necessary to know the magnitude of strain demand (applied strain) and strain capacity (strain limit) of two limit states: tensile rupture and compressive buckling. Tensile rupture is an ultimate limit state that is related to the breach of the pressure boundary. Compressive buckling could be either a service limit state resulting from excessive displacement or an ultimate limit state caused by the compressive limits of the material.

With the exception of offshore pipe reeling in which the strain demand is easily computed from the geometry of the lay vessel, determining strain demand can be a very complex undertaking. For onshore pipelines estimating strain demand involves multiple disciplines such as seismology, soil mechanics, as well as soil and pipe interaction. Strain demand could be a one-time event such as the strain at a fault crossing in a seismic event, but most often the strain demand can vary and/or accumulate over time (a time-dependent accumulative event) such as in the case of frost heave and differential settlement.

Several tensile strain capacity prediction models are available that are commonly based on a fracture mechanics approach to the welded joint [24]. Local discontinuities or welded joints can concentrate strain in a small area and cause the linepipe to experience tensile rupture below its intended design pressure. Due consideration must be given to both the ductility and capacity of the welded joints as well as the linepipe steels.

When forces or displacements are applied to a pipeline and cause the steel to exceed its elastic capacity, it is advantageous to distribute the plastic strain over a large area rather than localize the strain to a small area such as the pipe joint. When strain is distributed over a large area, a higher overall strain can be reached before any individual area exceeds its strain capacity. Strain hardening of plastically deformed steel will help to distribute the strains over a large area as the overall plastic strain increases [13]. Hence there is a need to develop prediction methods for bounding strain capacity based on the ductility and capacity of the linepipe steel.

4.1 STRESS-BASED ANALYSIS METHODS

Engineering stress analysis is based on the theory of elasticity and infinitesimal strain. It is fundamentally concerned with ensuring that the stress throughout the structure remains below the yield strength of the material and does not undergo permanent distortion. The stress-based analysis methods can be divided into two categories based on material properties: isotropic and anisotropic.

4.1.1 Isotropic Material Properties

Elastic, stress-based analysis for engineering materials that are isotropic and homogeneous requires only two elastic constants: Young's Modulus of Elasticity and Poisson's ratio. The compliance matrix for Hooke's law in three dimensions for an isotropic, linearly elastic material in compliance form can be written as follows:

$$\begin{bmatrix} \varepsilon_{xx} \\ \varepsilon_{yy} \\ \varepsilon_{zz} \\ \varepsilon_{yz} \\ \varepsilon_{zx} \\ \varepsilon_{xy} \end{bmatrix} = \frac{1}{E} \begin{bmatrix} 1 & -\upsilon & -\upsilon & 0 & 0 & 0 \\ -\upsilon & 1 & -\upsilon & 0 & 0 & 0 \\ -\upsilon & -\upsilon & 1 & 0 & 0 & 0 \\ 0 & 0 & 0 & 1+\upsilon & 0 & 0 \\ 0 & 0 & 0 & 0 & 1+\upsilon & 0 \\ 0 & 0 & 0 & 0 & 0 & 1+\upsilon \end{bmatrix} \begin{bmatrix} \sigma_{xx} \\ \sigma_{yy} \\ \sigma_{zz} \\ \sigma_{yz} \\ \sigma_{zx} \\ \sigma_{xy} \end{bmatrix}$$

These basic stress-strain relationships are used to derive formulas for thick walled, pressurized cylinders. Thick-wall cylinder formulas, known as the Lamé solution, date from 1833 and incorporate the theory of elasticity [55]. These formulas are based on an axisymmetric, elastic analysis approach to cylinders where nothing varies with the circumferential coordinate θ, and the circumferential, longitudinal, and radial stresses are all principal stresses. The cylinder stresses include (Fig. 13):

- Circumferential stress σ_θ—also referred to as hoop stress, acts perpendicular to both the longitudinal axis and radius of the pipe primarily because of internal pressure.

- Longitudinal stress σ_z—Stress along the axis of the pipe, generally caused by either capping the internal pressure on the pipe ends or pipe displacement.

- Radial stress σ_r—stress through the wall of the pipe generally cause by internal pressure and the Poisson effects of the circumferential and longitudinal stresses.

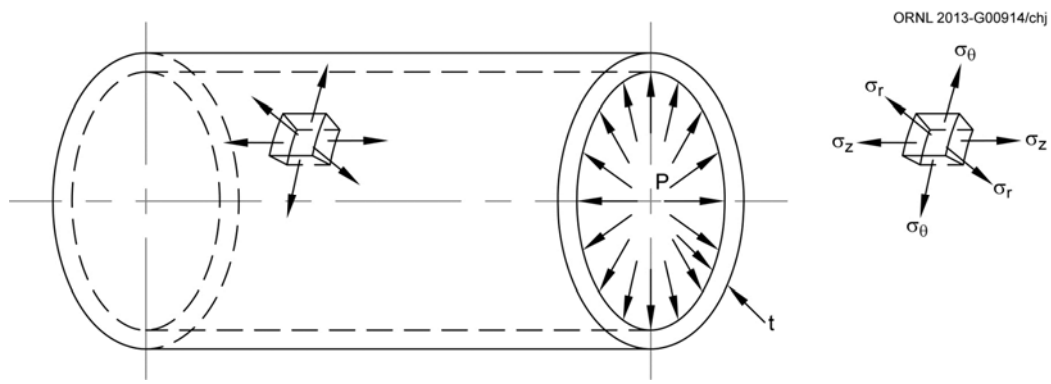

Fig. 13. Pipe element.

The basic cylinder equations assume the material to be homogeneous, isotropic, and linearly elastic and adequate only when displacements and strains are small. States of stress and strain are assumed not to vary along the length of the cylinder being analyzed. Several additional assumptions have to be made for the analysis:

- Local imperfections in geometry and material are ignored.

- The cross section of the pipe remains circular throughout the deformation process.

- Axial strain is idealized as a linear distribution through the pipe cross section.

- The volume of pipe steel is assumed to be constant at plastic deformation, which means pipe steel is incompressible when the plastic deformation dominates the elastic deformation [15].

A material is said to be in plane stress when one of the three principle stresses is zero. This is often considered to be the case for thin plates when the stress across the thickness of plate is very small in relation to the other two principle stresses. Pipelines are often assumed to be in a plane stress state since the pipe wall stress is small compared with the circumferential and longitudinal stress. The stresses are considered negligible with respect to the smaller dimension and compared with the in-plane stresses. For example, when a cylinder outer-diameter-to-wall-thickness ratio is equal to 10, the stresses between the inner and outer wall (D/t) will vary by less than 5%. This allows for a considerably simplified and often acceptable stress analysis. In the case of high strength, large diameter pipelines operating at high pressures, the D/t ratio may exceed 40, making the plane-stress assumption even more realistic. The ASME Boiler and Pressure Vessel Code, as well as piping codes, provide common rules that assume plane stress when D/t exceeds 10.

Barlow's formula for transverse stress for a cylinder is easily derived from static equilibrium equations and the free-body diagram of the cylinder half. The stress around the wall of the pipe must equal the internal pressure across the cross section. The transverse stress is determined by the internal pressure (p) of the fluid in a pipe of diameter, d, yielding transverse, or hoop stress:

$$\sigma_\theta = \frac{pr}{t} \ .$$

The same can be done for the longitudinal stress:

$$\sigma_z = \frac{pr}{2t} \ .$$

The preceding basic equations are incorporated in ASME B31.8 in a slightly modified fashion. The calculation for circumferential stress also accounts for other factors and can be rewritten in terms of stress:

$$\sigma_\theta = \frac{pd}{2t} FET \ ,$$

where:

F	=	design factor based on geographic location, number and proximity of buildings, and other characteristics involving human occupancy (ranging from 0.40 to 0.80)
E	=	longitudinal welding joint design factor (E = 1.00 for API Specification 5L pipe submerged-arc welded)
T	=	temperature derating factor (T = 1.00 for operating temperatures less than 250°F)

The longitudinal stress component caused by internal pressure only is incorporated into ASME B31.8 as:

$$\sigma_z = 0.5\sigma_\theta \ .$$

When a uniaxial force is applied to linepipe, it deforms in the direction of the applied force, but it also expands or contracts laterally. If the material is isotropic, homogeneous, and remains elastic, the lateral strain has a constant relationship to the axial strain. This constant, Poisson's ratio (ν), is an intrinsic

material property just like Young's Modulus. Poisson's ratio is used for the design of structures where all dimensional changes, stresses, and strains need to be taken into account and in the general application of elastic or elastic-plastic analysis. Poisson's ratio can be obtained during a tensile test from diametric measurements resulting from uniaxial stress-strain only. Most codes and standards generally consider Poisson's ratio to be approximately 0.3 for common linepipe steels. For isotropic material, directionality is not a consideration. Standardized test methods to determine Poisson's ratio from tension tests are specified in ASTM E132 *Standard Test Method for Poisson's Ratio at Room Temperature* [59]. Poisson's ratio can be difficult to accurately determine during testing. It is typically limited by the measurement accuracy of transverse strain. Poisson's ratio is defined as:

$$\nu = -\frac{transverse\ strain}{longitudinal\ strain} = -\frac{d\varepsilon_h}{d\varepsilon_l} \ .$$

Although Poisson's ratio may vary slightly within a certain isotropic, homogeneous material, it is usually considered small in relation to other uncertainties. The values might be close enough for a reasonably accurate answer but should be regarded as a ballpark figure. For restrained pipe, the longitudinal stress component resulting from internal pressure only would be a function of Poisson's ratio. From Hooke's Law:

$$\varepsilon_l = -\nu\varepsilon_h \ ,$$

and

$$\nu = -\frac{\varepsilon_l E}{\sigma_h} \ .$$

The calculation incorporated into ASME B31.8 assumes isotropic material with ν = 0.3 and is written as:

$$\sigma_z = 0.3\sigma_\theta \ .$$

To evaluate protection against failure, the results from an elastic stress analysis of the pipeline subject to defined loading conditions are compared to a limiting value. The equivalent stress at a point in a component is calculated from stress components using a yield failure criterion, which is compared with the mechanical strength properties of the material obtained in tests under uniaxial tension. The pipeline yield criterion in ASME B31.8 is based the assumption of ductile failure using the maximum distortion energy yield criterion. In this case, the equivalent stress is equal to the von Mises equivalent stress given by:

$$\sigma_{eq} = \sqrt{\frac{1}{2}[(\sigma_\theta - \sigma_z)^2 + (\sigma_z - \sigma_r)^2 + (\sigma_r - \sigma_\theta)^2]} \ .$$

Based on the limitations stated in ASME B31.8, the maximum permitted stress in the circumferential direction is 80% of SMYS. The maximum permitted stress in the longitudinal direction of unrestrained pipe is 75% of SMYS. For loads of "long duration," the maximum permitted equivalent stress limit is 90% of SMYS.

All popular failure criteria rely on data from small-scale testing, such as uniaxial tensile testing. Pipelines are typically subjected to multi-axial loading. Validation of actual failure involving full-scale testing typically requires extensive, complicated, and expensive methods. Failure is not only dependent on

strength but also on other factors such as stress concentrations and fatigue. Failure prediction for elastic analysis using the preceding failure theory should be considered only as an approximation.

4.1.2 Orthotropic Material Properties

Although the majority of stress-based analyses presented in codes and regulations are based on the assumption of isotropic material properties, this approach might be inappropriate for modern steels, particularly high-strength, microalloyed TMCP linepipe steels. These types of steel are sometimes anisotropic with the longitudinal, circumferential, and through-wall mechanical properties significantly dissimilar.

Fully anisotropic steel without any planes of symmetry requires 21 elastic constants. An orthotropic elastic material, such as high strength linepipe materials, has three orthogonal symmetry planes. These planes occur because of the rolling direction of the material and the forming direction of the pipe. Pipe formed perpendicular to the rolling direction with a single longitudinal seam requires only nine elastic constants for analysis comprised of three Young's moduli E_x, E_y, E_z, the three Poisson's ratios ν_{xy}, ν_{xz}, ν_{yz}, and the three shear moduli G_{xy}, G_{xz}, and G_{yz}. The compliance matrix in three dimensions for an orthotropic, linearly elastic material in compliance form can be written as follows:

$$\begin{bmatrix} \varepsilon_{xx} \\ \varepsilon_{yy} \\ \varepsilon_{zz} \\ \varepsilon_{yz} \\ \varepsilon_{zx} \\ \varepsilon_{xy} \end{bmatrix} = \begin{bmatrix} \frac{1}{E_x} & -\frac{\upsilon_{xy}}{E_y} & -\frac{\upsilon_{zx}}{E_z} & 0 & 0 & 0 \\ -\frac{\upsilon_{xy}}{E_x} & \frac{1}{E_y} & -\frac{\upsilon_{zy}}{E_z} & 0 & 0 & 0 \\ -\frac{\upsilon_{xz}}{E_x} & -\frac{\upsilon_{yz}}{E_y} & \frac{1}{E_z} & 0 & 0 & 0 \\ 0 & 0 & 0 & \frac{1}{2G_{yz}} & 0 & 0 \\ 0 & 0 & 0 & 0 & \frac{1}{2G_{ZX}} & 0 \\ 0 & 0 & 0 & 0 & 0 & \frac{1}{2G_{xy}} \end{bmatrix} \begin{bmatrix} \sigma_{xx} \\ \sigma_{yy} \\ \sigma_{zz} \\ \sigma_{yz} \\ \sigma_{zx} \\ \sigma_{xy} \end{bmatrix},$$

where:

E_i = Young's modulus along axis *i*.
G_{ij} = Shear modulus in direction j on the plane whose normal is in direction i.
υ_{ij} = Poisson's ratio that corresponds to a contraction in direction *j* when an extension is applied in direction *i*.

and:

$$\frac{\upsilon_{yz}}{E_y} = \frac{\upsilon_{zy}}{E_z}, \quad \frac{\upsilon_{zx}}{E_z} = \frac{\upsilon_{xz}}{E_x}, \frac{\upsilon_{xy}}{E_x} = \frac{\upsilon_{yx}}{E_y}.$$

An anisotropic elastic stress analysis method is typically not applied to pipelines for evaluating protection against plastic collapse. The ASME Boiler and Pressure Vessel Code, Section VIII Division 2 [60]

provides rules for an elastic stress analysis method where stresses are classified into categories and are limited to allowable values that have been conservatively established. These procedures provide an approximation of the protection against plastic collapse and warn that a more accurate estimate can be obtained using an elastic-plastic stress analysis to develop limit and plastic collapse loads. Because the elastic stress analysis method is only an approximation, the equivalent stress limit would require that it be established at a conservative limit.

4.2 STRAIN-BASED ANALYSIS METHODS

The mechanics of materials approach to stress-based analysis presented in most codes and regulations may be inappropriate to modern steels, especially for displacement-controlled loads resulting from ground displacement. When pipelines experience large strains and displacements, particularly in the plastic region, the material behavior is no longer linearly elastic and therefore stresses cannot be accurately anticipated. This problem is compounded when material properties vary in anisotropic materials. Full solutions for tensile strain limits related to these factors do not yet exist in codes and standards [19]. A limit-load analysis incorporating elastic-plastic stress analysis and equivalent strains is required providing a more accurate assessment of the protection against plastic collapse.

For high-strength linepipe steels, the plastic region of the stress-strain curve is typically very flat. In the high strain regime, small changes in strains produce almost no change in stress. From a practical viewpoint, it is unlikely that these large strain values can be repeated consistently given the required precision and repeatability of the stress-strain curves [9]. Although the full stress-strain curves were used in the tensile strain capacity model developments, the exact shape of the stress-strain curves was not the focus and has not been thoroughly investigated. Therefore, it could be useful to investigate not only the engineering stress-strain curve but also the true stress-true strain behavior.

Engineering stress is calculated based on the undeformed cross-sectional area. For small-scale yielding, this is generally accurate enough within the scatter of the material properties. However, for extensive yielding, the assumption of the cross-sectional area remaining relatively constant ceases to be accurate. As the strain becomes large and the cross-sectional area decreases, the true stress can be much larger than the engineering stress because of the reduction of cross-sectional area. True stress is calculated using the applied load to the instantaneous cross-sectional area. True stress is related to the engineering stress assuming constant specimen volume where A_0 and l_0 are the initial area and initial length, respectively.

$$A \cdot l = A_0 \,.\, l_0 \ .$$

Substituting for stress, the true stress (σ_T) is related to the engineering stress (σ_E) and engineering strain (ε_E).

$$\sigma_T = \frac{P}{A} = \frac{P}{A_0} \cdot \frac{l}{l_0} = \sigma_E(1 + \epsilon_E) \ .$$

True strain is the sum of all the instantaneous engineering strains.

$$d\epsilon = \frac{dl}{l} \ .$$

True strain (ε_T) can be related to the engineering strain by:

$$\epsilon_T = \int d\epsilon = \int_{l_0}^{l_f} \frac{dl}{l} = ln\ \frac{l_f}{l_0}\ .$$

$$\epsilon_T = ln\ \frac{l_f}{l_0} = ln\ \frac{l_0+\Delta l}{l_0} = ln\ (1+\epsilon_E)\ \ .$$

Strain capacity is established from the stress-strain curve of the linepipe steel typically obtained from the uniaxial tensile test. Therefore, the mathematical equations used to represent the stress-strain curves need to be designed to capture the actual shape of the curves in real materials. Since changes in microstructure can alter the S-N curve and TMCP material properties vary with direction, one mathematical equation representing a group of materials or all axes might be unable to uniquely determine the full stress-strain curve using material parameters such as yield strength, ultimate strength, and uniform elongation.

The Ramberg-Osgood equation was formulated to describe the nonlinear relationship to characterize the elastic and plastic portions of the stress-strain curve as early as 1943 [5]. Before yielding, the relationship takes the form of Hooke's law. Beyond yielding, the strain is the sum of both the elastic and plastic strain:

$$\varepsilon = \varepsilon_e + \varepsilon_p\ .$$

The Ramberg-Osgood equation for strain in simple form is:

$$\varepsilon = \frac{\sigma}{E} + K\left(\frac{\sigma}{E}\right)^n\ ,$$

where: $\varepsilon_e = \frac{\sigma}{E}$ and $\varepsilon_p = K\left(\frac{\sigma}{E}\right)^n$.

K and *n* are constants and will depend on the material being considered. The Ramberg-Osgood equation can be customized in many forms, including true stress and true strain using a 0.2% offset method for the determination of the yield stress [36]:

$$\varepsilon_T = \frac{\sigma_T}{E} + 0.002\left(\frac{\sigma_T}{\sigma_0}\right)^m\ ,$$

where *E, m,* and σ_0 are the Young's modulus, strain hardening exponent, and reference stress, respectively. By definition, the reference stress σ_0 is the true stress corresponding to a plastic strain of 0.2% and is usually very close to the yield strength at 0.5% strain. The engineering stress-strain curve calculated from the Ramberg-Osgood equation usually consists of a natural peak (i.e., ultimate tensile strength and uniform elongation). By calibrating σ_0 and *m,* the Ramberg-Osgood equation can generate a stress-strain curve for given yield strength and ultimate tensile strength. The uniform elongation, however, is an outcome of the equation and must be independently varied.

In contrast to the Ramberg-Osgood equation, the equation given in CSA Z662 [61] can more uniquely determine a full stress-strain curve that satisfies the yield strength, ultimate tensile strength (or Y/T), and uniform elongation. The CSA equation defines the relationship between the engineering stress and engineering strain where σ_y is the yield strength at 0.5% strain and *n* is the strain hardening exponent of the CSA equation.

$$\varepsilon = \frac{\sigma}{E} + \left(0.005 - \frac{\sigma_y}{E}\right)\left(\frac{\sigma}{\sigma_y}\right)^n\ .$$

A unique *n* can be determined by the following equation using yield, ultimate tensile strength, and uniform elongation property values [9]:

$$n = \ln\left(\frac{UEL - \frac{\sigma_T}{E}}{0.005 - \frac{\sigma_y}{E}}\right) / ln\left(\frac{1}{\frac{Y}{T}}\right) \ .$$

There are common mathematical descriptions of the work-hardening phenomenon. Hollomon's equation, proposed in 1949, is a power law relationship between stress and plastic strain:

$$\sigma = K\varepsilon_p^n \ .$$

The Hollomon equation does not consider the elastic portion of the curve, and the true stress-strain information is needed. Ludwik's equation introduced the yield stress:

$$\sigma = \sigma_y + K\varepsilon_p^n \ .$$

These equations typically are evaluated by the slope of the log(σ)/log(ε) plot:

$$n = \frac{dlog(\sigma)}{dlog(\varepsilon)} = \frac{\varepsilon}{\sigma}\frac{d\sigma}{d\varepsilon} \ .$$

Both hardening exponents in the Hollomon and the Ramberg-Osgood equations are the parameters that describe the capacity of the steel hardening and reflect the strain hardening situation beyond the yield of the material. These two parameters determine the largest stress and uniform strain of the material. If the material has a higher hardening capacity, the hardening exponent in the Ramberg-Osgood equation is low and the hardening exponent in the Holloman equation is high. The work hardening exponents can be obtained from their own stress-strain equation [62].

Both equations create smooth stress-strain curves (i.e., the round-house shape). The discontinuities in the actual stress-strain curve, such as the Lüders strain, are not reflected in these models. The Lüders strain of the pipe material is highly detrimental to the compressive strain capacity of the pipeline, and therefore its inclusion is usually prohibited in SBD. The Lüders strain, on the other hand, can increase the tensile strain capacity because of the lower crack driving forces generated. Therefore, the omission of the Lüders strain in pipe stress-strain curve is deemed to be acceptable to the tensile strain capacity model development [21].

Uniform elongation has been shown to correlate to the strain at which plastic collapse will occur in the pipe body under the combined loading of internal pressure and longitudinal strain. Assuming homogeneous isotropic pipe material, analysis indicates that plastic collapse is estimated to occur at approximately 2/3 UEL [9, 24]. It has been shown that the uniform elongation created by the Ramberg-Osgood equation is almost independent of the yield strength and only depends on the Y/T. Most importantly, the uniform elongation calculated from the Ramberg-Osgood equation can be significantly lower than the actual uniform elongation from an experimentally measured stress-strain curve of the same yield strength and ultimate tensile strength (or Y/T). It is especially true for low-yield strength pipe materials [9]. The following equation was developed to estimate the minimum uniform elongation based on the Ramberg-Osgood expression [31]:

$$UEL = 1.25\varepsilon_o \ ,$$

where:

$$\varepsilon_o = \frac{\sigma_T}{E} + \left[0.005 - \frac{\sigma_Y}{E}\right]\left[\frac{1}{Y/T}\right]^n \ .$$

$$n = \frac{3.14}{1 - Y/T} \ .$$

When loadings are nonproportional, such as pipelines under internal pressure and large longitudinal strains, a critical plane approach is needed [36]. While no standardized methodology has been developed for the pipeline industry, the ASME Boiler and Pressure Vessel Code, Section VIII, Division 2, provides an assessment procedure using the von Mises yield criterion. The material model assessment includes hardening or softening using true stress-strain curves up to the true ultimate stress. This approach could provide insight into an assessment procedure that can be used for the SBD of pipelines.

4.3 LOW-CYCLE FATIGUE ANALYSIS METHODS

Fatigue is typically not a consideration in an elastic stress analysis. ASME B31.8 paragraph 805.2.6 states:

> *Design life may not pertain to the life of a pipeline system because a properly maintained and protected pipeline system can provide service indefinitely.*

Ferrous materials, particularly ductile carbon steels, exhibit a limit below which fatigue failure does not occur under ordinary situations. Lower strength carbon steel linepipe of sufficient ductility with a maximum internal operating pressure of 72% SMYS are often considered to operate below the fatigue limit or endurance limit. Although research suggests that endurance limits might not actually exist, the projected number of loading cycles is extremely high. In addition, periodic inspections using state-of-the-art in-line inspection tools are expected to detect flaws and crack initiations long before they reach a critical size. SBD refers to pipelines that experience significant plastic deformation and could experience low-cycle fatigue in just hundreds of cycles.

Since strain capacity is established from the stress-strain curve, it is beneficial to accurately represent the stress-strain curve based on cyclic behavior. The Ramberg-Osgood equation can be modified to also represent the cyclic stress-strain curve. For all values of stress, elastic and plastic strain are summed to obtain total strain amplitude resulting in a smooth curve from uniaxial loading:

$$\varepsilon_a = \frac{\sigma_a}{E'} + \left(\frac{\sigma_a}{H'}\right)^{\frac{1}{n'}} \ .$$

The constants *E', H',* and *n'* in the cyclic stress-strain equations are for the plastic terms fitting the cyclic rather than the monotonic stress-strain data to account for cyclic hardening or softening (Fig. 14). Fitting is accomplished using the power law:

$$\sigma = H' \varepsilon_p^{n'} \ .$$

When the data are fitted to stress versus life and to plastic strain versus life, separate power law relationships for plastic (not total) strain and stress can be used:

$$\varepsilon_e = \frac{\sigma_a}{E'} = \frac{\sigma_f'}{E'}\left(2N_f\right)^b \ .$$

$$\varepsilon_p = \varepsilon_f'\left(2N_f\right)^c$$

These power law relationships lead to the desired strain-life curve:

$$\varepsilon_a = \frac{\sigma_f'}{E'}\left(2N_f\right)^b + \varepsilon_f'\left(2N_f\right)^c \ .$$

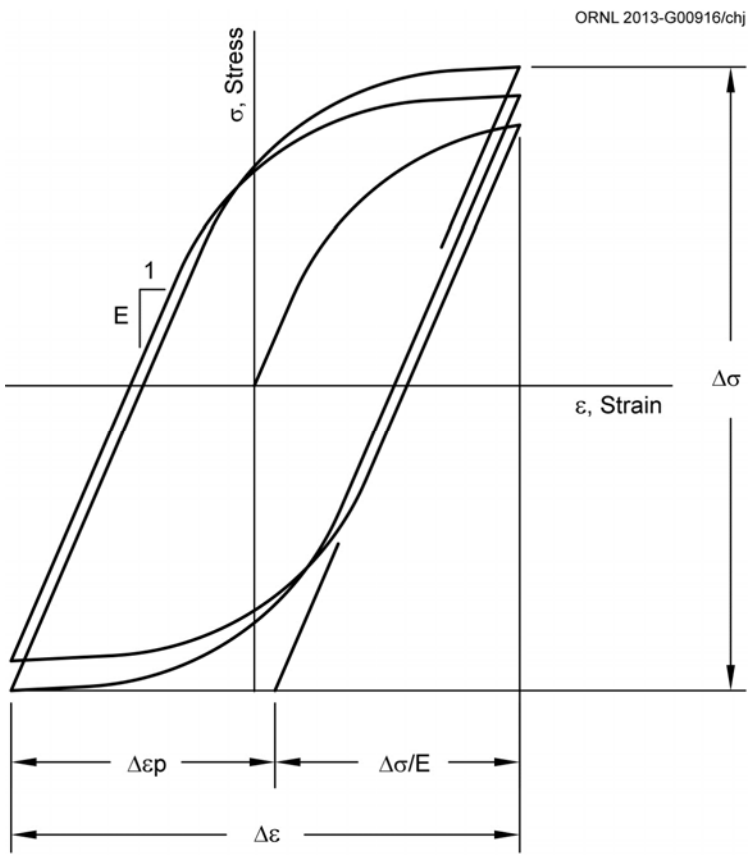

Fig. 14. Completely reversed cyclic loading hysteresis loop [36].

The stress or strain range is the difference between the minimum and maximum values. Half the range is referred to as the stress amplitude (σ_a), which is the variation about the mean (Fig. 15). When the mean is zero, the loading is said to be completely reversed. It is undoubtedly unreasonable to assume pipeline strain would be completed reversed. When the mean is non-zero, the cycle life can be affected because of a residual stress. The strain-life equations must be modified to a mean stress equation as follows:

$$\sigma_{ar} = f(\sigma_a, \sigma_m) \ .$$

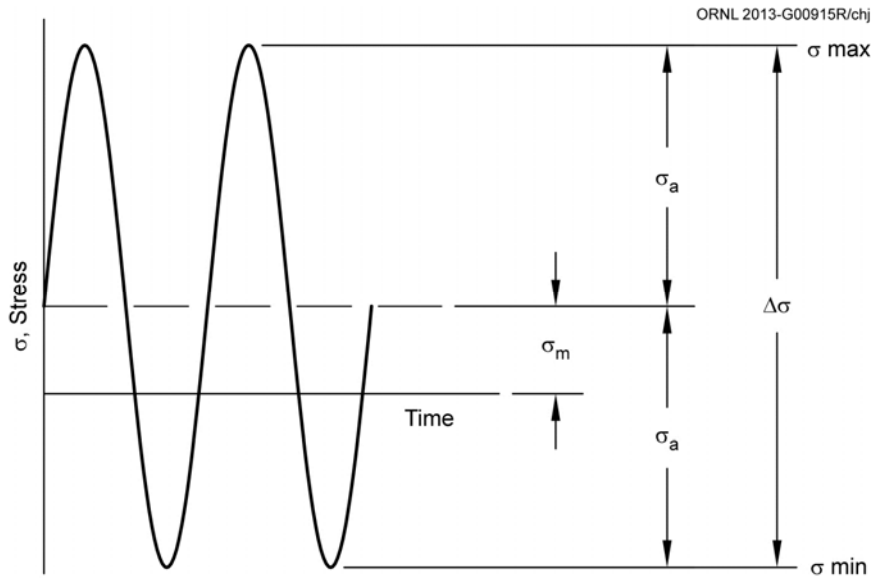

Fig. 15. Constant amplitude cyclic stress.

There are several approaches to account for the mean stress effects. An early fatigue life relationship was developed by J. O. Smith in 1942 based on an early proposal by Goodman [78]. The modified Goodman equation can be written as:

$$\frac{\sigma_a}{\sigma_{ar}} + \frac{\sigma_m}{\sigma_u} = 1 \ .$$

This relationship provides a straight-line fit, which is often called the Goodman diagram. The modified Goodman equation is highly inaccurate, often overly conservative, and should not be employed where life estimates are desired in fatigue analysis [36].

The Morrow equation uses the same form as the modified Goodman equation but is corrected to replace ultimate tensile strength with true fracture strength [79]. This equation is considered to be reasonably accurate for steels, but true fracture strengths are often unavailable and must be estimated. The modified Morrow equation can be written as:

$$\varepsilon_a = \frac{\sigma_f'}{E'}\left(1 - \frac{\sigma_m}{\sigma_f'}\right)\left(2N_f\right)^b + \varepsilon_f'\left(2N_f\right)^c \ .$$

The Smith, Watson, and Topper (SWT) parameter has the advantage of simplicity and does not rely on any material constant [77, 78]. The SWT strain-life equation provides good results in most cases and is somewhat more accurate than the Morrow equation, but it can be nonconservative for compressive mean stresses. The SWT equation can be written as [77]:

$$\sigma_{max}\varepsilon_a = \frac{\left(\sigma_f'\right)^2}{E'}\left(2N_f\right)^{2b} + \sigma_f'\varepsilon_f'\left(2N_f\right)^{b+c} \ .$$

The Walker equation gives superior results when data are available for fitting the adjustable parameter γ:

$$\gamma = -0.0002000\sigma_u + 0.8818\ (\sigma_u\ in\ MPa)\ .$$

For steels, this parameter can range between 0.4 to 0.8. If γ=0.5, the Walker and SWT equations yield the same result. The strain amplitude versus Walker-equivalent life curves can be written as:

$$\varepsilon_u = \frac{\sigma'_{fw}}{E'}(2N_w^*)^{b_w} + \varepsilon'_{fw}(2N_w^*)^{c_w}\ ,$$

where:

$$N_w^* = N_f\left(\frac{1-R}{2}\right)^{(1-\gamma)/b_w}\ .$$

When cyclic loading with plasticity is combined with a load-controlled loading in any direction, the result can be ratcheting. Ratcheting is the cycle-by-cycle increase of plastic strain. The increase in plastic strain is prominent in the direction of stress-controlled loading [13]. A completely displacement-controlled cycle that causes tensile and compressive plastic strain in the longitudinal direction of the pipe can cause ratcheting when it is combined with internal pressure. Ratcheting can occur on the circumferential strain, tending to expand the pipe under internal pressure. Increasing the longitudinal strain range will cause larger circumferential strains caused by pressure [13]. The longitudinal axis can also experience ratcheting extension or contraction when all or a significant fraction of the longitudinal loading is stress-controlled [13].

When multiple plastic cycles are applied, several methods are available for an assessment that sums the strains from each cycle to get an accumulated peak strain for assessment [13]. One method described in DNV-OS-F101 is the accumulated plastic strain approach, which defines the accumulated plastic strain as the sum of the plastic strain increments, irrespective of sign and direction [13]. The strain-life fatigue method combines the plastic strain increments into an estimate of the number of cycles that can be allowed [13]. These methods are based on limited data and might mean that these methods are conservative for many pipeline design situations to which they could be applied. Additional testing and analysis of cyclic behavior of pipelines are needed to improve the methods currently available [13].

Fatigue under multiaxial loading where plastic deformations occur is complex because of the rotation of the principle axes. An effective total equivalent stress amplitude and effective strain range can be used to evaluate fatigue damage. An elastic-plastic analysis can be performed based on cyclic curves obtained by material testing using a stabilized cyclic stress-strain curve or a specific cycle at a specified life under evaluation to obtain material properties. The ASME Boiler and Pressure Vessel Code, Section VIII, Division 2, provides an assessment procedure to evaluate protection against failure from cyclic loading using the effective stress and strain ranges. Other approaches have also been proposed for multi-axial stress effects using strain-life and stress-life curves. However, these approaches have not been adapted for the pipeline industry [36].

4.4 PROTECTION AGAINST FAILURE

Stress-strain diagrams clearly demonstrate that although the measured strains at the failure event can have large differences, the differences in the corresponding stresses at the same failure events are very small [25]. It should be noted that the strain range caused by the strength level variation is dominated by the shape of the stress-strain curve and the amount of the strength variation [25]. The most significant contributor to the tensile strain capacity variation and the difference between the measured and predicted tensile strain capacity is the strength variation in the specimens. From a practical viewpoint, it is unlikely that the large strain values produced in some of the tests can be repeated consistently given the required

precision and repeatability of the stress-strain curves. A relatively small variation of the pipe strength in the uniform strain zone can lead to a large variation of measured tensile strain capacity [9]. Therefore large tensile strain capacity variations are expected even under nominally identical conditions for high-strength, micro-alloyed linepipe steel with flat stress-strain curves [25].

The effect of the Y/T ratio and strain hardening on overall mechanical material and structural behavior is complex to assess because of several factors including the presence of Lüders plateau, fracture toughness, and the physical nature of strain hardening. The Y/T ratio merely addresses the singular point of uniaxial, monotonic stress-strain behavior. Historically, for material with low Y/T ratios, simplified equations and analysis were considered sufficient for assessing plastic deformation and providing a necessary margin of safety against ultimate failure. For pipe material with higher Y/T ratios, some of the safety margin against local failures has essentially been removed. This safety margin could be rebuilt by more extensive analysis of the local failure modes and the types of resistance available to prevent failures by those modes [13].

Some standards provide extensive guidance based on a FAD. This method uses a two-parameter technique to assess the possibility of plastic collapse and fracture separately (see Fig. 16). This approach leads to a need for fracture parameters to assess extensive plasticity. This approach can work reasonably well if material has strong strain hardening capacity, such as certain lower grade steels used in offshore applications. Modern high-strength linepipe steels (Grades X70 and above) typically exhibit low strain hardening [64]. When loadings are nonproportional, such as with pipelines, a critical plane approach is needed [36]. A methodology to evaluate fatigue damage, the effective strain range of longitudinal displacement, and circumferential stress effects from pressure to bound operating conditions is desired. The safety factor is expected to be within the range of 0.20-0.25 [64].

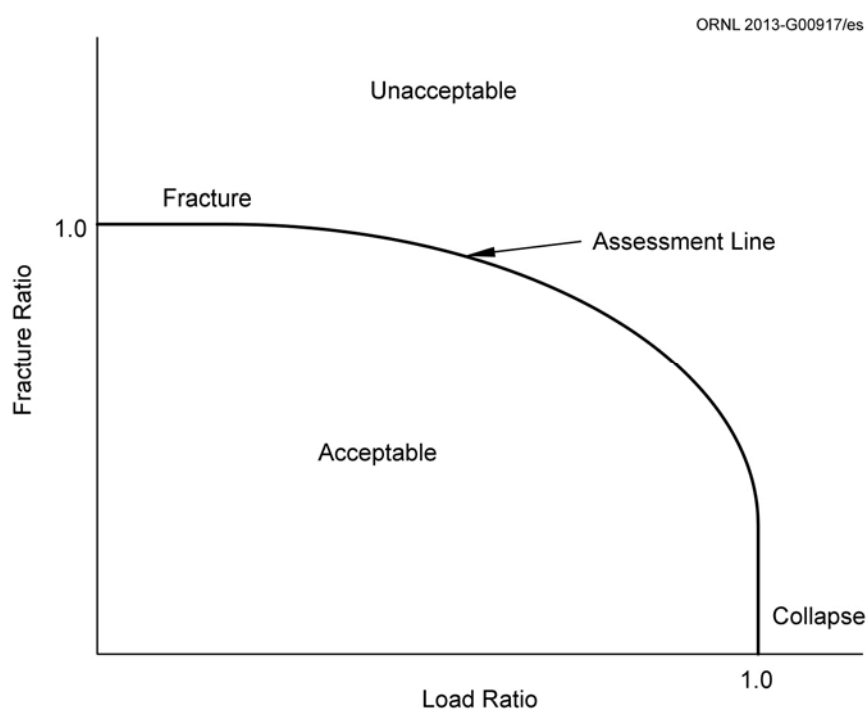

Fig. 16. Failure assessment diagram schematic.

5. PIPELINE DESIGN AND SAFETY ISSUES

Pipelines that undergo large longitudinal strain have been in service for many years. However, in the last 10 years, the design trend is evolving from a stress-based design approach to an SBD approach using high-strength linepipe. Existing federal pipeline safety regulations and national consensus codes for pipelines were not originally intended for high-strength linepipe, and very limited service experience exists. Consequently, current rules for stress-based design and high-strength linepipe steel are not sufficient to accurately predict mechanical properties, ensure safe operation, or predict a reliable service history. For instance, after years of service, structural integrity problems have been noted in petroleum and natural gas transmission pipelines in off-shore service because of the cyclic effects of waves and currents. The following discussions about material standards, design codes, construction practices, and regulatory compliance issues characterize some key problem areas that are not adequately addressed by stress-based design of pipelines constructed with high-strength linepipe.

5.1 DESIGN CODE AND MATERIAL STANDARD ISSUES

Specific prescriptive and performance requirements will likely be codified as additional research and operational histories become available because design codes and material standards are the primary vehicles for advancing the SBD approach and establishing acceptable consensus requirements. It is important to identify the key requirements for validating SBD, determine applicable standard practices, codify developmental efforts, and begin implementation of protocols for the industry. Codes, standards, and recommended practices provide criteria and recommended guidelines on concept development, design, construction, operation, maintenance, repair, and abandonment of equipment when invoked by applicable regulations or company specifications. They might also serve as a requirement or guideline between a purchaser and contractor. SBD is addressed in a number of design codes, but the codes do not give sufficient guidance in nonlinear structural analysis. Appropriate national, international, and consensus standards should be followed in conjunction with specific recommendations for SBD.

A challenge in estimating strain demand is accounting for potential error in analytical strain demand prediction methods. There are discrepancies between finite element analysis results, experiments, and operational histories. Because of the complexity and expense of full-scale testing and the limited data on small-scale testing of high-strength linepipe, it is difficult to estimate errors in analytical methods. There are many factors affecting strain capacity; therefore, it is unrealistic to experimentally determine optimum specifications of full-scale testing. It is essential to determine the parameters for the validation of strain capacity through small-scale testing.

As SBD methods are not yet fully mature, some problems still exist, such as lack of test results, field experience, and different definitions of yield strength for high-strength linepipe steel. Understanding the true material response is critically important for all SBD applications because the effects of low strain hardening, which has been observed for certain high-strength steels, can result in reduced service life.

5.2 LINEPIPE MATERIAL PROPERTY ISSUES

Although significant advances and theories have been developed over the past decade to support SBD, most of the previous work has relied on monotonic testing techniques. The studies published to this point have focused on stress or strain limits but have limited application to predicting service life or failure caused by cyclic behavior at these stress and strain limits. A unique opportunity currently exists for further exploration of high-strength linepipe material properties as manufacturers consider their use for near-term projects.

Considerable work remains to develop an SBD approach for pipelines that takes full advantage of the nonlinear behavior of linepipe steel because this behavior has far greater influence on the strain capacity than stress capacity. The long-term goal should be to achieve near-optimum designs that provide the best economy over the life time of the pipelines and at quantifiable reliability levels. Full stress-strain curves are needed for SBD. This is particularly true in light of the problem with differing yield strength definitions and the nonlinear shapes of stress-strain curves. For most pipelines, the design is governed by the pressure-induced transverse stress intensity produced by the maximum internal operating pressure. To ensure safe pipeline operation, the maximum allowable operating pressure (MAOP) for SBD should be determined using the actual material properties for the linepipe steel determined by tensile testing of representative material samples.

Deficiencies in the current state of knowledge that are preventing effective use of the SBD approach for pipeline applications have been identified. Some areas are the focus of current research, but many of the following potential problems still remain.

- Pipeline steels are often assumed to be isotropic. Previous studies assuming isotropic properties of the longitudinal direction might be nonconservative [65].

- Strain aging from the pipe coating process has been shown to increase pipe yield strength and even ultimate tensile strength. Its effect is thought to be larger in the transverse direction [10].

- The predictive models have no inherent safety factor [9].

- Numerical analysis in the last few years and more recent experimental work has shown that the longitudinal tensile strain capacity could be significantly reduced by transverse stress [10].

- There exists the possibility of failure from large tensile strain induced longitudinally in a pipe based on values expected to be acceptable from measured transverse properties only [13].

- The widely accepted assumption that the tensile and compressive strain capacities are affected only by the longitudinal tensile properties is not rigorously correct. Both transverse and longitudinal properties have impact on the strain capacity. This could be particularly true in the presence of transverse stress [10].

- There have not been sufficient data regarding biaxial stress from transverse stress caused by high design pressure and large longitudinal strain from large deformation [66].

- The definition of yield strength needs to be reviewed to accommodate high-strength linepipes [10].

- There is a need to develop prediction methods for bounding strain capacity [14].

Although the use of higher strength linepipe has economic advantages, it is essential to understand the material behaviors over the life cycle of a transmission pipeline. Establishing the technical basis for these compliance and performance issues and formulating appropriate regulatory requirements for ensuring pipeline safety requires an understanding of the root causes and contributing factors for these problems. SBD requires the consideration of more complex analytical approaches that maintain compliance resulting from lateral displacements without exceeding acceptable longitudinal strain limits. It requires the consideration of plastic deformations that are “non-recoverable” beyond the elastic limit, the interaction of the biaxial stress state and the potential for anisotropic effects on the linepipe steel. The advanced nature of the required analyses places a large burden on the correct interpretation and implementation of mechanical properties data. Because methods to predict strain capacity are still

relatively new technologies, there is a need to provide confidence in pipeline behavior with adequate design safety when the pipeline is subjected to significant lateral displacements. Significant experimental and analytical work remains to ensure uniformity of application within the industry while facilitating regulatory acceptance and compliance. Establishing the technical basis for strain-based performance issues and formulating appropriate regulatory requirements requires an understanding of the material behavior. Consequently, a comprehensive validation program of high-strength material properties is key to accomplishing this goal.

6. GRADE X80 LINEPIPE

The material samples supplied for this study met the requirements in API Specification 5L for Grade X80M PSL2 linepipe. The linepipe was fabricated using a three-roll bending process from plate that was thermomechanically rolled. After rolling, the single longitudinal seam was welded using a submerged-arc welding process (SAWL). Following welding, the linepipe was shipped by barge to a separate facility for mechanical expansion to the final dimensions. Final delivery conditions satisfied the rules in 49 C.F.R §192.112 (a)(3) and (4) for additional design requirements for steel pipe using alternative maximum allowable operating pressure and requirements for general standards including chemical composition.

The Grade X80M SAWL PSL2 linepipe that was supplied for this study was manufactured specifically to evaluate the effects of mechanical expansion of X80 pipe and not explicitly to evaluate SBD requirements. Consequently, the linepipe was received in two conditions; in the as-rolled condition before mechanical expansion and after mechanical expansion. As-received linepipe dimensions for each delivery condition are shown in Table 1. These dimensional data were not evaluated for compliance to any other specification.

Table 1. Pipe body dimensions

Delivery Condition	Pipe Dimensions	Maximum Outer Fiber Strain (%)	Cold Expansion (%)
As-Rolled	D = 47 5/8 in. t = 0.950 in.	2.03	--
Post-Expansion	D = 48 1/8 in. t = 0.933 in.	3.11	1.05

Tensile test data was provided by the pipe mill following mechanical expansion, but before shipment. Due to the nature of shipping and fabrication facility schedules, the time between linepipe fabrication and delivery was approximately18 months.

6.1 CHEMICAL ANALYSIS

The chemical composition of the post-expanded linepipe was determined at the Oak Ridge National Laboratory using Spectro Analytical Instrument Spectroport, Model #TPF7B02F. Results of the chemical analysis are shown in Table 2.

Additional requirements for steel pipe meeting the alternative maximum allowable operating pressure requirements that are referenced in 49 C.F.R §192.112 (a) include:

(1) *The plate, skelp, or coil used for the pipe must be micro-alloyed, fine grain, fully killed, continuously cast steel with calcium treatment.*

(2) *The carbon equivalents of the steel used for pipe must not exceed 0.25 percent by weight as calculated by the Ito-Bessyo formula (Pcm formula) or 0.43 percent by weight, as calculated by the International Institute of Welding (IIW) formula.*

Table 2. Chemical analysis results

Element*	Chemical analysis results for post-expanded linepipe (%)	Chemical analysis limits in API Specification 5L/ISO 3183 (2013) (max. %)
C	0.068	0.18
Si	0.20	0.45
Mn*	2.04	1.90
P	0.013	0.025
S	0.001	0.015
V**	0.004	
Nb**	0.037	Nb + V + Ti ≤ 0.15
Ti**	0.002	
Cu	0.25	0.50
Ni	0.27	1.00
Cr	0.008	0.50
Mo	0.22	0.50
CE_{IIW}	0.149	0.43
CE_{Pcm}	0.209	0.25

*Up to a maximum of 2.00% based on reductions below maximum C or as agreed.

**Nb + V + Ti = 0.037 + 0.004 + 0.002 = 0.043.

Based on these chemical analysis results, the material supplied for this study satisfies the chemical requirements for Grade X80M PSL2 linepipe prescribed in both 49 C.F.R §192 and API Specification 5L.

6.2 TENSILE PROPERTIES

Transverse and longitudinal rectangular tensile specimens and round bar transverse tensile specimens were machined from the Grade X80M PSL2 linepipe that was supplied for this study. Tensile test data reported by the pipe mill are shown in Table 3. Mechanical property requirements prescribed in API Specification 5L for Grade X80M PSL2 linepipe are shown in Table 4.

Table 3. Tensile test data acquired at the pipe mill

	Before Expansion				After Expansion			
	Yield Strength, psi (MPa)	Tensile Strength, psi (MPa)	Elongation, %	Y/T	Yield Strength psi (MPa)	Tensile Strength, psi (MPa)	Elongation, %	Y/T
Transverse Body	77,885	95,435	41.5	0.82	77,450	96,740	40.0	0.85
Longitudinal Body	78,175	92,534	41.0	0.84	76,579	93,694	40.0	0.82
Round Bar	78,289	96,450	26.0	0.79	86,877	97,900	24.5	0.89

Table 4. Mechanical property requirements prescribed in API Specification 5L for Grade X80M PSL2 linepipe

Yield Strength, Y (psi)		Tensile Strength, T (psi)		Ratio, Y/T	Elongation, %
Minimum	**Maximum**	**Minimum**	**Maximum**	**Maximum**	**Minimum**
80,500	102,300	90,600	119,700	0.93	13%

Comparison of yield strength values reported in Tables 3 and 4 reveals that the yield strength test results for the after expansion rectangular tensile specimens fell below the minimum API Specification 5L yield strength requirement of 80,000 psi. However, the yield strength test results for round bar tensile specimens after expansion exceed the minimum yield strength requirement of 80,000 psi and, therefore, satisfies this API Specification 5L requirement.

6.3 TEST SPECIMENS

In order to accurately assess the mechanical properties and establish design limits for Grade X80 linepipe, studies were conducted to compare the life-cycle effects of material processing and operational conditions. These studies included testing of specimens in the as-rolled, post-expansion, and post-expansion, strain-aged conditions. Conditioning of the post-expanded, strain-aged linepipe specimens was achieved by heating the pipe segments to 550°F for 30 minutes and then allowing the segments to air cool. This conditioning process simulated strain aging and thermal treatments corresponding to coating application.

The location and orientation of circumferential and longitudinal test specimens is shown in Fig. 17.

Key

1 – Circumferential sample, 90° from longitudinal weld joint

2 – Longitudinal sample, 90° from longitudinal weld joint

3 – Circumferential sample, 180° from longitudinal weld joint

4 – Longitudinal sample, 180° from longitudinal weld joint

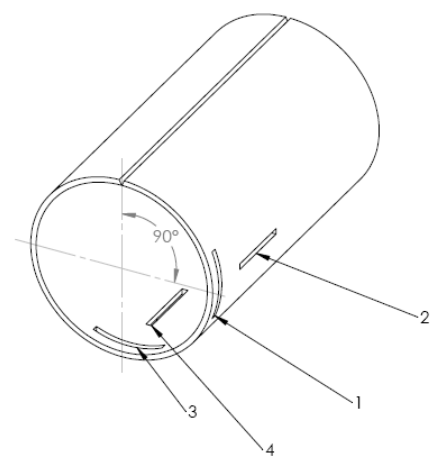

Fig. 17. Specimen locations and orientations.

After machining, each specimen was marked with “A”, “B”, “C”, or “D” to identify material condition and location as follows:

“A” – As-rolled, pre-expanded pipe 90° from longitudinal weld joint

“B” – Post-expanded pipe 90° from longitudinal weld joint

“C” – Strain-aged, post-expanded 90° from longitudinal weld joint

“D” – Strain-aged, post-expanded 180° from longitudinal weld joint

6.4 MICROSTRUCTURE

Approximately square samples were taken from all three material conditions to investigate the grain structure. The circumferential and longitudinal faces were ground, polished, and etched as shown in Fig. 18. Images of the grain structure were produced using a scanning electron microscope (SEM) for each of the four (4) pipe conditions labeled “A”, “B”, “C”, and “D” as described in Section 6.3. The SEM images are shown in Figs. 19-26.

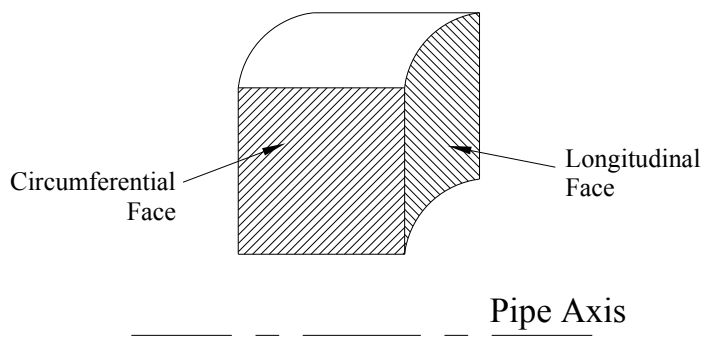

Fig. 18. Pipe Sample.

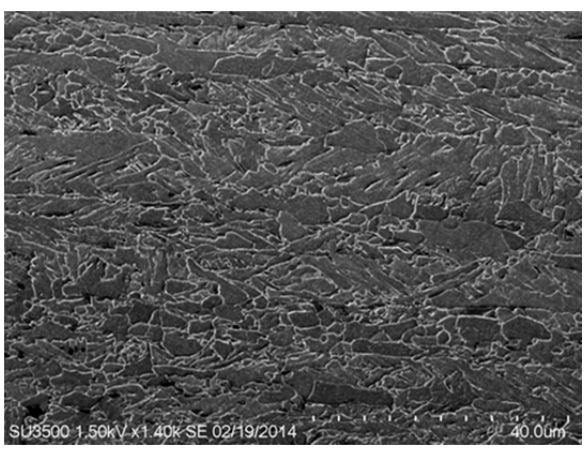

Fig. 19. Specimen A Circumferential.

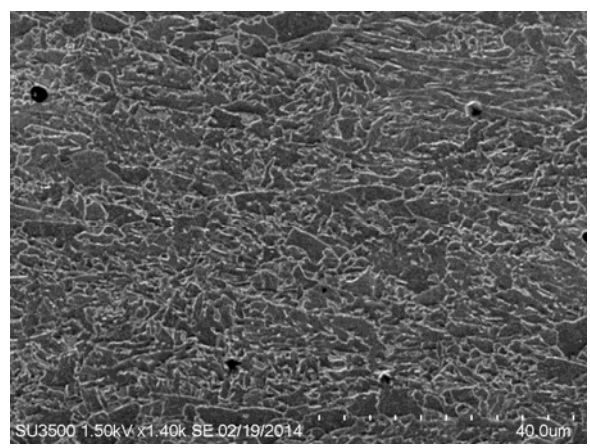

Fig. 20. Specimen A Longitudinal.

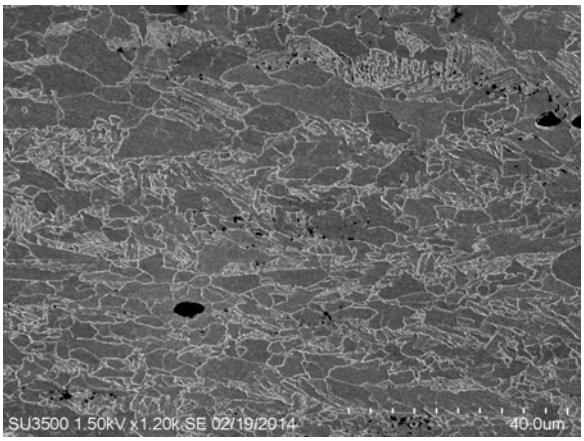

Fig. 21. Specimen B Circumferential.

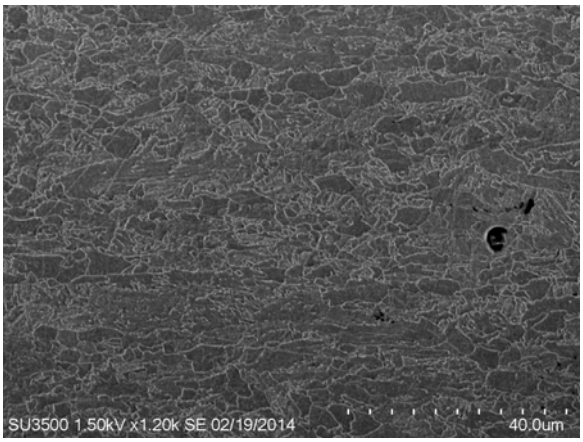

Fig. 22. Specimen B Longitudinal.

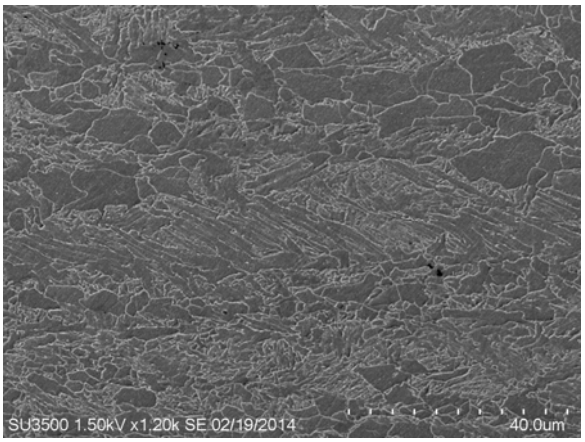

Fig. 23. Specimen C Circumferential.

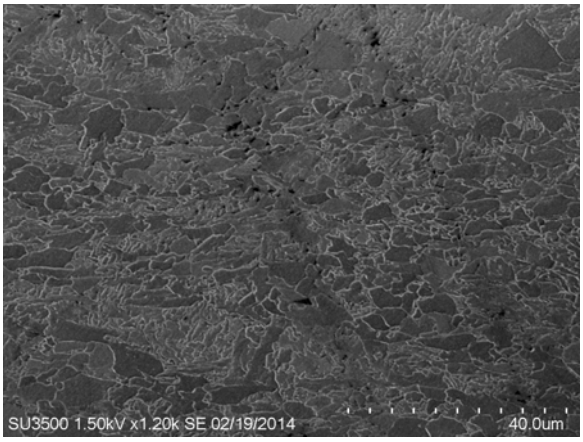

Fig. 24. Specimen C Longitudinal.

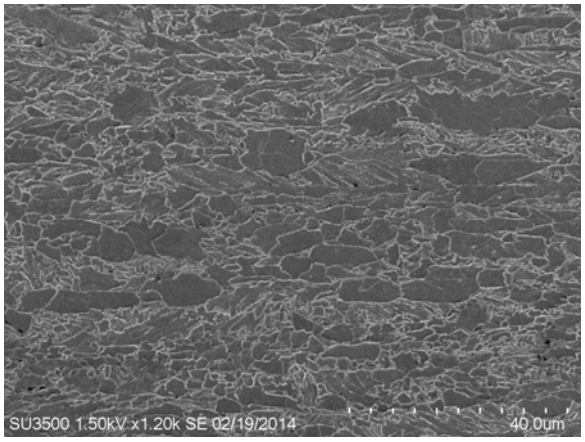

Fig. 25. Specimen D Circumferential.

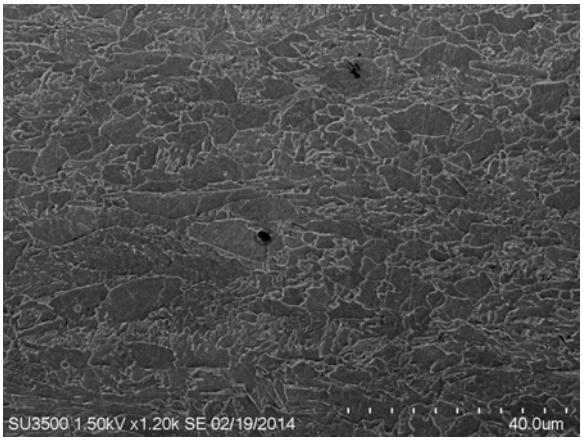

Fig. 26. Specimen D Longitudinal.

6.5 HARDNESS

Through-wall hardness variation was determined for all three material conditions using a Versitron Series Rockwell hardness testing machine. The hardness was measured along both the circumferential and longitudinal faces shown in Fig. 18. Rockwell hardness values varied from 10 to 19 HRC depending on the distance from the inner wall surface and the material condition as shown in Fig. 27. This range is well below the API Specification 5L lower limit of 35 HRC. No discernable patterns of through-wall hardness properties were noted.

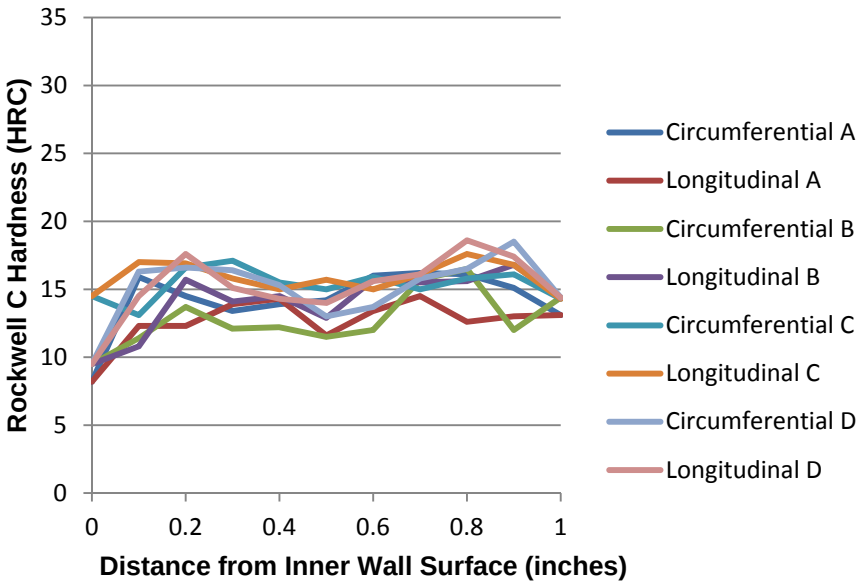

Fig. 27. Through-Wall Hardness.

7. MONOTONIC LINEPIPE MATERIAL PROPERTIES AND BEHAVIOR

Implementation of the elastic-plastic analysis and assessment method described in Sect. 9 requires an understanding of monotonic properties and behavior of Grade X80 linepipe steel. In an effort to develop the knowledge base needed to assess the effectiveness of this method, tensile testing of representative linepipe steel samples were conducted in the laboratory using servo-controlled hydraulic testing equipment and automated instrumentation suitable for loading, measuring, and acquiring stress-strain data. The key objective of these laboratory tests was to produce material properties for Grade X80 linepipe steel in the as-rolled, expanded, and expanded and aged conditions.

7.1 TEST SPECIMEN SELECTION CONSIDERATIONS AND ANALYSIS

Round bar specimens with a uniform cross section and rectangular full-thickness specimens were chosen as representative test samples based on the following considerations.

- testing equipment capacity
- specimen size limitations
- gripping constraints
- material strength
- laboratory accessibility
- economic factors

Round tensile test specimens met the requirements of ASTM E8/E8M-13a for small-size specimens with a gage length of five times the diameter. Rectangular tensile test specimens met the requirements of ASTM E8/E8M-13a for standard plate-type specimens with a full wall thickness. The number of specimens, sample location, and gage length do not necessarily comply with any other code requirements. Flattening of test specimens was not permitted. Pipe curvature over the gage length of the longitudinal specimens was maintained. However, due to the loads required for the longitudinal flat tensile specimens, the pipe curvature over the grip length was removed. Based on the API Specification 5L requirement of 13% minimum test elongation, ring expansion tests could not produce completed stress-strain curves and therefore were not conducted.

The general test requirements were intended to yield tensile properties for the material including measured stress-strain curves. The specimens were labeled “A”, “B”, “C”, and “D” as described in Section 6.3. The specified minimum yield strength (SMYS) was defined by using the 0.5 extension under load (EUL) method. Tests were conducted at room temperature (≈75°F) in accordance with testing requirements in ASTM A 370-09a and ASTM E8/E8M-13a.Round bar and rectangular full-thickness specimens were prepared from the wall of large diameter X80 rolled linepipe. The general pipe wall specimen configuration is shown in Fig. 28. The round bar specimens were machined and ground while the rectangular specimens were cut directly from the pipe wall using waterjet cutting technology.

The tensile test results were intended to provide tensile properties and stress-strain curves for comparison to cyclic material properties and analysis. Engineering and true stress-strain curves were generated and true stress-strain material constants were determined after testing.

- The strength coefficient, H, and strain hardening coefficient, n, was determined using a power law fit based on the true stress versus true plastic strain curve. The slope of the plastic strain curve is the strain hardening exponent and the strength coefficient is the intercept when the plastic strain is equal to 1.

$$\bar{\sigma} = H\bar{\varepsilon}_p^n$$

- True fracture strength is obtained from the load at fracture and the final area. The major and minor axis was measured using an optical comparator.

$$\bar{\sigma}_f = \frac{P_f}{A_f}$$

- True fracture strain was obtained as a ratio of the initial and final area.

$$\bar{\varepsilon}_f = ln\frac{A_i}{A_f}$$

Fig. 28. Tensile specimens.

7.2 CIRCUMFERENTIAL TENSILE TESTING

Round bar tensile testing followed the general practices set forth in ASTM E 8/E 8M-08. The tests consisted of 3 specimens of the same configuration and material condition as described in Sect. 6.3. The specimens had a 0.250" diameter within the 1.5" gage length. All circumferential tensile tests were conducted at a strain rate of 0.090 inches per minute.

A summary of circumferential round bar tensile properties is shown in Tables 5 through 8. The strain hardening exponent values reported in these tables were calculated based on the true stress-strain data; the strength coefficient, H, was computed based on true strain at ε_p=1; and the true fracture strength and true fracture strain were determined using post mortem measurements of specimens. The engineering and true stress-strain curves are shown in Figs. 29 and 30 with a detailed view of the 0.5% EUL and 0.2% offset yield point determination shown in Fig. 31. Fracture surface pictures of the tensile specimens are shown in Figs. 32 through 35.

Table 5. Summary of Circumferential Round Bar Tensile Properties, As-Rolled
(* Necking occurred outside limits of clip gage)

Specimen	ENGINEERING							TRUE			
	Yield Strength (0.2% off-set) (ksi)	Yield Strength (0.5% EUL) (ksi)	Ultimate Strength (ksi)	Y/T	Elastic Modulus (Msi)	UEL (%)	Maximum Test Elongation (%)	True Fracture Strength (ksi)	Strength Coefficient (ksi)	True Fracture Strain	Strain Hardening Exponent
A-Circ-01	75.69	77.95	96.77	0.81	31.14	8.70	21.06	217.06	85.29	1.513	0.100
A-Circ-02*	76.44	78.54	97.61	0.80	32.00	9.42	13.50	221.95	85.67	1.510	0.100
A-Circ-03	78.42	80.30	98.57	0.81	31.39	7.69	17.47	227.94	87.37	1.543	0.098
Average	76.85	78.93	97.65	0.81	31.51	8.60	17.34	222.32	86.11	1.522	0.099
Standard Deviation	1.410	1.223	0.901	0.006	0.440	0.869	3.782	5.449	1.103	0.018	0.001

Table 6. Summary of Circumferential Round Bar Tensile Properties, Expanded

Specimen	ENGINEERING							TRUE			
	Yield Strength (0.2% off-set) (ksi)	Yield Strength (0.5% EUL) (ksi)	Ultimate Strength (ksi)	Y/T	Elastic Modulus (Msi)	UEL (%)	Maximum Test Elongation (%)	True Fracture Strength (ksi)	Strength Coefficient (ksi)	True Fracture Strain	Strain Hardening Exponent
B-Circ-01	94.94	94.95	99.72	0.95	32.01	7.17	20.57	216.45	92.10	1.548	0.077
B-Circ-02	95.91	95.92	98.75	0.97	32.14	6.47	18.81	222.81	91.55	1.563	0.076
B-Circ-03	93.48	93.48	98.84	0.95	31.68	7.07	20.43	216.23	91.11	1.539	0.078
Average	94.78	94.78	99.10	0.96	31.94	6.90	19.94	218.50	91.59	1.550	0.077
Standard Deviation	1.223	1.229	0.536	0.013	0.237	0.379	0.978	3.737	0.493	0.012	0.001

Table 7. Summary of Circumferential Round Bar Tensile Properties, Expanded and Strain-Aged, 90° from Weld Seam

Specimen	ENGINEERING							TRUE			
	Yield Strength (0.2% off-set) (ksi)	Yield Strength (0.5% EUL) (ksi)	Ultimate Strength (ksi)	Y/T	Elastic Modulus (Msi)	UEL (%)	Maximum Test Elongation (%)	True Fracture Strength (ksi)	Strength Coefficient (ksi)	True Fracture Strain	Strain Hardening Exponent
C-Circ-01	94.26	94.23	98.70	0.95	32.93	8.38	21.67	227.25	87.25	1.543	0.090
C-Circ-02	95.02	94.90	100.55	0.94	32.52	6.95	19.22	211.16	89.79	1.467	0.085
C-Circ-03	92.86	91.87	97.73	0.94	32.68	6.79	19.50	197.98	88.79	1.449	0.082
Average	94.05	93.67	98.99	0.95	32.71	7.37	20.13	212.13	88.61	1.486	0.086
Standard Deviation	1.096	1.592	1.433	0.008	0.207	0.875	1.341	14.659	1.283	0.050	0.004

Table 8. Summary of Circumferential Round Bar Tensile Properties, Expanded and Strain-Aged, 180° from Weld Seam

Specimen	ENGINEERING							TRUE			
	Yield Strength (0.2% off-set) (ksi)	Yield Strength (0.5% EUL) (ksi)	Ultimate Strength (ksi)	Y/T	Elastic Modulus (Msi)	UEL (%)	Maximum Test Elongation (%)	True Fracture Strength (ksi)	Strength Coefficient (ksi)	True Fracture Strain	Strain Hardening Exponent
D-Circ-01	94.81	94.81	102.47	0.93	32.61	8.76	21.02	227.57	88.06	1.545	0.097
D-Circ-02	95.32	95.28	103.13	0.92	32.68	8.44	22.18	210.47	88.73	1.476	0.094
D-Circ-03	94.86	94.86	102.66	0.92	32.71	9.71	23.18	220.87	88.32	1.535	0.096
Average	95.00	94.98	102.75	0.92	32.67	8.97	22.13	219.64	88.37	1.519	0.095
Standard Deviation	0.281	0.258	0.340	0.001	0.051	0.661	1.081	8.616	0.339	0.037	0.001

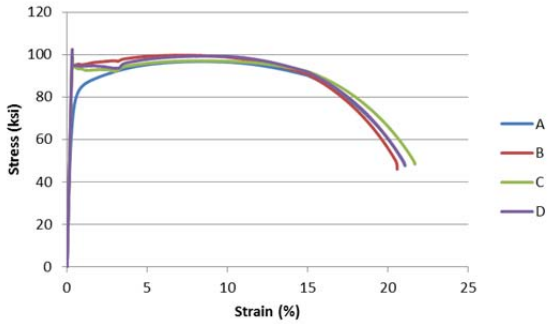

Fig. 29. Engineering stress strain curves for circumferential tensile specimens.

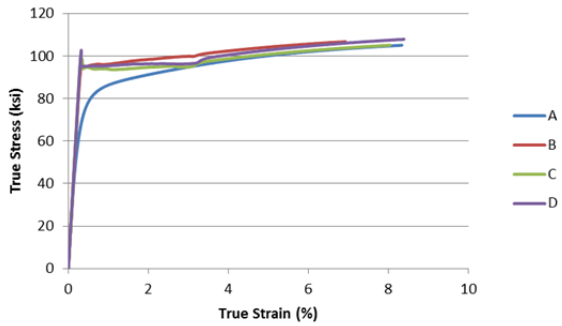

Fig. 30. True stress strain curves for circumferential tensile specimens.

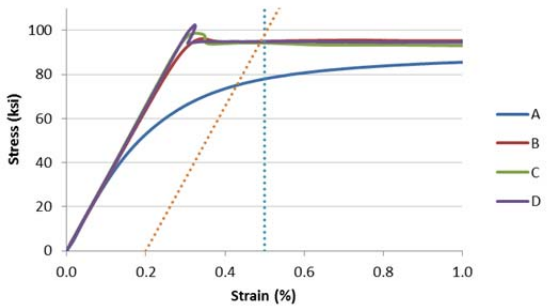

Fig. 31. 0.5% EUL and 0.2% Offset yield points for circumferential tensile specimens.

Fig. 32. Fracture surface for as-rolled circumferential tensile test specimen.

Fig. 33. Fracture surface for expanded circumferential tensile test specimen.

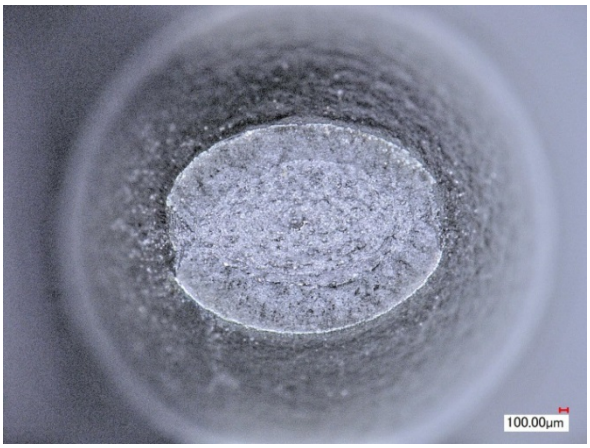

Fig. 34. Fracture surface for expanded and strain-aged circumferential tensile test specimen 90° from weld seam.

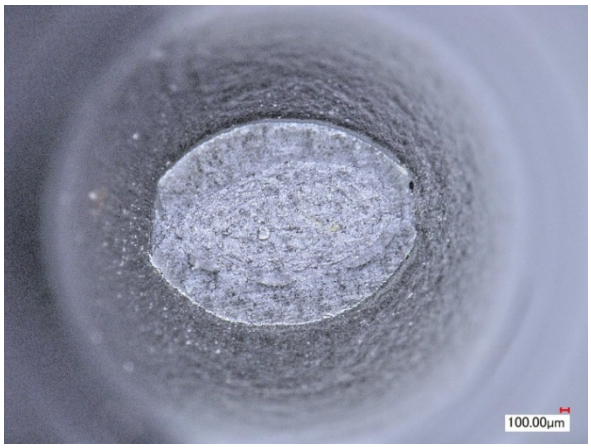

Fig. 35. Fracture surface for expanded and strain-aged circumferential tensile test specimen 180° from weld seam.

7.3 LONGITUDINAL TENSILE TESTING

7.3.1 Round Bar Tensile Test Specimens

Round bar tensile testing followed the general practices set forth in ASTM E 8/E 8M-08. The tests consisted of 3 specimens of the same configuration and material condition as described in Sect. 6.3. The specimens had a 0.250” diameter within the 1.5” gage length. All circumferential tensile tests were conducted at a strain rate of 0.090 inches per minute.

A summary of round bar tensile properties is shown in Tables 9 through 12. The engineering and true stress-strain curves are shown in Figs. 36 and 37 with a detailed view of the 0.5% EUL and 0.2% offset yield point determination shown in Fig. 38. Fracture surface pictures of the tensile specimens are shown in Figs. 39 through 42.

7.3.2 Rectangular Tensile Specimens

Full wall thickness rectangular tensile specimens were also tested following the general practices set forth in ASTM E 8/E 8M-08. The tests consisted of 3 specimens of the same configuration for each material condition.

The full wall specimens had a width of 1 ½ in. and a minimum gage length of 2 ¼ in. The specimens were cut using waterjet technology in an effort to not flatten the specimens. Due to the material strength, specimens were tested on a 200 kip test machine. Original specimens, with a grip length of 3 in. could not be held sufficiently to conduct the tests. Subsequent specimens were cut with a grip length of 6 in. and machined flat over the grip length (see Fig. 28). For these specimens, the curved pipe diameter was retained over the gage length.

Table 9. Summary of Longitudinal Round Bar Tensile Properties, As-Rolled

Specimen	ENGINEERING							TRUE			
	Yield Strength (0.2% off-set) (ksi)	Yield Strength (0.5% EUL) (ksi)	Ultimate Strength (ksi)	Y/T	Elastic Modulus (Msi)	UEL (%)	Maximum Test Elongation (%)	True Fracture Strength (ksi)	Strength Coefficient (ksi)	True Fracture Strain	Strain Hardening Exponent
A-Axial-01	78.05	78.37	94.27	0.83	29.49	9.16	21.00	219.15	80.65	1.552	0.113
A-Axial-02	76.41	77.05	92.98	0.83	31.22	10.71	24.07	238.67	79.11	1.656	0.114
A-Axial-03	77.11	77.65	93.57	0.83	29.92	9.29	22.15	207.35	81.00	1.527	0.107
Average	77.19	77.69	93.61	0.83	30.21	9.72	22.41	221.72	80.25	1.578	0.111
Standard Deviation	0.823	0.661	0.646	0.001	0.900	0.860	1.551	15.818	1.007	0.068	0.004

Table 10. Summary of Longitudinal Round Bar Tensile Properties, Expanded

Specimen	ENGINEERING							TRUE			
	Yield Strength (0.2% off-set) (ksi)	Yield Strength (0.5% EUL) (ksi)	Ultimate Strength (ksi)	Y/T	Elastic Modulus (Msi)	UEL (%)	Maximum Test Elongation (%)	True Fracture Strength (ksi)	Strength Coefficient (ksi)	True Fracture Strain	Strain Hardening Exponent
B-Axial-01	78.84	79.49	92.46	0.86	29.21	9.08	22.63	225.97	83.16	1.578	0.088
B-Axial-02	80.97	82.30	96.53	0.85	28.73	6.82	21.16	235.46	90.41	1.704	0.069
B-Axial-03	78.33	79.83	93.79	0.85	29.30	7.38	20.51	221.85	85.73	1.627	0.082
Average	79.38	80.54	94.26	0.85	29.08	7.76	21.43	227.76	86.43	1.636	0.080
Standard Deviation	1.400	1.534	2.075	0.005	0.309	1.177	1.086	6.979	3.677	0.063	0.010

Table 11. Summary of Longitudinal Round Bar Tensile Properties, Expanded and Strain-Aged, 90° from weld seam

Specimen	ENGINEERING							TRUE			
	Yield Strength (0.2% off-set) (ksi)	Yield Strength (0.5% EUL) (ksi)	Ultimate Strength (ksi)	Y/T	Elastic Modulus (Msi)	UEL (%)	Maximum Test Elongation (%)	True Fracture Strength (ksi)	Strength Coefficient (ksi)	True Fracture Strain	Strain Hardening Exponent
C-Axial-01	83.36	88.22	95.46	0.92	29.01	8.37	22.86	225.61	84.66	1.620	0.097
C-Axial-02	82.74	82.85	94.39	0.88	29.07	8.39	22.26	224.87	84.02	1.627	0.094
C-Axial-03	85.11	85.13	93.47	0.91	30.26	8.72	21.79	215.43	81.52	1.557	0.105
Average	83.74	85.40	94.44	0.90	29.45	8.49	22.30	221.97	83.40	1.601	0.099
Standard Deviation	1.229	2.695	0.996	0.024	0.704	0.197	0.536	5.676	1.662	0.038	0.005

Table 12. Summary of Longitudinal Round Bar Tensile Properties, Expanded and Strain-Aged, 180° from weld seam

Specimen	ENGINEERING							TRUE			
	Yield Strength (0.2% off-set) (ksi)	Yield Strength (0.5% EUL) (ksi)	Ultimate Strength (ksi)	Y/T	Elastic Modulus (Msi)	UEL (%)	Maximum Test Elongation (%)	True Fracture Strength (ksi)	Strength Coefficient (ksi)	True Fracture Strain	Strain Hardening Exponent
D-Axial-01	85.55	85.57	94.98	0.90	29.85	9.50	23.17	219.54	81.94	1.576	0.109
D-Axial-02	85.63	85.64	95.33	0.90	30.08	9.56	22.52	218.81	82.44	1.566	0.108
D-Axial-03	85.88	85.91	95.77	0.90	29.80	8.97	20.96	211.20	83.10	1.486	0.107
Average	85.69	85.71	95.36	0.90	29.91	9.34	22.22	216.52	82.49	1.543	0.108
Standard Deviation	0.172	0.180	0.396	0.002	0.149	0.325	1.136	4.619	0.582	0.049	0.001

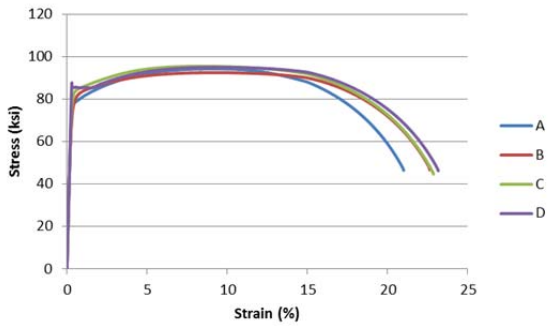

Fig. 36. Engineering stress strain curves for longitudinal round bar tensile specimens.

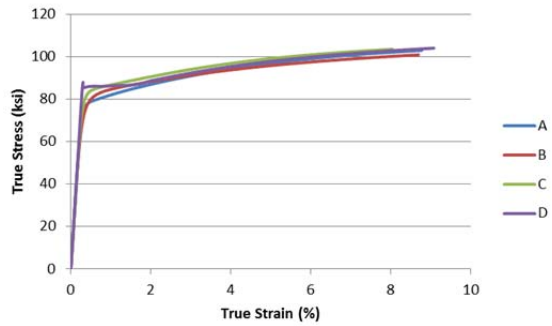

Fig. 37. True stress strain curves for longitudinal round bar tensile specimens.

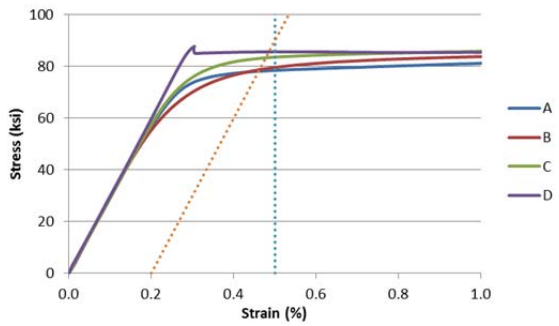

Fig. 38. 0.5% EUL and 0.2% Offset yield points for longitudinal round bar tensile specimens.

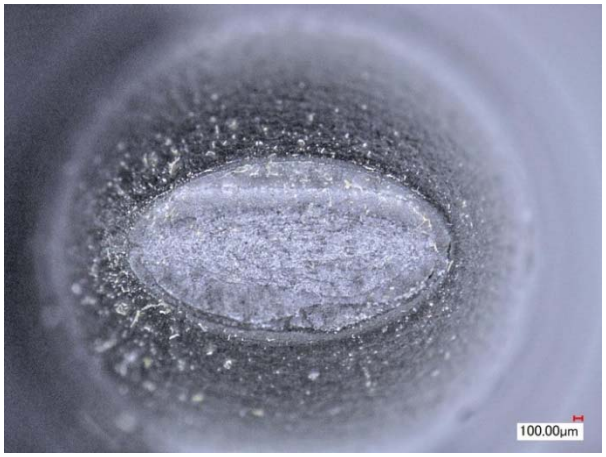

Fig. 39. Fracture surface for as-rolled longitudinal tensile test specimen.

Fig. 40. Fracture surface for expanded longitudinal tensile test specimen.

Fig. 41. Fracture surface for expanded and strain-aged longitudinal tensile test specimen 90° from weld seam.

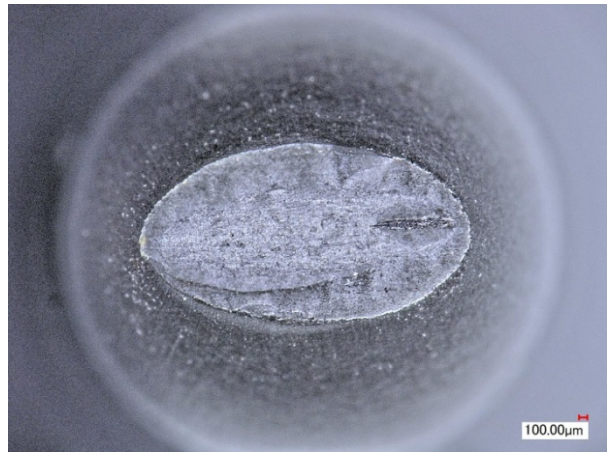

Fig. 42. Fracture surface for expanded and strain-aged longitudinal tensile test specimen 180° from weld seam.

A summary of longitudinal full wall thickness tensile properties is shown in Tables 13 through 16. The engineering and true stress-strain curves are shown in Figs. 43 and 44. A detailed view of the 0.5% EUL and 0.2% offset yield point determination shown in Fig. 45.

Midline cracking of the full thickness longitudinal specimens was observed (Figs. 46 through 51). The visual observation occurred after the onset of plastic yielding. Due to testing safety considerations, close proximity visual inspection during testing was not feasible and it was not obvious if cracking occurred before localized thinning of the specimen. In addition, slight rotation of the through-wall edges of the specimens was observed after completion of the tests.

7.4 STRAIN RATIO TESTING

Strain ratio testing, usually described as Poisson's ratio testing, experimentally determines the negative ratio of transverse to axial strain. Strain ratio determinations involved circumferential and longitudinal tensile specimens labeled "A," "B," and "C" as described in Sect. 6.3 and followed general testing guidance in ASTM E 132-04 (R 2010). In contrast to ASTM E 132, round tensile specimens were used in place of flattened rectangular specimens to determine strain ratio because this approach avoided use of flattened specimens. Test data were evaluated above the proportional limit up to 6% EUL.

The specimens were mounted in a tensile test machine used to perform standard tensile tests. A 1-in. extensometer was attached to the gage section of the specimen to measure and record the axial strain history. A digital micrometer was used to measure the minimum and maximum specimen diameters in the gage section during the test. Transverse strains were plotted in relation to axial strains rather than the applied load due the plastic behavior of the material. Round bar orientation was determined based on strain comparisons to the rectangular flat specimens. The axial strain versus strain ratio test results are plotted in Figs. 52 through 57. The plastic ratios were determined using the least squares method after the Lüder's yielding and are shown in Table 17.

Table 13. Summary of Longitudinal Rectangular Specimen Tensile Properties, As-Rolled

Specimen	ENGINEERING							TRUE			
	Yield Strength (0.2% off-set) (ksi)	Yield Strength (0.5% EUL) (ksi)	Ultimate Strength (ksi)	Y/T	Elastic Modulus (Msi)	UEL (%)	Maximum Test Elongation (%)	True Fracture Strength (ksi)	Strength Coefficient (ksi)	True Fracture Strain	Strain Hardening Exponent
AL-Axial-01	77.67	78.18	91.32	0.86	27.69	10.29	28.65	220.43	82.63	0.992	0.085
AL-Axial-02	78.10	78.68	91.20	0.86	28.31	10.60	41.93	132.61	82.81	1.006	0.083
AL-Axial-03	77.23	76.10	91.52	0.83	22.85	10.99	41.22	110.84	82.85	0.945	0.084
Average	77.67	77.65	91.35	0.85	26.28	10.63	37.27	154.63	82.76	0.981	0.084
Standard Deviation	0.435	1.368	0.162	0.016	2.993	0.351	7.471	58.018	0.117	0.032	0.001

Table 14. Summary of Longitudinal Rectangular Specimen Tensile Properties, Expanded

Specimen	ENGINEERING							TRUE			
	Yield Strength (0.2% off-set) (ksi)	Yield Strength (0.5% EUL) (ksi)	Ultimate Strength (ksi)	Y/T	Elastic Modulus (Msi)	UEL (%)	Maximum Test Elongation (%)	True Fracture Strength (ksi)	Strength Coefficient (ksi)	True Fracture Strain	Strain Hardening Exponent
BL-Axial-01	84.64	83.09	93.43	0.89	22.89	6.64	39.69	86.20	88.69	1.037	0.062
BL-Axial-02	93.32	93.87	96.23	0.98	25.63	7.46	39.05	103.66	87.15	0.987	0.086
BL-Axial-03	94.12	94.04	96.98	0.97	26.86	4.71	36.65	99.59	95.57	0.955	0.037
Average	90.69	90.33	95.55	0.94	25.13	6.27	38.46	96.48	90.47	0.993	0.062
Standard Deviation	5.258	6.273	1.871	0.048	2.031	1.412	1.603	9.135	4.480	0.041	0.024

Table 15. Summary of Longitudinal Rectangular Specimen Tensile Properties, Expanded and Strain-Aged, 90° from weld seam

Specimen	ENGINEERING							TRUE			
	Yield Strength (0.2% off-set) (ksi)	Yield Strength (0.5% EUL) (ksi)	Ultimate Strength (ksi)	Y/T	Elastic Modulus (Msi)	UEL (%)	Maximum Test Elongation (%)	True Fracture Strength (ksi)	Strength Coefficient (ksi)	True Fracture Strain	Strain Hardening Exponent
C-Axial-01	79.09	73.01	92.69	0.79	18.34	6.62	41.29	123.92	87.82	1.016	0.062
C-Axial-02	93.43	93.96	96.81	0.97	28.43	8.05	50.19	103.01	87.00	1.011	0.091
C-Axial-03	92.41	92.69	95.79	0.97	29.20	14.75	39.73	109.73	86.86	1.013	0.093
Average	88.31	86.55	95.10	0.91	25.32	9.81	43.74	112.22	87.23	1.013	0.082
Standard Deviation	8.001	11.746	2.146	0.105	6.055	4.340	5.643	10.675	0.521	0.003	0.018

Table 16. Summary of Longitudinal Rectangular Specimen Tensile Properties, Expanded and Strain-Aged, 180° from weld seam

Specimen	ENGINEERING							TRUE			
	Yield Strength (0.2% off-set) (ksi)	Yield Strength (0.5% EUL) (ksi)	Ultimate Strength (ksi)	Y/T	Elastic Modulus (Msi)	UEL (%)	Maximum Test Elongation (%)	True Fracture Strength (ksi)	Strength Coefficient (ksi)	True Fracture Strain	Strain Hardening Exponent
DL-Axial-01	90.49	88.34	98.34	0.90	23.75	6.20	39.77	104.58	94.27	1.004	0.056
DL-Axial-02	94.66	95.03	98.02	0.97	29.27	7.62	39.05	111.69	88.79	0.998	0.086
DL-Axial-03	92.41	92.69	95.79	0.97	29.20	14.75	39.73	99.88	86.40	0.988	0.086
Average	92.52	92.02	97.38	0.95	27.41	9.52	39.52	105.38	89.82	0.997	0.076
Standard Deviation	2.087	3.395	1.389	0.041	3.170	4.582	0.405	5.946	4.032	0.008	0.018

Table 17. Summary of Plastic Strain Ratio Specimens

	$\nu_{r\theta}$	$\nu_{\theta z}$	ν_{rz}
L-A-3		0.379	0.504
C-A-8	0.502	0.378	
L-B-2		0.383	0.571
C-B-8	0.523	0.385	
L-C-2		0.358	0.527
C-C-4	0.445	0..437	
Average	0.512	0.383	0.534

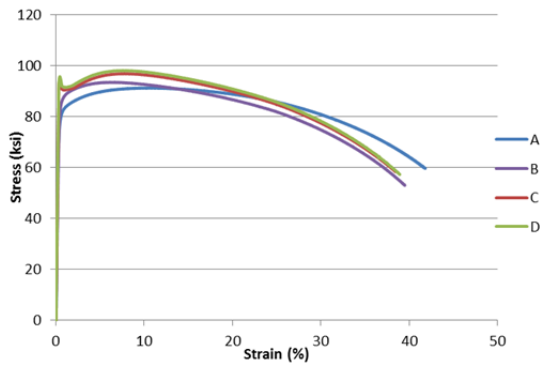

Fig. 43. Engineering stress strain curves for longitudinal rectangular tensile specimens.

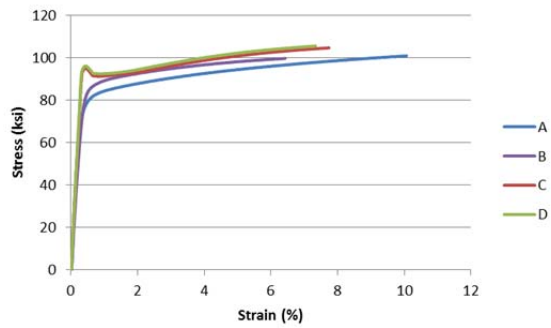

Fig. 44. True stress strain curves for longitudinal rectangular tensile specimens.

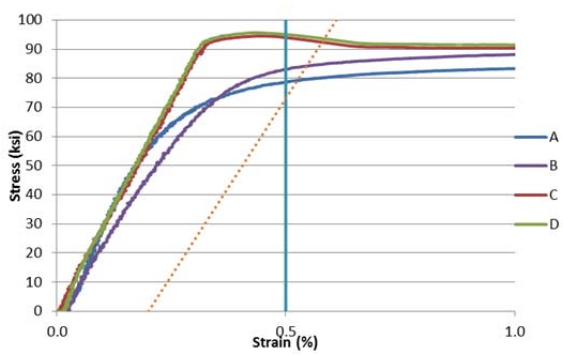

Fig. 45. 0.5% EUL and 0.2% Offset yield points for longitudinal rectangular tensile specimens.

Fig. 46. Top view of fracture surface for as-rolled longitudinal tensile test specimen.

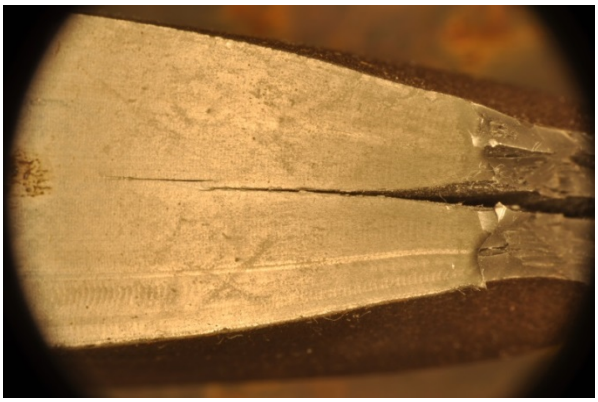

Fig. 47. Side view of fracture surface for as-rolled longitudinal tensile test specimen.

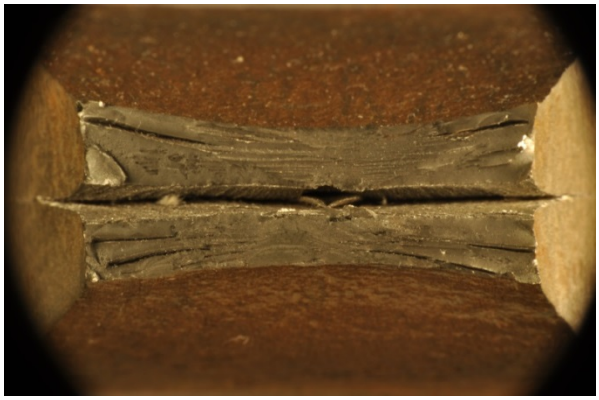

Fig. 48. Top view of fracture surface for expanded longitudinal tensile test specimen.

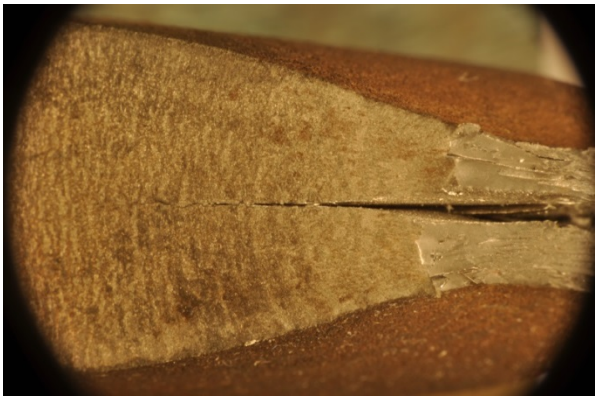

Fig. 49. Side view of fracture surface for expanded longitudinal tensile test specimen.

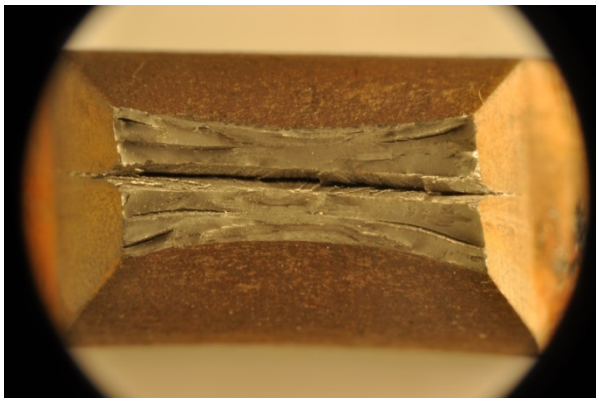

Fig. 50. Top view of fracture surface for expanded and strain-aged longitudinal tensile test specimen 90° from weld seam.

Fig. 51. Side view of fracture surface for expanded and strain-aged longitudinal tensile test specimen 90° from weld seam.

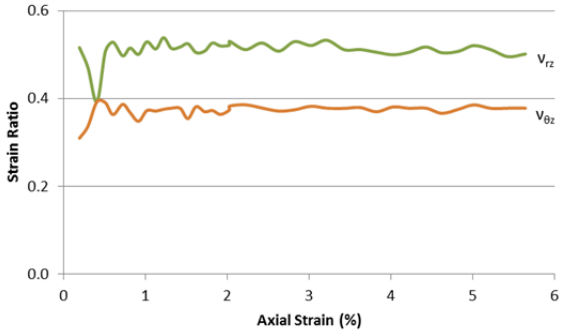

Fig. 52. Strain Ratio curves for as-rolled material from longitudinal round bar tensile specimens (specimen L-A-3).

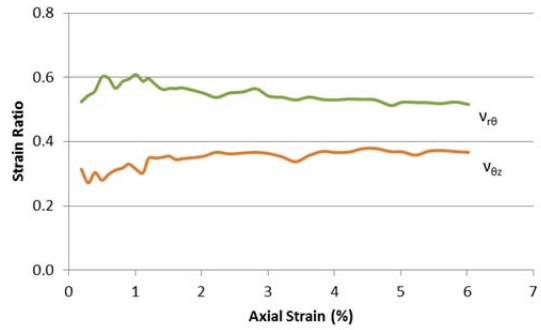

Fig. 53. Strain Ratio curves for as-rolled material from circumferential round bar tensile specimens (specimen C-A-8).

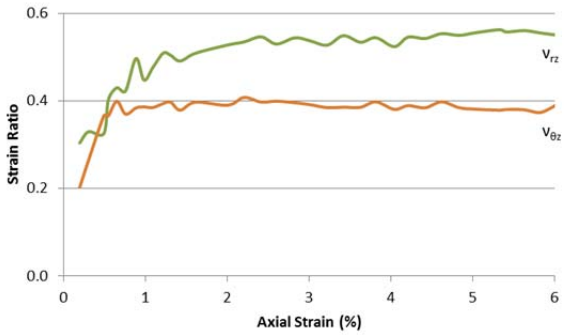

Fig. 54. Strain Ratio curves for expanded material from longitudinal round bar tensile specimens (specimen L-B-2).

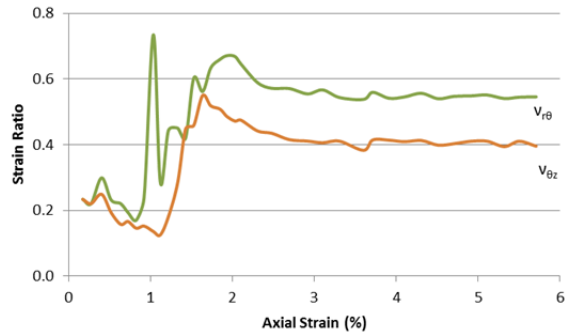

Fig. 55. Strain Ratio curves for expanded material from circumferential round bar tensile specimens (C-B-8).

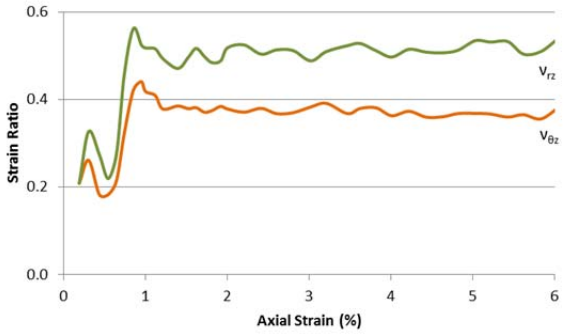

Fig. 56. Strain Ratio curves for expanded, strain-aged material from longitudinal round bar tensile specimens (specimen L-C-2).

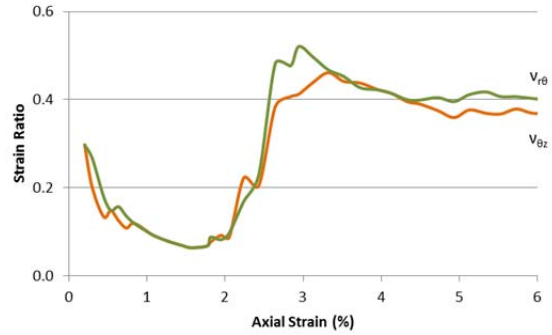

Fig. 57. Strain Ratio curves for expanded, strain-aged material from circumferential round bar tensile specimens (specimen C-C-9).

7.5 DISCUSSION AND CONCLUSIONS

Compared to plate test results obtained using standard testing techniques, the monotonic test results show very different mechanical properties and behavioral characteristics that are influenced by material processing, aging, specimen orientation, and test method. The following observations were noted.

- The tensile test results show that as-rolled linepipe material exhibits roundhouse stress-strain response in the transition region from elastic to plastic deformation. However, the yield point for as-rolled linepipe test specimens is below the minimum yield strength required by API Specification 5L.

- Cold forming associated with rolling and expanding operations leads to a distinct increase in the yield strength but no significant effect on the ultimate tensile strength for specimens oriented in the circumferential direction. Cold forming associated with rolling and expanding operations had no significant effect on the yield strength of specimens oriented in the longitudinal direction. The shape of the stress strain curve was very sharp in the transition region for specimens oriented in the circumferential direction, but the shape of the stress strain curve in the transition region for specimens oriented in the was not significantly affected for specimens oriented in the longitudinal direction.

- Cold forming associated with rolling and expanding operations slightly reduces uniform elongation and has no significant effect on maximum elongation.

- Expansion and aging have no significant effect on the yield point of test specimens oriented in the circumferential direction but contribute to varied results in test specimens oriented in the longitudinal direction.

- A combination of cold-forming and aging causes both yield and ultimate tensile strength to elevate and increases the Y/T ratio.

- Maximum test elongation was consistently much greater than the minimum required by API Specification 5L.

- No significant increase in the yield strength in the longitudinal direction was noted due to the expansion process.

- Obvious Lüder's elongation was observed for test specimens oriented in both the circumferential and longitudinal directions.

- Aging does not contribute to significant changes to the uniform elongation or maximum elongation of tensile test specimens.

- Small changes were noted between 90° and 180° test specimen results, but these changes are not considered significant.

- Significant differences in test results were observed between flat and round specimens in terms of the shapes of stress-strain curves in the transition region and maximum tensile elongation (see Fig. 58).

- Mid-wall separation of fracture surfaces for all flat specimens was observed.

- Mid-wall separation occurred after yield and after the engineering ultimate strength occurred.

- Mid-wall separation may affect small specimen elongation properties more significantly than flat specimens due to the centerline effects over the gage length (see Fig. 59).

- Anisotropy was observed in fractured specimens and strain ratio data.

- While most design standards set strain ratio at 0.5 for plastic deformation, this assumption may be slightly conservative for Grade X80 linepipe.

- The stress-strain relationships outlined in CSA Z662 are not accurate for Grade X80 linepipe and tend to be highly conservative.

- The Ramberg-Osgood relationship using the strength coefficient is more accurate in predicting the stress-strain behavior of Grade X80 linepipe including discontinuities around the yield point. The Ramberg-Osgood relationship can be written in the following form.

$$\varepsilon = \frac{\sigma}{E} + \left(\frac{\sigma}{H}\right)^{\frac{1}{n}}$$

- Material properties determined from expanded and aged Grade X80 linepipe steel test specimens should be represented in pipeline design and analysis methods because these linepipe manufacturing processes can potentially have a marked effect on the performance characteristics of pipelines constructed with these steels. In addition, the following plastic strain ratio values should also be represented in pipeline design and analysis methods due to anisotropy of this material.

$$\upsilon_{r\theta} = 0.50$$

$$\upsilon_{\theta z} = 0.40$$

$$\upsilon_{rz} = 0.55$$

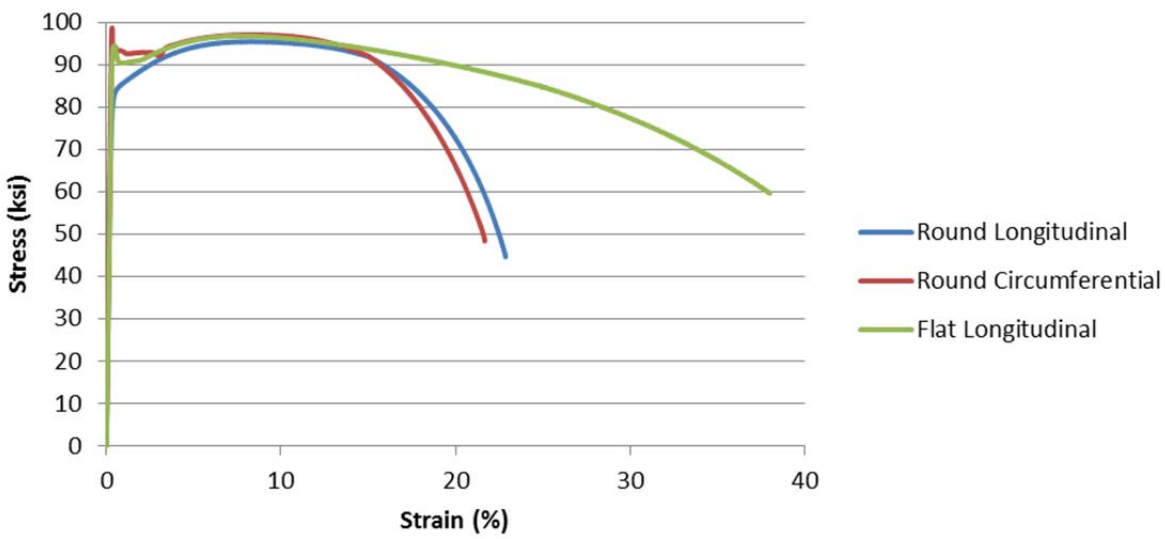

Fig. 58. Engineering stress strain curves for expanded and strain-aged tensile specimens 90° from weld seam.

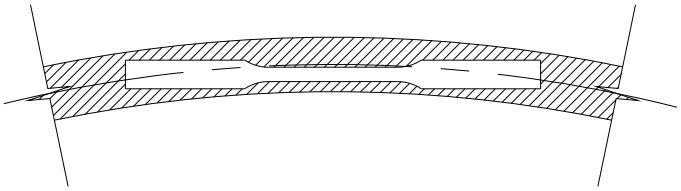

Fig. 59. Round circumferential tensile specimen from pipe wall.

8. CYCLIC LINEPIPE MATERIAL PROPERTIES AND BEHAVIOR

Implementation of the fatigue analysis and assessment method described in Sect. 10 requires an understanding of cyclic properties and fatigue behavior of Grade X80 linepipe steel. In an effort to develop the knowledge base needed to assess the effectiveness of this method, force-controlled and stain-controlled tests of representative linepipe steel samples were conducted in the laboratory using servo-controlled hydraulic testing equipment and automated instrumentation suitable for loading, measuring, and acquiring stress-strain hysteresis loop data. The key objective of these laboratory tests was to produce cyclic material properties for Grade X80 linepipe steel in the as-rolled, expanded, and expanded and aged conditions.

8.1 TEST SPECIMEN SELECTION CONSIDERATIONS

Round bar specimens with a uniform cross section were chosen as representative test samples based on the following considerations.

- testing equipment capacity
- specimen size limitations
- gripping constraints
- material strength
- laboratory accessibility
- economic factors

The number of specimens, sample locations, and gage lengths of the round bar specimens did not necessarily comply with any code requirements or applicable linepipe testing standards primarily because Grade X80 linepipe steel is an anisotropy material. As discussed in Sect. 7, Grade X80 linepipe steel properties (1) vary with sample location and orientation and (2) do not exhibit isotropic material behavior on which testing requirements for conventional linepipe steels are based. Consequently, hourglass-shaped test sections with axial strain gages were not considered suitable test specimens for this material because they would not produce the types of data needed to achieving the key test objective. Instead, round test specimens with uniform gage lengths were chosen based on the physical restrains of attaching an extensometer capable of measuring large axial strains. Strain gages are limited in their ability to measure plastic stains.

Material samples used to produce the required number of test specimens were taken at 90 degrees from the longitudinal weld seam and represented three (3) pipe conditions labeled “A”, “B”, and “C” as described in Sect. 6. The round bar specimens were machined from the wall of large diameter Grade X80 rolled linepipe segments into the configurations as shown in Fig. 60. Flattening of test specimens prior to machining was not permitted.

The fatigue test results were intended to cyclic tensile properties and stress-strain curves for comparison to monotonic material properties and analysis. Cyclic stress-strain curves were generated and cyclic material property constants were determined after testing.

- The cyclic strength coefficient, H’, and cyclic strain hardening coefficient, n’, was determined using a power law fit stress versus alternating plastic strain curve. The slope of the plastic strain curve is the cyclic strain hardening exponent and the cyclic strength coefficient is the intercept when the cyclic plastic strain is equal to 1.

$$\sigma_a = H' \varepsilon_{pa}^{n'}$$

- Fitting constants were determined from fitting the strain versus life relationship:

$$\sigma_a = \sigma_f'(2N_f)^b$$

and:

$$\varepsilon_{pa} = \varepsilon_f'(2N_f)^c$$

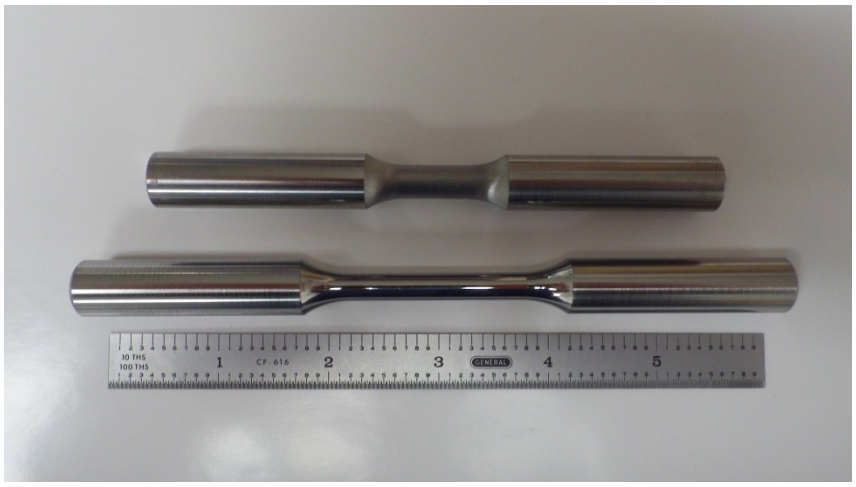

Fig. 60. Fatigue Test Specimens.

8.2 FORCE-CONTROLLED FATIGUE TESTING

Force-controlled fatigue testing of the circumferential specimens discussed in Section 6.3 followed the general practices set forth in ASTM E 466-07. The specimens had a test section diameter of 0.250 in. with a uniform gage length of 1.5 in. All force-controlled tests were conducted at a frequency of 2 Hz and at room temperature (≈ 75°F). Testing continued until either the specimen fractured or the number of loading cycles equaled 100,000. A summary of the circumferential round bar fatigue properties derived from the force-controlled fatigue testing are shown in Table 18.

Table 18. Summary of Circumferential Round Bar Fatigue Properties

Specimen				Selected Cycle Near Start				Strain Life				Selected Cycle Near Half-Life				Strain-Life				
Material Condition	ID	Target Stress Amplitude (ksi)	Strain Ratio (R)	Cycle	Cyclic Modulus E' (Msi)	H'	n'	σ'_f	b	ε'_f	c	Cycle	Cyclic Modulus E' (Msi)	H'	n'	σ'_f	b	ε'_f	c	N_f
A	C-A-2	58.35	-1	20	31.82	284.33	1.0300	109.60	-0.0520	0.3963	-0.0505	50,000	32.02	224.73	0.9935	109.6	-0.0520	0.485411	-0.05234	100,000
	C-A-5	64.40	-1	20	32.56	238.03	0.9956	109.60	-0.0520	0.4589	-0.0522	7,000	31.38	124.3	0.8117	109.6	-0.0520	0.856365	-0.06406	14,490
	C-A-6	68.43	-1	20	31.20	223.09	0.9866	109.60	-0.0520	0.4866	-0.0527	2,000	30.2	118.74	0.7296	109.6	-0.0520	0.896027	-0.07127	5,346
	C-A-7	72.45	-1	20	31.30	199.30	0.9392	109.60	-0.0520	0.5290	-0.0554	700	30.56	103.32	0.6421	109.6	-0.0520	1.096251	-0.08098	1,420
B	C-B-2	58.35	-1	7	32.98	170.18	0.6093	108.61	-0.0510	0.4785	-0.0837	50,000	32.09	147.98	0.4879	108.61	-0.0510	0.530482	-0.10453	100,000
	C-B-5	64.40	-1	20	32.54	145.12	0.4054	108.61	-0.0510	0.4893	-0.1258	7,000	30.11	92.277	0.2206	108.61	-0.0510	2.09332	-0.23119	15,940
	C-B-6	68.43	-1	20	31.60	148.02	0.4167	108.61	-0.0510	0.4757	-0.1224	2,000	30.66	91.173	0.1933	108.61	-0.0510	2.472804	-0.26384	4,995
	C-B-7	72.45	-1	5	32.00	122.56	0.2802	108.61	-0.0510	0.6497	-0.1820	600	30.31	84.25	0.0926	108.61	-0.0510	15.52901	-0.55076	1,357
C	C-C-5	58.35	-1	20	31.56	290.26	0.9302	105.91	-0.0480	0.3383	-0.0516	50,000	30.66	150.29	0.5161	105.91	-0.0480	0.507571	-0.09301	100,000
	C-C-6	64.40	-1	2	32.28	285.60	0.9182	105.91	-0.0480	0.3395	-0.0523	8,000	30.22	97.893	0.2629	105.91	-0.0480	1.349061	-0.18258	16,624
	C-C-7	68.43	-1	25	31.70	237.95	0.7964	105.91	-0.0480	0.3619	-0.0603	2,000	30.07	91.6820	0.2216	105.91	-0.0480	1.917475	-0.21661	4,092
	C-C-8	72.45	-1	5	32.32	236.26	0.7652	105.91	-0.0480	0.3504	-0.0627	500	30.15	95.207	0.2032	105.91	-0.0480	1.689263	-0.23622	1,185

Stress versus life data plots for round bar test specimens that were subjected to force-controlled fatigue testing are shown in Fig. 61. Stress-strain responses for circumferential force-controlled fatigue specimens in the as-rolled, expanded, and expanded and strain aged conditions are plotted in Figs. 62, 63, and 64, respectively.

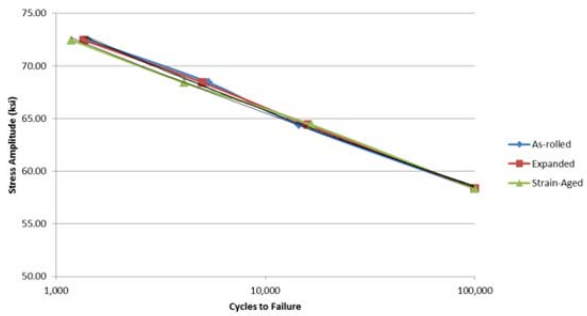

Fig. 61. Stress versus life curves for round bar test specimens.

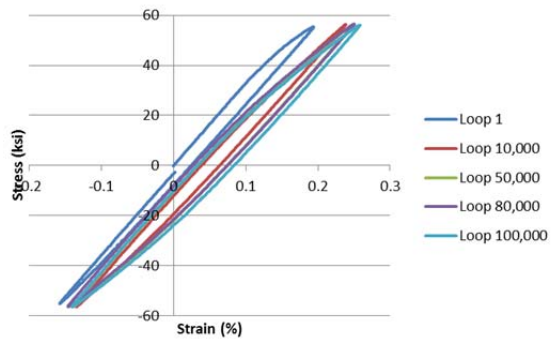

Fig. 62. Circumferential force-controlled fatigue specimen stress-strain response for as-rolled linepipe (C-A-2).

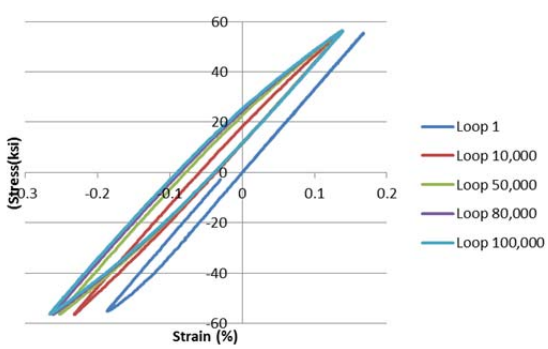

Fig. 63. Circumferential force-controlled fatigue specimen stress-strain response for expanded linepipe (C-B-2).

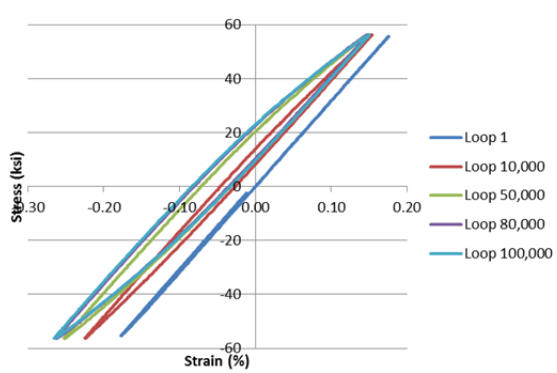

Fig. 64. Circumferential force-controlled fatigue specimen stress-strain response for expanded and strain-aged linepipe (C-C-5).

8.3 STRAIN-CONTROLLED FATIGUE TESTING

Strain-controlled fatigue testing of the longitudinal specimens discussed in Section 6.3 followed the general testing practices set forth in ASTM E606/E606M-12. The specimens had a test section diameter of 0.300 in. with a uniform gage length of 0.5 in. All strain-controlled tests were conducted at a frequency of 0.1 Hz and testing continue until the specimen fractured. A summary of the longitudinal cyclic properties are shown in Table 19.

Stress versus life data plots for round bar test specimens that were subjected to strain-controlled fatigue testing are shown in Figs. 65 and 66. Stress-strain responses for longitudinal strain-controlled fatigue specimens in the as-rolled, expanded, and expanded and strain aged conditions are plotted in Figs. 67 through 72.

8.4 DISCUSSION AND CONCLUSIONS

Fatigue testing results discussed in Sects. 8.2 and 8.3 show cyclic response characteristics that vary depending on the material processing, aging, specimen orientation, and test method. The following observations were noted.

- The load-controlled stress-strain hysteresis loops for all specimens exhibited ductile behavior and cycle dependent softening with an increase in strain with increasing number of cycles.

- The strain-controlled stress-strain hysteresis loops for all specimens also exhibited cycle dependent softening with a decrease in stress with increasing number of cycles.

- There were multiple reasons for discontinuing fatigue tests including termination at 100,000 cycles, fracture, and bucking of the specimen. This may be affect the accuracy of the stress-life relationships.

- The load-controlled specimens tested at stresses greater than 80% SMYS were discontinued due to buckling. Changing the specimen size and configuration may lead to greater fatigue life.

- All but one of the strain-controlled fatigue tests were discontinued prior to achieving the 100,000 cycle limit due to fracturing of the specimen.

- While slight differences exist for material conditions at high stress and strain, fatigue life converges at lower tested values of stress and strain.

- The strain hardening exponent is dependent on stress levels and decreases as the alternating stress amplitude increases.

Table 19. Summary of Longitudinal Round Bar Fatigue Properties

Specimen				Selected Cycle Near Start								Selected Cycle Near Half-Life									
Material Condition	ID	Target Strain Amplitude (%)	Strain Ratio (R)	Cycle	Cyclic Modulus E' (Msi)	H'	n'	σ'_f	b	ε'_f	c	Cycle	Cyclic Modulus E' (Msi)	H'	n'	σ'_f	b	ε'_f	c	N_i	N_f
A	LCF1	2.00	0	1	30.50	84.66	0.059	97.71	-0.024	11.25	-0.403	100	26.27	64.96	0.160	95.78	-0.065	11.25	-0.403	124	223
	LCF2	1.50	0	1	25.10	84.17	0.062	97.75	-0.025	11.25	-0.403	200	26.61	64.32	0.182	99.91	-0.073	11.25	-0.403	247	486
	LCF3	1.00	0	1	26.70	85.24	0.047	95.49	-0.019	11.25	-0.403	400	27.57	63.82	0.232	111.98	-0.094	11.25	-0.403	705	804
	LCF4	0.50	0	3	28.25	87.76	0.573	350.88	-0.231	11.25	-0.403	3,000	27.98	64.75	0.592	271.25	-0.238	11.25	-0.403	4,702	6,950
B	LCF11	2.00	0	1	24.40	89.98	0.039	96.12	-0.013	5.34	-0.327	40	24.43	70.74	0.111	85.13	-0.036	5.34	-0.327	87	89
	LCF12	1.50	0	1	24.80	87.68	0.049	95.18	-0.016	5.34	-0.327	70	25.35	67.69	0.137	85.19	-0.045	5.34	-0.327		148
	LCF13	1.00	0	1	26.10	85.60	0.049	92.86	-0.016	5.34	-0.327	200	25.06	63.35	0.208	89.81	-0.068	5.34	-0.327	451	485
	LCF14	0.50	0	1	27.60	84.14	0.061	93.21	-0.020	5.34	-0.327	2,000	28.49	62.20	0.508	145.64	-0.166	5.34	-0.327	5,394	5,849
C	LCF21	2.00	0	1	25.30	84.80	0.056	92.65	-0.018	4.84	-0.320	50	24.78	66.66	0.169	86.98	-0.054	4.84	-0.320	104	111
	LCF22	1.50	0	1	25.90	83.39	0.064	92.17	-0.020	4.84	-0.320	100	25.24	66.23	0.171	86.74	-0.055	4.84	-0.320	170	202
	LCF23	1.00	0	1	25.96	85.71	0.052	93.02	-0.017	4.84	-0.320	200	26.22	63.61	0.242	93.24	-0.078	4.84	-0.320	407	451
	LCF24	0.50	0	1	27.20	86.53	0.088	99.41	-0.028	4.84	-0.320	3,000	26.71	63.10	0.565	153.93	-0.181	4.84	-0.320	6,213	6,713
A	LCF7	2.00	-1	3	26.14	91.22	0.029	97.04	-0.011	8.64	-0.374	100	26.20	78.80	0.046	86.98	-0.017	8.64	-0.374	195	218
	LCF6	1.50	-1	1	27.00	86.93	0.025	91.70	-0.009	8.64	-0.374	100	25.87	78.47	0.054	88.18	-0.020	8.64	-0.374	200	253
	LCF5	1.00	-1	1	27.10	87.15	0.013	89.56	-0.005	8.64	-0.374	500	27.04	72.30	0.075	84.99	-0.028	8.64	-0.374	907	1,006
	LCF8	0.50	-1	6	27.90	97.00	0.250	166.14	-0.093	8.64	-0.374	3,000	28.01	73.58	0.212	116.17	-0.079	8.64	-0.374	5,437	6,681
B	LCF15	2.00	-1	1	25.60	84.10	0.046	89.91	-0.014	4.29	-0.302	40	26.74	81.92	0.038	86.52	-0.011	4.29	-0.302		86
	LCF16	1.50	-1	1	26.59	88.76	0.048	95.18	-0.014	4.29	-0.302	60	26.33	79.43	0.045	84.87	-0.014	4.29	-0.302		124
	LCF17	1.00	-1	1	26.70	87.13	0.070	96.53	-0.021	4.29	-0.302	200	26.13	74.03	0.077	82.87	-0.023	4.29	-0.302	484	557
	LCF18	0.50	-1	1	28.30	94.40	0.228	131.63	-0.069	4.29	-0.302	3,000	27.88	71.13	0.204	95.78	-0.062	4.29	-0.302	6051	6,687
C	LCF25	2.00	-1	1	26.10	85.69	0.057	93.00	-0.017	4.26	-0.305	40	26.02	83.61	0.043	88.95	-0.013	4.26	-0.305		86
	LCF26	1.50	-1	1	26.40	84.90	0.055	91.89	-0.017	4.26	-0.305	100	25.68	78.62	0.058	85.48	-0.018	4.26	-0.305	113	234
	LCF27	1.00	-1	1	27.70	83.89	0.079	94.06	-0.024	4.26	-0.305	200	27.46	74.73	0.093	85.51	-0.028	4.26	-0.305	441	484
	LCF28	0.50	-1	1	28.00	89.99	0.208	121.71	-0.064	4.26	-0.305	4,000	27.85	70.99	0.210	96.24	-0.064	4.26	-0.305	7312	8,129

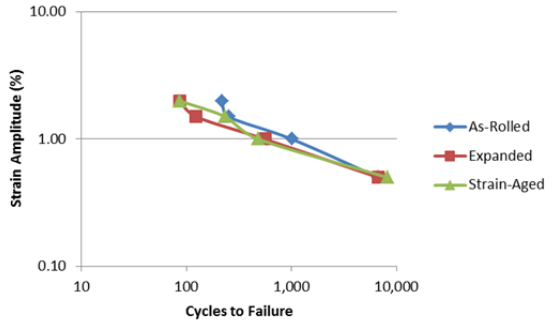

Fig. 65. Strain versus life curves for round bar test specimens, R = -1.

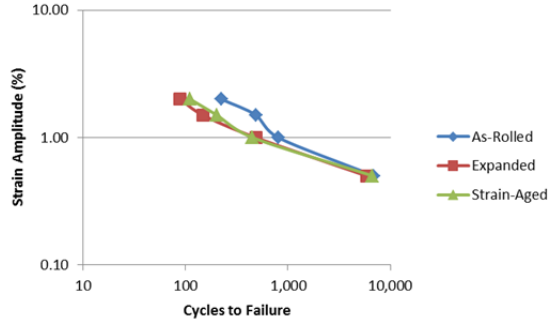

Fig. 66. Strain versus life curves for round bar test specimens, R = 0.

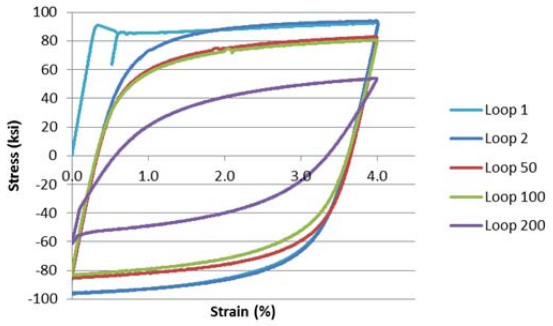

Fig. 67. Longitudinal strain-controlled fatigue specimen stress-strain response for as-rolled linepipe (LCF-1).

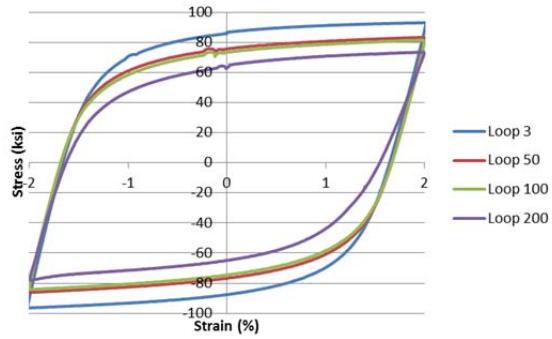

Fig. 68. Longitudinal strain-controlled fatigue specimen stress-strain response for as-rolled linepipe (LCF-7).

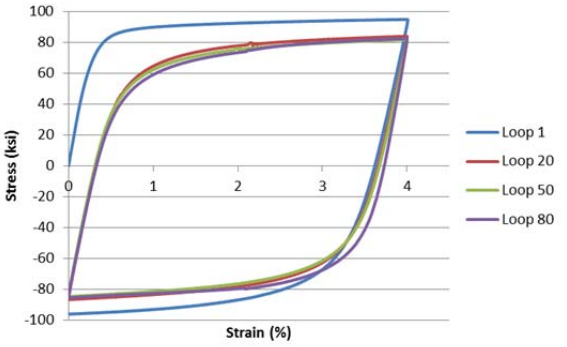

Fig. 69. Longitudinal strain-controlled fatigue specimen stress-strain response for expanded linepipe (LCF-11).

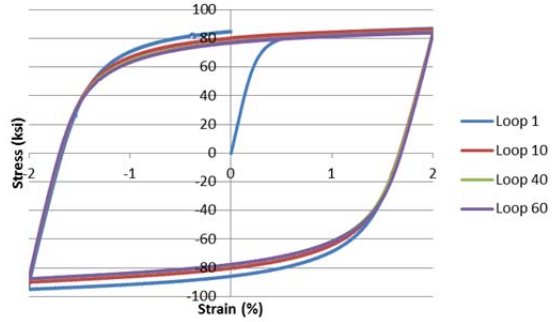

Fig. 70. Longitudinal strain-controlled fatigue specimen stress-strain response for expanded linepipe (LCF-15).

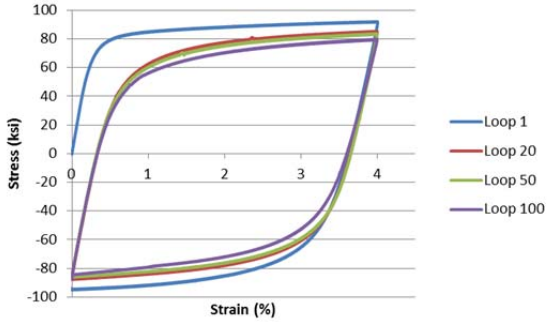

Fig. 71. Longitudinal strain-controlled fatigue specimen stress-strain response for expanded and strain-aged linepipe (LCF-21).

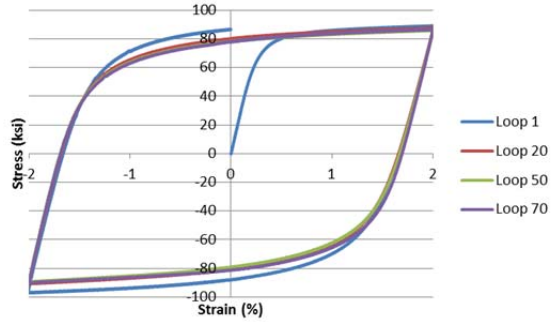

Fig. 72. Longitudinal strain-controlled fatigue specimen stress-strain response for expanded and strain-aged linepipe (LCF-25).

9. PROTECTION AGAINST PLASTIC COLLAPSE

The experimental monotonic stress-strain relationships were presented and various material properties for the uniaxial stress state were defined in Chapter 7. For linepipe subjected to a single stress component, the uniaxial failure criteria may be applied. However, when a pipeline is subjected to a multiaxial state of stress or strain, failure criteria must account for the multiaxial nature of the stress and strain state. It is essential to accurately predict the initiation of the inelastic response of materials under multiaxial stress states. In the case of linepipe steels, specific criteria for the initiation of yield of ductile materials need to be developed and compared from material properties obtained through uniaxial material testing.

In order to quantify the nonlinear response of pipelines subjected to large longitudinal strain beyond yield, it is assumed that the linepipe is rotationally symmetrical and can be reasonably represented using D/t ratios much greater than 10. For long-distance transmission pipelines, this assumption is justified because these pipelines are typically constructed using large diameter linepipe with a relatively thin wall making the plane stress assumption valid. In addition, it is assumed that these pipelines are subjected to uniform internal pressure. However, these assumptions may need further consideration depending on elevation changes and proximity to pumping or compressor stations. Where applicable, the internal pressure resulting from static head or other static or dynamic loads must be considered in the design basis. After taking localized anomalies into consideration, it can generally be stated that pipeline design solutions based on these assumptions are applicable to locations sufficiently far from external constraints and structural discontinuities.

Stresses from temperature have not been considered in establishing the governing equations. The material fracture toughness must be established in correlation with upper-bound stresses, lower-bound fracture toughness, and upper-bound flaw size, in addition to meeting the minimum toughness requirements as required by API Specification 5L. It is essential that the operating temperatures are greater than the minimum design metal temperature based on the design loading conditions.

The load case combinations for the elastic-plastic stress analysis method are based on separate global load cases. The type of load combinations expected for strain-based design pipeline applications involve both “load-controlled” and “strain-controlled” loads. In this context, the term “load-controlled” refers to loads such as internal pressure and externally applied reactions due to weight effects and the term “strain-controlled” refers to imposed displacements that produce strains that are primarily in the longitudinal direction. Except for dead loads or other permanent loads, most “load-controlled” and “strain-controlled” loads can vary with time.

9.1 ELASTIC-PLASTIC DESIGN CONSIDERATIONS

Over long spans, the external loads are primarily due to soil weight. Operating internal pressures are based on the limits set in the CFRs or referenced in the ASME design codes. Stresses in the longitudinal direction are limited based on allowable tensile strain.

Because of radial symmetry, no shear stresses act on the volume element such that:

$$\sigma_{r\theta} = \sigma_{\theta z} = \sigma_{rz} = 0$$

The non-zero stress components then are principal stresses σ_r, σ_θ, and σ_z. Based on the assumption of large D/t ratios and plane stress, the stress variations through the wall thickness are comparably small. Therefore, the structural element can be reduced to two dimensions assuming $\sigma_r \approx 0$. Circumferential and longitudinal stresses are the sum of stress components produced by internal pressure and the strain effects

due to longitudinal strain. Strain across the wall thickness is due to the strain effects of the internal pressure and applied longitudinal displacement. Circumferential stress due to internal pressure is load-controlled and less than the yield stress while the longitudinal stress is strain-controlled and above the yield stress. However, applied longitudinal strain is less than the uniform elongation verified by testing. This loading combination is expected to be cyclic but with different frequencies.

Care must be exercised when selecting parameters such as the full range of operating conditions, including upset conditions, to consider during pipeline design. However, it is important to provide an additional margin of safety to ensure reliable long-term pipeline performance throughout its intended service life that may involve emergency situations, unexpected loads, misuse, and degradation.

9.2 ELASTIC-PLASTIC ANALYSIS METHOD

An elastic-plastic stress analysis method for transmission pipelines involves the derivation of a collapse load algorithm that includes both the applied loading and deformation characteristics of the linepipe. Elastic-plastic stress analysis that is based on non-linear stress-strain response provides a more accurate assessment of the protection against plastic collapse of a pipeline compared to elastic stress analysis that is based on the theory of elasticity because actual structural behavior is more closely approximated. The redistribution of stress that occurs as a result of inelastic deformation (plasticity) and deformation characteristics of the linepipe are considered directly in the analysis. When using this non-linear stress-strain material model, the hardening behavior should be included up to the true ultimate stress and perfect plasticity behavior (i.e. the slope of the stress-strain curves is zero) beyond this limit.

The governing equations can be written as a function of the circumferential stress due to internal pressure and the applied tensile strain in the longitudinal direction based on the assumption of plane stress. Since the stress in the circumferential direction due to internal pressure is less than the specified minimum yield strength, strain in the circumferential direction due to internal pressure will remain in the elastic region and preferably below the proportional limit. Since the strain in the longitudinal direction is expected to be greater than 0.5%, both elastic and plastic stress components are necessary to accurately model structural behavior. The stress in the circumferential direction due to pressure is determined based on the ASME piping codes and can be as high as 80% of SMYS (see Sect. 4.1.1).

Based on the Ramberg-Osgood equations for modelling full stress-strain curves, the orthotropic elastic-plastic triaxial strain equations can be developed for the load combinations. Using a uniaxial curve that fits the Ramberg-Osgood form in terms of elastic and plastic components, the elastic and plastic strain equations due to the applied tensile displacement in the longitudinal direction is written as follows.

$$\varepsilon_z = \varepsilon_{ze} + \varepsilon_{zp}$$

Where:

$$\varepsilon_{ez} = \frac{\sigma_z}{E_z}$$

$$\varepsilon_{pz} = \left(\frac{\sigma_z}{H_z}\right)^{\frac{1}{n_z}}$$

The elastic-plastic governing strain equations based on plane stress (σ_r=0) and anisotropic material is written as follows using the monotonic material constants.

$$\varepsilon_r = -\upsilon_{r\theta e}\left(\frac{\sigma_\theta}{E_\theta}\right) - \upsilon_{rze}\left(\frac{\sigma_z}{E_z}\right) - \upsilon_{rzp}\left(\frac{\sigma_z}{H_z}\right)^{\frac{1}{n_z}}$$

$$\varepsilon_\theta = \left(\frac{\sigma_\theta}{E_\theta}\right) - \upsilon_{\theta ze}\left(\frac{\sigma_z}{E_z}\right) - \upsilon_{\theta zp}\left(\frac{\sigma_z}{H_z}\right)^{\frac{1}{n_z}}$$

$$\varepsilon_z = -\upsilon_{\theta ze}\left(\frac{\sigma_\theta}{E_\theta}\right) + \left(\frac{\sigma_z}{E_z}\right) + \left(\frac{\sigma_z}{H_z}\right)^{\frac{1}{n_z}}$$

The equivalent stress in terms of principal stresses is given by:

$$\sigma_e = \sqrt{\frac{1}{2}[(\sigma_\theta - \sigma_z)^2 + (\sigma_\theta)^2 + (\sigma_z)^2]}$$

The effective strain is a function of the principal strains and the weighted average of the strain ratio and written as follows.

$$\bar{\varepsilon} = \frac{1}{\sqrt{2}(1+\bar{\upsilon})}\sqrt{(\varepsilon_r - \varepsilon_\theta)^2 + (\varepsilon_\theta - \varepsilon_z)^2 + (\varepsilon_z - \varepsilon_r)^2}$$

The weighted average of the strain ratio ($\bar{\upsilon}$) can be viewed as the generalized strain ratio and the weighted average of the strain ratio in the elastic and plastic ranges. When strains are small and the elastic component is dominant, $\bar{\upsilon}$ is approximately equal to 0.3. As strain increases and the plastic component dominates, $\bar{\upsilon}$ is replaced by 0.5, which is equivalent to the assumption that plastic strains do not contribute to volume change. For purposes of elastic-plastic analysis, $\bar{\upsilon}$ equals $= 0.5$ for strains greater than 1.0%.

9.3 ELASTIC-PLASTIC ASSESSMENT

In 2009, the ASME Boiler and Pressure Vessel Code committee responsible for Section VIII Division 2 developed elastic-plastic local strain limit criterion to determine the allowable plastic strain at a point as a function of triaxiality in the component and the uniaxial strain limits for the material. The limit criterion was developed considering the local damage accumulation in metals during plastic deformation at temperatures below the creep range. Prediction models were benchmarked against numerous results of notch-bar and tensile tests under high-pressure conditions taking into account post-necking strain behavior. The microstructure damage accumulates exponentially depending on the degree of triaxiality and microstructure, is directly proportional to applied stress and strain, and can be described as follows [80, 67, 71].

$$\frac{dDamage}{d\varepsilon_{tp}} = f(stress, triaxiality, material\ properties)$$

The following was proposed for the development of the strain limit function.

$$\frac{dDamage}{d\varepsilon_{tp}} = \sigma_T * \gamma * exp[\alpha_{sl} * T]$$

Where: σ_T is the true stress,

γ is a material constant dependent on factors such as grain size, cleanliness, and inclusion content that contribute to voiding and microcrack initiation,

α_{sl} is a material constant dependent on metallurgical (crystallographic) structure,

$d\varepsilon_{tp}$ is an incremental change in the true plastic strain, and

T is the Davis-Connelly triaxiality factor based on principal stresses given by the following [75].

$$T = \frac{\sigma_r + \sigma_\theta + \sigma_z}{3\sigma_e}$$

The relationship between true stress and true strain is given by:

$$\sigma_T = S_0 * \varepsilon_{tp}^{m_s}$$

Where: S_0 is a stress material constant where the true stain is equal to unity (see Fig. 73), and

m_2 is the strain hardening coefficient that is estimated from the ratio of the engineering yield to tensile strength [60, 70]

The uniaxial strain limit material coefficients, m_2 and α_{sl} for ferritic steel are based on definitions provided in the ASME Boiler and Pressure Vessel Code, Section VIII Division 2 as follows.

$$\alpha_{sl} = 2.2$$

$$m_2 = 0.60\left[1.00 - \frac{SMYS}{SMTS}\right]$$

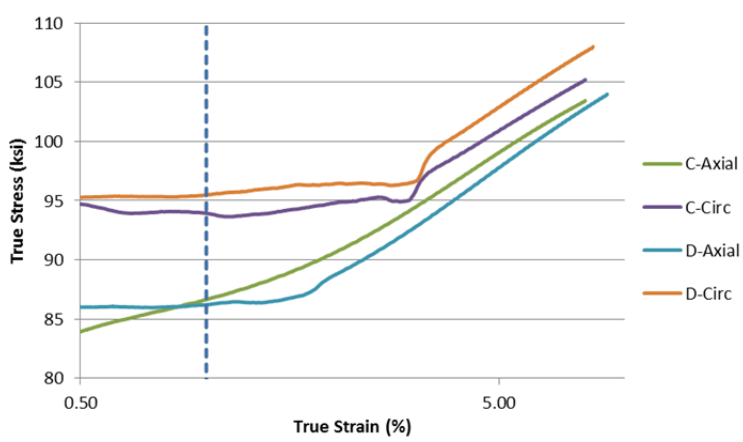

Fig. 73. True stress true strain relations at large strains for expanded and strain-aged linepipe.

Engineering stress-strain relationships may be calculated from the true stress vs true strain diagram. The ultimate strength shown is reached when the true strain is numerically equal to the strain hardening

coefficient. Substituting the above true stress and damage equations, the differential equation for damage is written as follows.

$$dDamage = S_0 * \gamma * exp[\alpha_{sl} * T] * \varepsilon_{tp}^{m_2} * d\varepsilon_{tp}$$

Integrating the above equation and solving for the fracture strain for multiaxial conditions, ε_{fm}, at a given triaxiality becomes:

$$\int_0^1 dDamage = S_0 * \gamma * exp[\alpha_{sl} * T] \int_0^{e_f} \varepsilon_{tp}^{m_2} * d\varepsilon_{tp}$$

$$1 = \left(\frac{S_0 * \gamma}{(1 + m_2)}\right) * exp[\alpha_{sl} * T] * \varepsilon_f^{(1+m_2)}$$

Solving the above equation by rearranging all other terms, except the fracture strain, to the opposite side of the equation and taking the root, gives the fracture strain, ε_{fm}, for multiaxial conditions or the general case at any triaxiality.

$$\varepsilon_{fm} = \sqrt[\frac{1}{(1+m_2)}]{\frac{(1 + m_2)}{s_0 * \gamma}} * exp\left[-\left(\frac{\alpha_{sl}}{1 + m_2}\right) * T\right]$$

For the uniaxial fracture strain case (ε_{fu}), the triaxiality factor T = $\frac{1}{3}$, or is set by inspection of test results.

$$\varepsilon_{fu} = \sqrt[\frac{1}{(1+m_2)}]{\frac{(1 + m_2)}{s_0 * \gamma}} * exp\left[-\left(\frac{\alpha_{sl}}{1 + m_2}\right) * \frac{1}{3}\right]$$

Taking the ratio of the multiaxial fracture strain to the uniaxial fracture strain, $\frac{\varepsilon_{fm}}{\varepsilon_{fu}}$, becomes:

$$\frac{\varepsilon_{fm}}{\varepsilon_{fu}} = \frac{\sqrt[\frac{1}{(1+m_2)}]{\frac{(1 + m_2)}{s_0 * \gamma}} * exp\left[-\left(\frac{\alpha_{sl}}{1 + m_2}\right) * T\right]}{\sqrt[\frac{1}{(1+m_2)}]{\frac{(1 + m_2)}{s_0 * \gamma}} * exp\left[-\left(\frac{\alpha_{sl}}{1 + m_2}\right) * \frac{1}{3}\right]} = exp\left[-\left(\frac{\alpha_{sl}}{1 + m_2}\right) * \left(T - \frac{1}{3}\right)\right]$$

The multiaxial strain limit, $\varepsilon_{Lm} = \varepsilon_{fm}$, as a function of the uniaxial strain limit $\varepsilon_{Lu} = \varepsilon_{fu}$ is:

$$\varepsilon_L = \varepsilon_{Lu} * exp\left[-\left(\frac{\alpha_{sl}}{1 + m_2}\right)\left(\left\{\frac{\sigma_1 + \sigma_2 + \sigma_3}{3\sigma_e}\right\} - \frac{1}{3}\right)\right]$$

The strain limit of the linepipe is acceptable if the forming strain ε_f and effective strain $\bar{\varepsilon}$ are less than the limiting strain such that:

$$\bar{\varepsilon} + \varepsilon_f \leq \varepsilon_L$$

The forming strain ε_f is defined in the ASME Boiler and Pressure Vessel Code, Section VIII Division 2 as:

$$\varepsilon_f = \frac{50t}{R_f}\left(1 - \frac{R_f}{R_o}\right)$$

Where: t = plate thickness before forming
R_o = original mean radius (∞ for flat plate)
R_f = Final mean radius

However, the forming strain above accounts for forming flat plate into a cylinder only and does not account for the additional strain associated with expansion. Therefore, the total forming strain is the forming strain from rolling the plate into pipe and expansion of the pipe to the final dimensions. The total forming strain can be written as follows.

$$\varepsilon_{tf} = 100\left(\frac{R_{fe} - R_f}{R_f}\right) + \varepsilon_f$$

Where: R_{fe} = Final mean radius after expansion

9.4 GRADE X80 ELASTIC-PLASTIC MODEL DEVELOPMENT

The governing equations for strain as proposed in Section 9.2.1 have little sensitivity to actual material properties. However, using the minimum material requirements from API Specification 5L will provide more conservative safety margins than actual material properties when yield and tensile strengths exceed the minimum requirements. Using the minimum API Specification 5L requirements for yield strength, elastic modulus equal to 30 msi, and the strain hardening coefficient equal to 0.10 for expanded and aged linepipe steel which is discussed in Sect. 7, the governing equations for strain can be written as follows (σ_θ in psi).

$$\varepsilon_r = \frac{-0.30}{30 * 10^6}\sigma_\theta - \frac{0.30}{30 * 10^6}\sigma_z - 0.55\left(\frac{\sigma_z}{80.5 * 10^3}\right)^{\frac{1}{0.10}}$$

$$\varepsilon_\theta = \frac{\sigma_\theta}{30 * 10^6} - \frac{0.30}{30 * 10^6}\sigma_z - 0.40\left(\frac{\sigma_z}{80.5 * 10^3}\right)^{\frac{1}{0.10}}$$

$$\varepsilon_z = \frac{-0.3}{30 * 10^6}\sigma_\theta + \frac{\sigma_z}{30 * 10^6} + \left(\frac{\sigma_z}{80.5 * 10^3}\right)^{\frac{1}{0.10}}$$

Based on the ferritic steel coefficients specified in the ASME Boiler and Pressure Vessel Code, Section VIII Division 2, and the requirement for minimum elongation of Grade X80 linepipe steel in API Specification 5L, strain limit can be determined from the following equation.

$$\varepsilon_L = 0.13 * exp\left[-\left(\frac{2.2}{1 + 0.042}\right)\left(\frac{\sigma_\theta + \sigma_z}{3\sigma_e} - \frac{1}{3}\right)\right]$$

The forming strain for the pipe under consideration is (see chapter 6):

$$\varepsilon_{tf} = 1.1 + 2.0 = 3.1\%$$

Based on the plastic forming strain in the circumferential direction where $\sigma_r = \sigma_z = 0$, the effective forming strain, $\bar{\varepsilon}_{tf}$, can be determined as follows.

$$\varepsilon_r = -\upsilon_{r\theta e}\left(\frac{\sigma_\theta}{E_\theta}\right) - \upsilon_{r\theta p}\left(\frac{\sigma_\theta}{H_\theta}\right)^{\frac{1}{n_\theta}}$$

$$\varepsilon_\theta = \left(\frac{\sigma_\theta}{E_\theta}\right) + \left(\frac{\sigma_\theta}{H_\theta}\right)^{\frac{1}{n_\theta}}$$

$$\varepsilon_z = -\upsilon_{\theta ze}\left(\frac{\sigma_\theta}{E_\theta}\right) - \upsilon_{\theta zp}\left(\frac{\sigma_\theta}{H_\theta}\right)^{\frac{1}{n_\theta}}$$

Using the experimental monotonic properties from Chapter 7 and setting $\varepsilon_{tf} = \varepsilon_\theta$, the effective forming strain becomes:

$$\bar{\varepsilon}_{tf} = 3.0$$

Using this equation, the results of an elastic-plastic analysis based on the strain limit criterion are shown in Table 20 and Fig. 74. Values were determined for the limiting triaxial strain, effective plus forming strain, and the ratio of limiting strain to effective plus forming strain. Cyclic test data was generated for maximum total strain values up to 4%. Maximum longitudinal strain values of 5% have been generated. These values are outside the test data and should be considered for comparison purposes only. The effective strain is considered acceptable if:

$$\frac{\varepsilon_L}{\bar{\varepsilon} + \bar{\varepsilon}_{tf}} \geq 1.0$$

Values less than 1.0 shown in Table 21 as determined from the analysis would be considered unacceptable.

Table 20. Results of elastic-plastic analysis

Maximum Longitudinal Strain (%)	Internal Pressure (% SMYS)	ε_r	ε_θ	ε_z	σ_θ (ksi)	σ_z (ksi)	σ_e (ksi)	$\bar{\varepsilon}$	ε_L	$\bar{\varepsilon}+\bar{\varepsilon}_{tf}$	$\frac{\varepsilon_L}{\bar{\varepsilon}+\bar{\varepsilon}_{tf}}$
1	0.00	-0.40	-0.55	1.00	0.0	80.48	80.48	0.99	13.00	3.99	3.26
	0.50	-0.40	-0.55	1.00	40.3	80.48	69.70	0.99	7.77	3.99	1.95
	0.72	-0.40	-0.55	1.00	58.0	80.48	71.20	0.99	6.78	3.99	1.70
	0.80	-0.40	-0.55	1.00	64.4	80.48	80.50	0.99	6.60	3.99	1.65
	0.85	-0.40	-0.55	1.00	68.4	80.48	75.18	0.99	6.52	3.99	1.63
	0.90	-0.40	-0.55	1.00	72.5	80.49	76.79	0.99	6.47	3.99	1.62
2	0.00	-0.80	-1.10	2.00	0.0	86.27	86.27	1.98	13.00	4.98	2.61
	0.50	-0.80	-1.10	2.00	40.3	86.27	74.77	1.97	7.99	4.97	1.61
	0.72	-0.80	-1.10	2.00	58.0	86.27	76.17	1.97	6.93	4.97	1.39
	0.80	-0.80	-1.10	2.00	64.4	86.27	77.68	1.97	6.71	4.97	1.35
	0.85	-0.80	-1.10	2.00	68.4	86.27	78.88	1.97	6.61	4.97	1.33
	0.90	-0.80	-1.10	2.00	72.5	86.27	80.26	1.97	6.53	4.97	1.31
3	0.00	-1.20	-1.65	3.00	0.0	89.84	89.84	2.96	13.00	5.96	2.18
	0.50	-1.20	-1.65	3.00	40.3	89.84	77.94	2.96	8.12	5.96	1.36
	0.72	-1.20	-1.65	3.00	58.0	89.84	78.89	2.96	7.03	5.96	1.18
	0.80	-1.20	-1.65	3.00	64.4	89.84	80.21	2.96	6.79	5.96	1.14
	0.85	-1.20	-1.65	3.00	68.4	89.84	81.28	2.96	6.68	5.96	1.12
	0.90	-1.20	-1.65	3.00	72.5	89.84	82.53	2.96	6.59	5.96	1.10
4	0.00	-1.60	-2.20	4.00	0.0	92.46	92.46	3.95	13.00	6.95	1.87
	0.50	-1.60	-2.20	4.00	40.3	92.46	80.30	3.95	8.21	6.95	1.18
	0.72	-1.60	-2.20	4.00	58.0	92.46	80.93	3.95	7.10	6.95	1.02
	0.80	-1.60	-2.20	4.00	64.4	92.46	82.11	3.95	6.85	6.95	0.99
	0.85	-1.60	-2.20	4.00	68.4	92.46	83.09	3.95	6.73	6.95	0.97
	0.90	-1.60	-2.20	4.00	72.5	92.46	84.26	3.95	6.63	6.95	0.95
5	0.00	-2.00	-2.75	5.00	0.0	94.55	94.55	4.94	13.00	7.94	1.64
	0.50	-2.00	-2.75	5.00	40.3	94.55	82.18	4.93	8.28	7.93	1.04
	0.72	-2.00	-2.75	5.00	58.0	94.55	82.58	4.93	7.16	7.93	0.90
	0.80	-2.00	-2.75	5.00	64.4	94.55	83.65	4.93	6.90	7.93	0.87
	0.85	-2.00	-2.75	5.00	68.4	94.55	84.57	4.93	6.77	7.93	0.85
	0.90	-2.00	-2.75	5.00	72.5	94.55	85.67	4.93	6.66	7.93	0.84

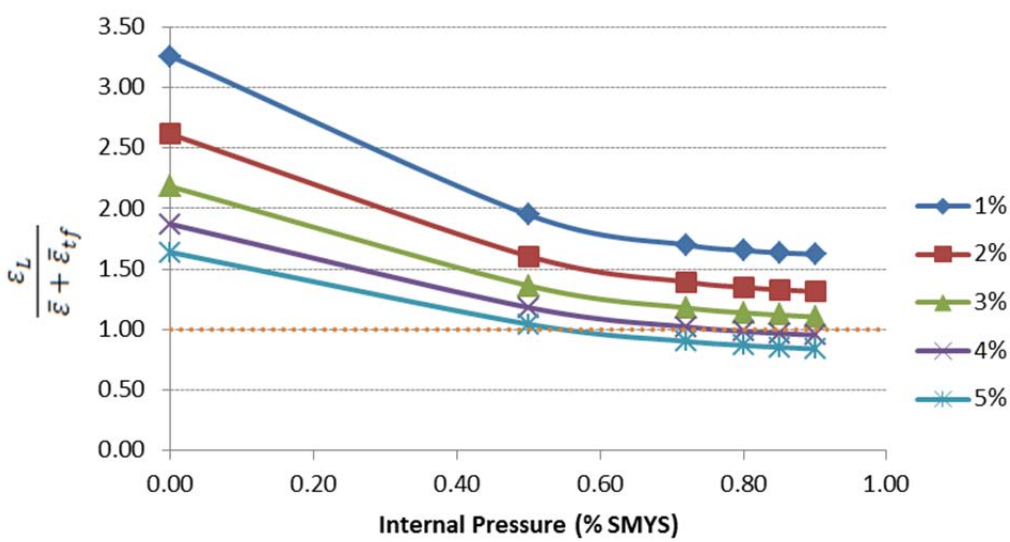

Fig. 74. Internal pressure vs $\frac{\varepsilon_L}{\bar{\varepsilon}+\bar{\varepsilon}_{tf}}$ based on maximum longitudinal strain.

10. PROTECTION AGAINST FAILURE FROM CYCLIC LOADING

10.1 OVERVIEW

The fatigue or endurance limit for linepipe steel is a value of stress at which the number of cycles becomes so large that fatigue failure is no longer a plausible pipeline design consideration. Typical values of the endurance limit for conventional linepipe steels are approximately half of the ultimate strength. Based on the minimum ultimate strength of Grade X80 linepipe steel in the API 5L Specification, the estimated endurance limit stress for this material is 45 ksi. However, according to the elastic-plastic analysis method described in Sect. 9, a fatigue evaluation must be performed for Grade X80 linepipe steel on the basis of the number of applied cycles of stress and strain.

The Twice Yield ($2S_y$) fatigue assessment method that is based on the calculation of an effective strain range to evaluate fatigue damage and results obtained from an elastic-plastic stress analysis was originally described by Kalnins [31, 32] and later incorporated into rules in the ASME Boiler and Pressure Vessel Code Section VIII Division 2. This Twice Yield Method is an elastic-plastic stress analysis approach that is performed in a single loading step. It is based on a stabilized cyclic stress-range-strain-range curve and a specified load range that represents one cycle. Stress and strain ranges are the direct output from this analysis. This method is performed in the same manner as a monotonic analysis and does not require cycle-by-cycle analysis. However, discussions in Sect. 8 indicate that use of cyclic stress-strain curves and determinations of material constants from uniaxial loading is an important design consideration for pipeline constructed using Grade X80 linepipe steel.

10.2 FATIGUE ANALYSIS METHOD

The cyclic stress-strain equations needed for a fatigue analysis are derived in the same manner as the elastic-plastic stress-strain equations that are derived using the Ramberg-Osgood format except with cyclic loading constants rather than monotonic loading constants. The alternating elastic and plastic components of the strain equations for the k_{th} cycle due to applied cyclic tensile displacement in the longitudinal direction are written as follows.

$$\varepsilon_{az,k} = \varepsilon_{aze,k} + \varepsilon_{azp,k}$$

Where:

$$\varepsilon_{aze,k} = \frac{\sigma_{az,k}}{E'_z}$$

$$\varepsilon_{azp,k} = \left(\frac{\sigma_{az,k}}{H'_z}\right)^{\frac{1}{n'_z}}$$

As discussed in Sect. 8, the cyclic alternating strain equations for the k_{th} cycle is written as follows using the cyclic material constants. These equations are based on the assumptions of plane stress (σ_r=0) and anisotropic material properties.

$$\varepsilon_{ar,k} = -\upsilon_{r\theta e}\left(\frac{\sigma_{a\theta,k}}{E'_\theta}\right) - \upsilon_{rze}\left(\frac{\sigma_{az,k}}{E'_z}\right) - \upsilon_{rzp}\left(\frac{\sigma_{az,k}}{H'_z}\right)^{\frac{1}{n'_z}}$$

$$\varepsilon_{a\theta,k} = \left(\frac{\sigma_{a\theta,k}}{E'_\theta}\right) - \upsilon_{\theta ze}\left(\frac{\sigma_{az,k}}{E'_z}\right) - \upsilon_{\theta zp}\left(\frac{\sigma_{az,k}}{H'_z}\right)^{\frac{1}{n'_z}}$$

$$\varepsilon_{az,k} = -\upsilon_{\theta ze}\left(\frac{\sigma_{a\theta,k}}{E'_\theta}\right) + \left(\frac{\sigma_{az,k}}{E'_z}\right) + \left(\frac{\sigma_{az,k}}{H'_z}\right)^{\frac{1}{n'_z}}$$

The equivalent cyclic stress in terms of principal cyclic stresses for the k_{th} cycle is given by the following equation.

$$\sigma_{ae,k} = \sqrt{\frac{1}{2}\left[\left(\sigma_{a\theta,k} - \sigma_{az,k}\right)^2 + \left(\sigma_{a\theta,k}\right)^2 + \left(\sigma_{az,k}\right)^2\right]}$$

The effective strain equation, which is a function of the principal strains for the k_{th} cycle and the weighted average of strain ratio, can be written as follows.

$$\bar{\varepsilon}_{a,k} = \frac{1}{\sqrt{2}(1+\bar{\upsilon})}\sqrt{\left(\varepsilon_{ar,k} - \varepsilon_{a\theta,k}\right)^2 + \left(\varepsilon_{a\theta,k} - \varepsilon_{az,k}\right)^2 + \left(\varepsilon_{az,k} - \varepsilon_{ar,k}\right)^2}$$

10.3 FATIGUE ASSESSMENT

Resistance to fatigue damage for smooth round-bar Grade X80 linepipe steel test specimen is given by the S-N (stress vs. fatigue life) curves shown in Sect. 8. The design fatigue curves published in ASME Boiler and Pressure Vessel Code Section VIII Division 2 are based primarily on strain controlled fatigue tests of small polished smooth round-bar test specimens. These design fatigue curves are included in the ASME Code to serve as the basis for fatigue assessments. In this study, these design fatigue curves are used as the basis for development of similar design fatigue curves needed to assess fatigue damage to pipelines constructed using Grade X80 linepipe steel discussed in Sect. 10.4.

A best-fit to the experimental data used as the basis for the design fatigue curves in the ASME Code was obtained by applying the method of least squares to the logarithms of the experimental values. The resulting design stress values are based on a factor of two (2) on stress or a factor of twenty (20) on cycles, whichever is more conservative. These design stress margins are not intended to be factors of safety, but rather to account for real effects identified by cyclic testing [71]. However, a margin for atmospheric conditions was implemented to reflect industrial atmospheric environmental effects on material behavior in comparison to the relatively benign air-conditioned environment in a testing laboratory.

The factor of twenty used in the ASME Code design fatigue curves is based on the following subfactors [30, 71].

- Scatter of data – 2.0
- Size effect – 2.5
- Surface finish, atmosphere – 4.0

A factor of twenty on the number of cycles has no significant effect at a high number of cycles so a factor of two on stress was introduced as a margin at the higher number of cycles. It was found that a factor of two on stress produced a border between low-cycle fatigue and high-cycle fatigue at approximately 10,000 cycles.

Most S-N curves are based on zero mean stress (R = -1). If data approximate a straight line on a log-linear plot, the following equation can be fitted to obtain a mathematical expression of the data.

$$\sigma_a = \sigma'_f \left(2N_f\right)^b$$

A strain versus life curve can be employed in the strain-based approach for making life estimates in a manner similar to the S-N curve in the stress-based approach. The elastic strains often give a straight line of shallow slope on a log-log plot. Equations can be fitted to provide the strain-life constants as follows.

$$\varepsilon_{pa} = \varepsilon'_f \left(2N_f\right)^c$$

However, S-N curves that include data for various mean stresses are available for commonly used engineering materials. When specific data are not available, there are several approaches to account for mean stress effects as discussed in Sect. 4.3. Conclusions from other fatigue assessment studies are summarized below [63].

- At very short lives, it is expected that stress-life data will approach true fracture strength from a monotonic tension test, which is noted to be the intercept at one-half cycle. However, where the data flatten at short lives, cyclic true fracture strength may considerably exceed the monotonic true fracture strength depending on curve fit and range of data available [36]

- The Goodman method employing the ultimate tensile strength $\sigma_u$is highly inaccurate and should not be employed where life estimates are desired in fatigue analysis.

- The Morrow equation with the true fracture strength $\bar{\sigma}_{fB}$ is reasonably accurate in most cases when the true fracture strengths are available. However, it is highly inaccurate and nonconservative for materials with log-log stress behavior that flattens at short lives.

- The Morrow method with the intercept constant σ'_f is also reasonably accurate for steels

- The Smith, Watson, Topper (SWT) method provides good results in most cases. The SWT method has the advantage of simplicity and is a good choice for general use although not as accurate as the Morrow method with σ'_f.

- Where data are available for fitting the adjustable parameter γ, the Walker method gives superior results.

- Values of the Walker parameter γ decrease with ultimate tensile strength σ_u. For steels, values range from around 0.8 for low σ_u down to around 0.4 for high σ_u. The Walker parameter can be estimated from:

$$\gamma = -.0002000\sigma_T + 0.8818 \ (\sigma_T \ in \ MPa)$$

The trend of decreasing Walker parameter for higher strength steels indicates an increasing sensitivity to mean stress. Using the Walker parameter that varies from 0.4 to 0.8 based on material properties is preferable to the SWT method which corresponds to a fixed $\gamma = 0.5$ [81].

When loading occurs under a multiaxial stress or stain state with plastic deformation, uncertainty exists for complex nonproportional loadings where the ratios of the principal stresses change and where the principal axes may also rotate. For these situations, the cyclic stress-strain curves and strain-life curves need to be used in a more general form. For biaxial loading under constant amplitude and approximately proportional loadings, a modification to the strain-life equation has been proposed based on the triaxiality factor-effective strain as discussed in Sect. 9.3 [73]. This modification is reflected in the following equations.

$$\bar{\varepsilon}_a = \frac{\sigma_f'}{E'}\left(2N_f\right)^b + 2^{1-T}\varepsilon_f'\left(2N_f\right)^c$$

where:

$$T = \frac{\sigma_r + \sigma_\theta + \sigma_z}{\sigma_a}$$

The effective strain approach is limited in combined loadings that are in phase or 180° out-of-phase provided there are no steady loadings that cause substantial rotation of the principal stress axes during cyclic loadings. When loadings are nonproportional to a significant degree, a critical plane approach is appropriate for estimating fatigue life [36]. In the critical plane approach, stresses and strains during cyclic loading are determined for various orientations (planes) in the material, and the stresses and strains acting on the most severely loaded plane are used to predict fatigue failure. Crack initiation and growth depends on many factors including magnitude of stress, strain, and material properties.
There are two distinct modes of crack initiation. Mode I loading occurs when the tensile stress is applied normal to the crack plane. This mode tends to open the crack. Mode II corresponds to in-plane shear loading acting parallel to the plane of the crack. This mode tends to slide one crack face with respect to the other. Tensile cracking is most likely to occur under equal biaxial stress loading conditions but is also common under uniaxial stress loading conditions. Shear cracking is most likely to occur at high strains, but may occur even at low strains under pure shear loading conditions. A reasonable approach for tensile stress dominated cracking is to employ the SWT parameter as follows.

$$\sigma_{max}\varepsilon_a = \frac{\left(\sigma_f'\right)^2}{E'}\left(2N_f\right)^{2b} + \sigma_f'\varepsilon_f'\left(2N_f\right)^{b+c}$$

Where:

ε_a = the largest amplitude of normal strain for any plane
$\sigma_{\max}$ = maximum normal stress on the same plane as ε_a

The largest amplitude of normal strain and maximum normal stress can be related to the principle strains and stresses as follows.

$$\varepsilon_a = \sqrt{\varepsilon_{ar}^2 + \varepsilon_{a\theta}^2 + \varepsilon_{az}^2}$$

$$\sigma_{max} = \sqrt{\sigma_r^2 + \sigma_\theta^2 + \sigma_z^2}$$

Crack growth due to shear stress alone is resisted by mechanical interlocking of the grain structure and friction effects due to irregularities of the crack face (see Fig. 75).

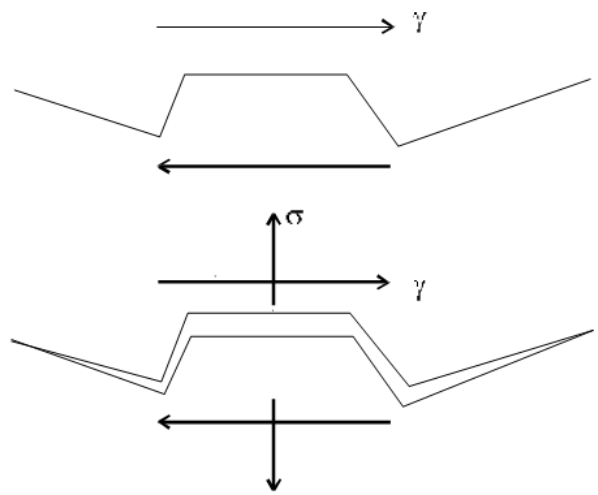

Fig. 75. Crack growth in pure shear and where normal stress enhances crack growth [74].

Several proposals for analyzing shear dominated cracking have been suggested. They are based on strain-life fatigue material constants obtained from completely reversed tests in pure shear such as torsion tests on thin-walled tubes. One such relationship proposed by Fatemi and Socie follows [74].

$$\gamma_{ac}\left(1+\frac{k\sigma_{n,max}}{\sigma'_Y}\right)=\frac{\tau'_f}{G}\left(2N_f\right)^b+\gamma'_f\left(2N_f\right)^c$$

Where:

γ_{ac} = largest amplitude of shear strain for any plane,
$\sigma_{n,max}$ = maximum tensile stress normal to the plane of γ_{ac} occurring during the γ_{ac} cycle
k = an empirical material constant (ranging from 0.6 to 1.0)
σ'_Y = yield strength for the cyclic stress-strain curve
τ'_f, b, γ'_f, c = constants from strain life curve

The shortest life estimate determined from the SWT and Fatemi and Socie equations becomes the final life estimate. The need to perform two separate calculations reflects the two possible modes of cracking.

10.4 GRADE X80 FATIGUE MODEL DEVELOPMENT

The cycle properties near half-life that are listed in Sect. 8 based on smooth bar fatigue curves are used to represent the stabilized stress-strain cycle for the Twice Yield Method fatigue evaluate of Grade X80 linepipe steel. Because pipelines usually do not operate at internal pressures ranging from ambient to slight vacuum, stress-controlled fatigue data may be more conservative for variable pressure loads. The same longitudinal strains and internal pressures reported in Sect. 9 are used to illustrate the Twice Yield Method for Grade X80 linepipe.

- Internal pressure loadings range from zero to a maximum operating pressure. The stress amplitude due to pressure is half the pressure range. A mean stress equation will be necessary to adjust for the predicted life estimate.

- Longitudinal strains range from a mean strain of zero. Therefore, the maximum range is twice the maximum strain.

While the Walker equation discussed in Sect. 4.3 can be used to fit fatigue life test data using completely reversed loading to establish the Walker parameter γ, this study did not provide enough data to accurately determine a stress-life relationship. However, the Walker parameter was estimated to be γ = 0.757 based on the minimum ultimate tensile strength as required by API Specification 5L. To determine the expected fatigue life from completely reversed data reported in Sect. 8, the Walker equation can be used to estimate the circumferential stress amplitude (R = 0) based on the maximum internal pressure follows.

$$\sigma_{ar} = \sigma_{max}\left(\frac{1-R}{2}\right)^{\gamma} = 0.592\sigma_{max}$$

For both restrained and unrestrained pipelines, the maximum circumferential stress is due to internal pressure is calculated as:

$$\sigma_{max} = \frac{PD}{2t}$$

Where:

P = internal pressure
D = outside diameter
t = wall thickness

Fatigue analysis models incorporate cyclic dependent material properties from the selected cycle near half-life as shown in Sect. 8 including $E'_{\theta} = 30$ msi and $E'_{z} = 26$ msi. The strain hardening exponent, n`, and fitting constant, *b*, were shown to be dependent on stress amplitude. A fatigue assessment based on an elastic-plastic stress analysis and equivalent strains results are shown in Table 21 and Fig. 76.

Table 21. Results of Fatigue Analyses

Longitudinal Strain Amplitude (%)	Internal Pressure (% SMYS)	Equivalent Stress Amplitude σ_{a0} (ksi)	n'_z	b	ε_{ar}	ε_{a0}	σ_{az}(ksi)	σ_{ae}(ksi)	$\bar{\sigma}$	Cycles based on Triaxiality Parameter	Cycles based on SWT Parameter
0.50	0.00	0.00	0.210	-0.064	-0.20	-0.27	69.52	69.52	0.49	341	173
	0.50	23.83			-0.20	-0.27	69.52	61.19	0.49	157	149
	0.72	34.31			-0.20	-0.27	69.52	60.21	0.49	114	129
	0.80	38.12			-0.20	-0.27	69.52	60.30	0.49	101	122
	0.85	40.51			-0.20	-0.27	69.52	60.48	0.49	94	116
	0.90	42.89			-0.20	-0.27	69.52	60.75	0.49	88	111
1.00	0.00	0.00	0.093	-0.028	-0.40	-0.55	80.48	86.27	0.99	51	26
	0.50	23.83			-0.40	-0.55	80.48	71.60	0.99	26	23
	0.72	34.31			-0.40	-0.55	80.48	69.95	0.99	19	21
	0.80	38.12			-0.40	-0.55	80.48	69.73	0.99	18	20
	0.85	40.51			-0.40	-0.55	80.48	69.70	0.99	17	19
	0.90	42.89			-0.40	-0.55	80.48	69.75	0.99	16	18
1.50	0.00	0.00	0.058	-0.018	-0.60	-0.83	82.41	82.41	1.48	15	8
	0.50	23.83			-0.60	-0.83	82.41	77.94	1.48	8	7
	0.72	34.31			-0.60	-0.83	82.41	71.70	1.48	6	6
	0.80	38.12			-0.60	-0.83	82.41	71.44	1.48	6	6
	0.85	40.51			-0.60	-0.83	82.41	71.37	1.48	5	6
	0.90	42.89			-0.60	-0.83	82.41	71.39	1.48	5	6
2.00	0.00	0.00	0.043	-0.013	-0.80	-1.10	82.93	82.93	1.97	7	4
	0.50	23.83			-0.80	-1.10	82.93	73.95	1.97	4	3
	0.72	34.31			-0.80	-1.10	82.93	72.18	1.97	3	3
	0.80	38.12			-0.80	-1.10	82.93	71.90	1.97	3	3
	0.85	40.51			-0.80	-1.10	82.93	71.83	1.97	3	3
	0.90	42.89			-0.80	-1.10	82.93	71.83	1.97	2	3

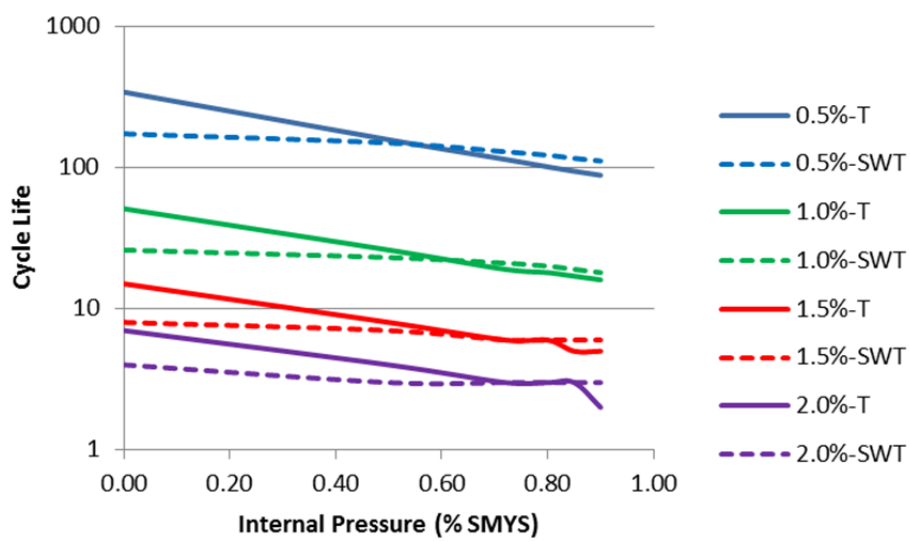

Fig. 76. Internal pressure vs cycle life based on allowable longitudinal strain amplitude using the triaxiality (T) Parameter and Smith, Watson, Topper (SWT) parameter.

11. OBSERVATIONS AND CONCLUSIONS

This research involved development of proposed tensile strain design models for use in design of natural gas and hazardous liquid transmission pipelines where ground movement could produce plastic strains in the linepipe steel. The models (1) are based on experimental data obtained from Grade X80 linepipe steel test specimens, (2) demonstrate the impact of material anisotropy on tensile strain capacity, and (3) characterize the overall trend of strain-based design of pipelines constructed using Grade X80 linepipe steel. The target optimum strain range of the proposed models is from 1% to 4%. Results of this research are intended to provide a technical basis for the development of industry guidelines for strain-based design of transmission pipelines and possible use by national code and consensus standard committees in the development of rules for pipelines construction using Grade X80 linepipe steel. Based on the results and analysis, the following observations have been made.

- Successful application of strain-based design methods compared to traditional stress-based design methods requires complete understanding of linear, nonlinear, and cyclic mechanical properties of the linepipe steel under the conditions in which the linepipe is installed. Linepipe can be expanded up to 1.5% to recover tensile strength and control the final dimensions. It is also important to note that the thermal cycle associated with the application of an external pipe coating can result in a change in the linepipe tensile and cyclic properties. Since the linepipe is received in the expanded condition and coated prior to installation, these final properties will govern material behavior and should be given proper consideration in the final design analysis. The material specification provided by the purchaser needs to consider both the effect of expansion and thermal aging to ensure the properties are suitable for the operating conditions.

- For strain-based design methods, it is important to model the entire stress-strain behavior and to remember that tensile test data are affected by specimen dimensions, instrumentation, and even post-data processing. Research results discussed in this dissertation suggest that the effect of test procedures on test results should be factored into material specification development for Grade X80 linepipe. In addition, tensile properties can have variations within the same material specification and should also be considered in the design and material selection. Material specifications for Grade 80X linepipe should prescribe both the required minimum and maximum property values (yield, ultimate, and elongation) and the test protocols that will produce the required material properties data.

- Small-scale testing such as the testing that was conducted as part of this research effort typically produces more conservative results when compared to full-scale testing. Consequently, the proposed tensile strain design models that are based on these data have an inherent safety factor. Plastic collapse load calculations need to include applicable stress and strain limits that are derived from the envelope of test data and application of a design factor that is based on inspection of the test results.

- Most stress design methods prescribe stress reduction factors for use when various load case combinations are combined. However, for pipeline applications where it is unlikely that maximum magnitudes of multiple, time-varying loads, particularly multi-axial loads, will occur simultaneously, engineering judgment must be applied to establish appropriate reduction factors. These factors are applied to the type of stress or strain consistent with the loading conditions and depend on consideration and understanding of mechanical properties test results.

Based on the test results and analysis, the following conclusions can be made.

- Increasing strain capacity is possible by controlling material specification limits to provide confidence in material behavior. Material specifications should also lend consideration to specifying a minimum uniform longitudinal elongation to avoid strain localization. It is important that material specifications for strain-based design include the measurement of longitudinal properties that include minimum and maximum limits on tensile properties.

- Lüder's elongation which was observed in the expanded and aged condition is undesirable in strain-based design applications because it can lead to strain localization. Lüder's yielding is currently a focus of research for pipe mills to include sufficient carbon and nitride formers in combination with optimized processing to minimize the potential in the as-received and aged conditions. For strain-based design applications, it is desirable to avoid a sharp yield transition in the stress-strain curve or a drop in the yield strength. These characteristics can increase the strain demand while decreasing the strain capacity.

- When mean stress adjustments are needed in making strain-based fatigue life estimates, several methods are available using material data from completely reversed-controlled strain data where the mean strain or stress is at or near zero. The Walker mean stress equation with adjustable constant γ gives superior results where γ is known or can be estimated. However, not all standards require the designer to consider adjustment for the effects of mean stress and strain. The ASME Boiler and Pressure Vessel Code Section VIII Division 2 referenced design fatigue curves are already adjusted for the maximum possible effect of mean stresses and strains.

- Most codes apply fatigue strength reduction factors. They are defined as anything that reduces fatigue life compared to the polished smooth specimens used to generate the fatigue curves. They are a ratio of the fatigue strength without the reducing factor to the fatigue strength with the reducing factor and typically should be based on test data. These reduction factors are usually associated with welding but also apply to geometric abnormalities, local stress discontinuities, material flaws, or environmental concerns. The value of the reduction factor is dependent on the level of testing, inspection, and operational histories.

- The incorporation of the Walker equation into the strain-life curve is a promising approach that should be further evaluated and employed. Future work on mean stress equations should concentrate on the Walker relationship, such as identifying generic values of γ for pipeline steels, or developing correlations for estimating γ from monotonic tensile properties.

12. SUGGESTIONS FOR FUTURE WORK

Strain-based design technology for transmission pipeline applications using Grade X80 linepipe steel is not sufficiently validated and significant work remains. The tensile strain design models and recommendations presented are not intended to be used in lieu of applicable national and international codes and standards. Users of the prediction models will need to ensure the model is appropriate for their material, design, construction, as well as operational and environmental conditions. However, no single approach may be appropriate for all circumstances. It is expected further work introduced by this dissertation will be expanded and refined by additional work in this area.

- There is a need for a continued joint industry approach for establishment of testing requirements for validation of material properties and the possible development of minimum materials performance guidelines in lieu of prescriptive material requirements. The variation of linepipe tensile properties needs to be better understood and quantified. This process will involve more rigorous inspection of testing procedures and consistent post-data processing procedures. Statistical distributions for both the circumferential and longitudinal properties should be provided to include mean values and standard deviation for:

  - Yield strength
  - Ultimate strength
  - Uniform elongation
  - Total elongation

- Additional fatigue experimental data with varying mean stress is necessary to accurately predict the Walker parameter and provide better accuracy of the material fatigue constants.

- Continued development of closed-form solutions, expressed in terms of experimentally established stresses and strains from axial-torsional data, to be used to establish the material's damage parameter versus fatigue life would be useful for complex nonproportional loadings. The closed form solution would identify the most critical plane and hence the largest damage parameter for many widely adopted damage criteria.

Large-scale testing using full-scale pressurized linepipe covering all aspects of the proposed models and adequate ranges are important for model validation. It is not believed that sufficient material characterization and model validation exists to generate sufficient FEA models.

REFERENCES

[1] A. Liessem et al., *Investigation of the Stress-Strain Behaviour of Large-Diameter X100 Linepipe in View of Strain-Based Design Requirements,* Proceedings of IPC2008 7th International Pipeline Conference, Calgary, Alberta: Canada, 2008.

[2] M. Murata et al, *Development and Commercialization of High Strength Linepipe up to X120,* Proceedings of X80 & HGLPS 2008: International Seminar on X80 and Higher Grade Line Pipe Steel 2008, June 23-24, 2008, Xi'an, China, 185-191.

[3] R. Klein et al., *Determination of Mechanical Properties of High Strength Linepipe,* Proceedings of IPC2008 7th International Pipeline Conference*,* Calgary, Alberta: Canada, 2008.

[4] S. Felber, Pipeline Engineering Part 1, *Welding Research Council Bulletin 1001,* New York, NY: The Welding Research Council, 2009.

[5] W. Ramberg and W. R. Osgood, "Description of stress-strain curves by three parameters," *Technical Note No. 902*, National Advisory Committee for Aeronautics, Washington DC., 1943.

[6] H. Gao et al., *The Concepts for Pipeline Strain-Based Design.* Proceedings of the Seventeenth International Offshore and Polar Engineering Conference, Lisbon, Portugal, 476-482, 2010.

[7] S. T. Barbas and M. S. Weir, *Strain-based Design Methodology for Seismic and Artic Regions,* Proceedings of the Seventeenth International Offshore and Polar Engineering Conference, Lisbon, Portugal, July 1-6, 2007, 3073-3080, 2007.

[8] X. Wang et al., "Strain-based Design–Advances in Prediction Methods of Tensile Strain Capacity," *International Journal of Offshore and Polar Engineering*, 1-7. Retrieved from http://www.isope.org/publications, 2011.

[9] Y. Y. Wang et al., "Second Generation Models for Strain-Based Design," *Pipeline Research Council International,* Catalog No. L5XXXX, 2011.

[10] Y. Y. Wang et al., *Strain Based Design of Pipelines,* 16th Joint Technical Meeting of the Australian Pipeline Industry Association, 2007.

[11] A. Glover et al., *Technology approaches for Northern pipeline developments,* Proceedings of the International Pipeline Conference IPC*,* Calgary, Alberta, 503-515, 2002.

[12] K. Nagai et al., *Anisotropic Strain Aging Behavior of High Strength UOE Linepipes,* Proceedings of the Nineteenth (2009) International Offshore and Polar Engineering Conference, Osaka, Japan, June 21-26, 2009, 56-60, 2009.

[13] W. C. Mohr et al., *Strain-Based Design of Pipelines.* Edison Welding Institute, Project # 45892GTH, US Department of Interior and US Department of Transportation, Columbus, Ohio, 2003.

[14] M. L. Macia et al., *Approaches to Qualify Strain-Based Designed Pipelines*. Proceedings of the 8th International Pipeline Conference*,* Calgary, Alberta: Canada, 2010.

[15] ASME B31.8, *Gas Transmission and Distribution Piping Systems.* American Society of Mechanical Engineers*.* New York, New York, 2012.

[16] ASME B31.4, *Pipeline Transportation Systems for Liquids and Slurries*, American Society of Mechanical Engineers, New York, New York, 2012.

[17] X. K. Zhu and B. N., *Effect of Axial Tensile Strain on Yield Load-Carrying Capacity Of Pipelines,* Proceeding of the 8th International Pipeline Conference, 2010, Calgary, Alberta: Canada, 2010.

[18] S. Igi, and T. Sakimoto, *Tensile Strain Capacity of X80 Linepipe in Full Scale Test*, Proceedings of the Twentieth International Offshore and Polar Engineering Conference, 489-495, 2010.

[19] B. Liu et al., *Tensile Strain Capacity of Pipelines For Strain-Based Design.* Proceedings of IPC2008 7th International Pipeline Conference, Calgary, Alberta: Canada, 2008.

[20] W. Cimbali et al., Structural Reliability Approach to Strain Based Design of Offshore Pipelines. *Proceedings of the Seventeenth International Offshore and Polar Engineering Conference*, 56-60, 2002.

[21] M. Baker et al., "Strain-Based Design and Assessment: State-of-Art Review (SBDA-1)," Pipeline Research Council International, Catalog No. PR-415-124508-R01 (2012).

[22] Det Norske Veritas, *Fracture Control for Pipeline Installation Methods Introducing Cyclic Plastic Strain*, *Recommended Practice DNV-RP-F108*, 2006.

[23] Y. Y. Wang and M. Liu, *The Role of Anisotropy, Toughness Transferability, and Weld Misalignment in the Strain Based Design of Pipelines.* Proceedings of the Seventeenth International Offshore and Polar Engineering Conference, 3164-3171, 2007.

[24] S. Kibey et al., *Tensile Strain Capacity Equations For Strain-Based Design of Welded Pipelines.* Proceedings of the 8th International Pipeline Conference, Calgary, Alberta: Canada, 2010.

[25] M. Liu et al., *Multi-tier Tensile Strain-Based Design Part 2 – Development and Formulation of Tensile Strain Capacity Models,* Proceedings of the 2012 9th International Pipeline Conference, Calgary, Alberta: Canada, 2012.

[26] Y. Y. Wang et al., *A Quantitative Approach To Tensile Strain Capacity of Pipelines,* Proceedings of IPC2006 6th International Pipeline Conference 2006, Calgary, Alberta: Canada, 2006.

[27] W. Guijt et al., *Safety Concept in The New Dutch Pipeline Standard NEN 3650*, Proceeding of the Fourteenth International Offshore and Polar Engineering Conference, France, 2004.

[28] S. Hohler et al., *Analytical approach of limit state assessment for multi-axially loaded UOE linepipe,* Proceedings of the International Offshore and Polar Engineering Conference, 421-428, 2010.

[29] A. Liessem et al., "Production and Development Update of X100 for Strain-Based Design Application," *Journal of Pipeline Engineering, V.9,* 2010.

[30] Y. Shinohara et al., *Anisotropic Damage Behavior in High Strength Line Pipe Steels*, Proceedings of the Seventeenth International Offshore and Polar Engineering Conference, 446-452, 2010.

[31] American Petroleum Institute, *Specification for Line Pipe, ANSI/API Specification 5L*. (45th ed.), Washington, DC, 2012.

[32] M. Law, *Review of Strain Based Analysis for Pipelines,* ANSTO Materials and Engineering Science, 1-7, 2007.

[33] ASTM A370, *Standard Test Methods and Definitions for Mechanical Testing of Steel Products,* ASTM International, Pennsylvania, USA, 2009.

[34] ASTM E8/E8M. *Standard Test Methods for Tension Testing of Metallic Materials.* ASTM International, Pennsylvania, USA, 2012.

[35] D. G. Stalheim et al., *Alloy Design Concepts for High Strength Coil for Gas Transmission Spiral Pipe,* Proceedings of X80 and HGLPS 2008: International Seminar on X80 and Higher Grade Pipe Line Steel 2008, China, 2008.

[36] N. E. Dowling, *Mechanical Behavior of Materials: Engineering Methods for Deformation, Fracture, and Fatigue,* Upper Saddle River, NJ: Pearson Education, Inc., 2007.

[37] D. Porter et al., "Performance of TMCP steel with respect to mechanical properties after cold forming and post-forming heat treatment," *International Journal of Pressure Vessels and Piping* **81**, 867-877, 2004. Retrieved from http://www.elsevier.com/locate/ijpvp/.

[38] N. S. Mourino et al., "Texture Dependent Mechanical Anisotropy of X80 Pipeline Steel," *Advanc̃ed Engineering Materials* **12**(10), 973-980, 2010, doi:10.1002/adem.201000065.

[39] S. Neupane et al., *Modeling Approaches for Anistropic Material Properties of High Strength Steel Pipelines and the Effect on Differential Settlement*, Proceedings of the 8th International Pipeline Conference, Calgary, Alberta: Canada, 2010.

[40] Y.-Y. Wang, "Tensile Strain Limits and Material Specifications for Strain-Based Design of Pipelines," *International Forum on X100/X120 High Performance Pipe Steels,* 2005.

[41] Y. Bian et al., *Evaluation of UOE and Spiral-Welded Line Pipe for Strain Based Designs*, Proceedings of the 8th International Pipeline Conference, Calgary, Alberta: Canada, 2010.

[42] K. Kang et al., *Buckling Behavior of API-X80 Linepipe,* Proceedings of the Seventeenth International Offshore and Polar Engineering Conference, 3254-3260, 2007.

[43] C. M. J. Timms et al., *Compressive Strain Limits of Large Diameter X80 UOE Linepipe,* Proceedings of the Seventeenth International Offshore and Polar Engineering Conference, 181-189, 2009.

[44] Y. Shinohara et al., *Change of Mechanical Properties of High Strength Line Pipe by Thermal Coating Treatment,* Proceedings of the 24th International Conference on Offshore Mechanics and Artic Engineering, 27-34, 2005.

[45] E. Tsuru et al., *Evaluation Precept for Strain Capacity of High Strength UOE Line Pipes Used in Strain-based Design Applications,* Proceedings of the Seventeenth International Offshore and Polar Engineering Conference, 3172-3178, 2007.

[46] Y. Shinohara et al., *Development of A High Strength Steel Line Pipe for Strain-based Design Applications,* Proceedings of the Seventeenth International Offshore and Polar Engineering Conference, 2949-2954, 2007.

[47] M. Okatsu et al., *Development of High Deformability Linepipe With Resistance To Strain-Aged Hardening By Heat Treatment On-Line Process,* Proceedings of X80 & HGLPS 2008: International Seminar on X80 and Higher Grade Line Pipe Steel 2008, Xi'an, China, 2008.

[48] S. Zimmermann et al., *Resistance of High Strength Helical Seam Welded Line Pipe to Pressure Containment*. 3R International – Special Edition 2/2010, 2010.

[49] D. Duan et al., *Strain Aging Effects in High Strength Line Pipe Materials,* Proceedings of IPC2008 7th International Pipeline Conference, Calgary, Alberta: Canada, 2008.

[50] J.-Y. Yoo et al., *Development of X80/X100 Linepipe Steels with High Strain Aging Resistance,* Proceedings of the Eighteenth International Offshore and Polar Engineering Conference, 21-26, 2008.

[51] S. S. Yun and Y. W. Chang, "Influence of Baushinger Effect on Yield Strength after Pipe Forming," *Materials Science Forum* **475-479**, 4103-4108*,* 2005.

[52] L. Wang and P. Jia, "Study on Bauschinger Effect in X80 Steel Under Axial Loading and Bending," *Advanced Materials Research* **197-198**, 1686-1689*,* 2011.

[53] Det Norske Veritas, Offshore Standard DNV-OS-F10, *Submarine Pipeline Systems*, 2013.

[54] G. Hohl et al., *The Effect of Specimen Type on Tensile Test Results and its Implications for Linepipe Testing,* 13th Biennial European Pipeline Research Group (EPRG)—Pipeline Research Council International Inc. (PCRI) Joint Technical Meeting, New Orleans, LA, April 30−May 3, 2001, Paper 15.

[55] R. D. Cook and W. C. Young, *Advanced Mechanics of Materials* (2nd Ed.), Upper Saddle River, NJ: Pearson-Hall, Inc., 1999.

[56] W. C. Kan et al., *Strain-Based Pipelines: Design Consideration Overview,* Proceedings of the Eighteenth International Offshore and Polar Engineering Conference, Vancouver, British Columbia, July 6-11, 2008. 174-181, 2008.

[57] S. Herion et al., *Low-cycle Fatigue Behavior of High-strength Steel Butt Welds,* Proceedings of the Twenty-first (2011) International Offshore and Polar Engineering Conference, Maui, Hawaii, USA, June 19-24, 2011, 282-287, 2011.

[58] ASTM E606/E606M, *Standard Test Method for Strain-Controlled Fatigue Testing.* ASTM International*,* Pennsylvania, USA, 2012.

[59] ASTM E132, *Standard Test Method for Poisson's Ratio at Room Temperature*, ASTM International, Pennsylvania, USA, 2010.

[60] ASME Boiler and Pressure Vessel Code, Section VIII, *Rules for Construction of Pressure Vessels, Division 2 Alternative Rules*, American Society of Mechanical Engineers*.* New York, New York, 2013.

[61] CSA Z662, *Oil and Gas Pipeline Systems,* Canadian Standards Association*,* Ontario, Canada, 2011.

[62] W. R. Tyson, *Effect of Biaxial Stress on ECA of Pipelines under Strain-Based Design,* Proceedings of the Seventeenth International Offshore and Polar Engineering Conference, Lisbon, Portugal, 3107-3113, 2007.

[63] N. E. Dowling, "Mean stress effects in strain-life fatigue," *Fatigue and Fracture of Engineering Materials and Structures* **32**, 1004-1019, 2009.

[64] Y. Wang, *Strain Based Design of High Strength Pipelines*, Proceedings of the Seventeenth International Offshore and Polar Engineering Conference, 3186-3193, 2007.

[65] W. C. Mohr, *Pressure Effects on Strain Concentration and Constraint for Strain-Based Design.* Proceedings of the Seventeenth International Offshore and Polar Engineering Conference, 3121-3128, 2007.

[66] S Igi and N. Suzuki, *Tensile Strain Limits of X80 High-strain Pipelines,* Proceedings of the Seventeenth International Offshore and Polar Engineering Conference, 3081-3087, 2007.

[67] P. W. Bridgeman, *Studies in Large Plastic Flow and Fracture with Special Emphasis on the Effects of Hydrostatic Stress, Harvard University Press*, Cambridge, Massachusetts, 1964.

[68] A. W. Van Der Sluys, "PVRC's Position on environmental effects on fatigue life in LWR Applications," WRC Bulletin 487, Welding Research Council, New York, N.Y., 2003.

[69] NTIS, US Department of Commerce, *Tentative Structural Design Basis for Reactor Pressure Vessels and Directly Associated Components (Pressurized, Water Cooled Systems)*, PB-151-987, 1958.

[70] The American Society of Mechanical Engineers, *Fitness-for-Service*, API 579-1/ASME FFS-1. (Second Edition), 2007.

[71] D. A. Osage, PTB-1-2009, ASME Section VIII-Division 2 (2009). Criteria and Commentary. American Society of Mechanical Engineers. New York, NY.

[72] C. Chu, Fatigue Damage Calculation Using the Critical Plane Approach, *Journal of Engineering Materials and Technology,* Dearborn, MI, 1995.

[73] R. H. Marloff et al., ASTM STP 853 Multiaxial Fatigue. *Biaxial Low-Cycle Fatigue of Cr-Mo-V Steel at 538° By Use of Triaxiality Factors,* pp. 637-650, Philadelphia, PA., 1985.

[74] D. F. Socie, and G. B. Marquis, *Multiaxial Fatigue*, Society of Automotive Engineers, Warrendale, PA, 2000.

[75] E. A. Davis and F. M. Connelly, *Transactions.* American Society of Mechanical Engineers, *Journal of Applied Mechanics, Series E.* **81**(1), 1959, pp. 25-30.

[76] N. E. Dowling, *Mean Stress Effects in Stress-Life and Strain-Life Fatigue*. Society of Automotive Engineers, Warrendale, PA, 2004.

[77] K. N. Smith et al., "A Stress-Strain Function for the Fatigue of Metals," *ASTM Journal of Materials* **5**(4), 1970.

[78] J. Goodman, *Mechanics Applied to Engineering*, Longmans, Green, and Co. London, 1919.

[79] J. Morrow, *Fatigue Properties of Metal,* Society of Automotive Engineers, Warrendale, PA., 1964.

[80] M. Prager, "Development of a Local Strain Criteria for Use with Elastic-Plastic Analysis," *WRC Bulletin in Preparation.*

BIBLIOGRAPHY

API 5L. 2004. *Specification for Line Pipe (*43rd ed.). American Petroleum Institute Washington, DC.

API 5L. 2007. *Specification for Line Pipe (*44rd ed.). American Petroleum Institute, Washington, DC.

API Standard 1104. 2013. Welding of Pipelines and Related Facilities. (21st ed.). American Petroleum Institute. Washington, DC.

ASTM E466. 2007. Standard Practice for Conducting Force Controlled Constant Amplitude Axial Fatigue Tests of Metallic Materials. *ASTM International,* Pennsylvania, USA.

ASTM E468. 2004. Standard Practice for Presentation of Constant Amplitude Fatigue Test Results for Metallic Materials. *ASTM International,* Pennsylvania, USA.

ASTM E739. 2010. Standard Practice for Statistical Analysis of Linear or Linearized Stress-Life (S-N) and Strain-Life (ε-*N*) Fatigue Data. *ASTM International,* Pennsylvania, USA.

Baker, M. Jr., Inc., CC Technologies, RMH Welding Consulting, Inc., & Visitless Integrity Assessment Ltd. 2008. *Comparison of US and Canadian Transmission Pipeline Consensus Standards.*

Chi, Q., et al. 2010. *Investigation on Strain-age of Large Diameter and Thick Wall X80 Grade Cold Bends.* Proceedings of the Seventeenth International Offshore and Polar Engineering Conference, 436-440.

Crone, D. G., et al. 2010. *The Effect of Sample Flattening on Yield Strength Measurement in Line Pipe.* Proceedings of the Twelfth International Offshore and Polar Engineering Conference*,* 9-16.

Gao, H., et al. 2007. *Strain-Based Design of X80 Gas Pipeline in Seismic Area in China.* Proceedings of the Seventeenth International Offshore and Polar Engineering Conference, 3088-3092.

Glover, A., et al. 2004. *Construction and installation of X100 pipelines*. Proceedings of the Biennial International Pipeline Conference, 2379-2388.

Gordon, J. R., et al. 2007. *Crack Driving Force in Pipelines Subjected to Large Strain and Biaxial Stress Conditions.* Proceedings of the Seventeenth International Offshore and Polar Engineering Conference, 3129-3140.

Hertele, S., et al. 2010. *Determination of Full Range Stress-Strain Behavior of Pipeline Steels Using Tensile Characteristics.* Proceedings of the 8th International Pipeline Conference. Calgary, Alberta: Canada.

Igi, S., et al. 2009. *Compressive and Tensile Stain Limit and Integrity of X80 High Strain Pipelines.* Proceedings of the Seventeenth International Offshore and Polar Engineering Conference, 190-196.

Igi, S., et al. 2010. *Tensile Strain Capacity of X80 Pipeline Under Tensile Loading With Internal Pressure*. Proceedings of the 8th International Pipeline Conference. Calgary, Alberta: Canada.

Liessem, A., et al. 2007. *Strain Based Design—What the Contribution of a Pipe Manufacturer Can Be.* Proceedings of the Seventeenth International Offshore and Polar Engineering Conference, 3156-3163.

Liu, M., et al. 2012. *Multi-Tier Tensile Strain Models For Strain-Based Design Part 3 – Model Evaluation Against Experimental Data.* Proceedings of the 2012 9th International Pipeline Conference. Calgary, Alberta: Canada.

Liu, M., et al. 2008. *Stress Analysis Of Pipe Lowering-In-Process During Construction*. Proceedings of IPC2008 7th International Pipeline Conference. Calgary, Alberta: Canada.

Li, X., et al. 2009. *Ultimate Bending Capacity of Steel Pipes Considering Strain Hardening Effect.* Proceedings of the Nineteenth International Offshore and Polar Engineering Conference, 514-520.

Lourenco, M. I., and T. A. Netto, 2010. Low Cycle Fatigue of Corroded Pipes Under Cyclic Bending And Internal Pressure. *Proceedings of the 8th International Pipeline Conference.* Calgary, Alberta: Canada.

Murray, A. February 4, 2011. "The Design and Construction of High Pressure Pipelines." PowerPoint lecture presented in Seattle, Washington, at the ASME India Oil & Gas Pipeline Conference.

Nagai, K., et al. 2010. *Anisotrophy Of The Stress-Strain Curves For Line Pipe Steels.* Proceedings of the 8th International Pipeline Conference. Calgary, Alberta: Canada.

Pyshmintsev, Y., et al. 2009. "Effects of Microstructure and texture on shear fracture in X80 linepipes designed for 11.8MPa gas pressure." *Pipeline Technology Conference*. Ostend, Belgium.

Scott, C., et al. 2008. *An Analysis of the Stresses Incurred in Pipe During Laying Operations*. Proceedings of IPC 2008 7th International Pipeline Conference. Calgary, Alberta: Canada.

Scott-Emuakpor, O., et al. 2012. "A new Distortion energy-based equivalent stress for multiaxial fatigue life prediction." *International Journal of Non-Linear Mechanics* **47**, 29-37.

Seo, D. H., et al. 2009. *Development of X80/X100 Linepipe Steel Plates and Pipes for Strain Based Design Pipeline.* Proceedings of the Seventeenth International Offshore and Polar Engineering Conference, 61-66.

Shiozawa, K., et al. 1995. *Biaxial Low-Cycle Fatigue Behavior of Long-Term-Used Cr-Mo-V Steel at Elevated Temperatures*

Stephens, M. J., et al. 2009. An Experimental Basis for Improved Strain-based Design Models. Proceedings of the Seventeenth International Offshore and Polar Engineering Conference, 29-35.

Suzuki, N., and S. Igi, 2007. *Compressive Strain Limits of X80 High-Strain Line Pipes.* Proceedings of the Seventeenth International Offshore and Polar Engineering Conference, 3246-3253.

Takahashi, N., et al. 2009. *Strain Capacity of Large Diameter X80 Pipeline including Hot Bend.* Proceedings of the Seventeenth International Offshore and Polar Engineering Conference, 197-203.

Wang, Y. Y., et al. 2009. *Recent Development in Strain Based Design in North America.* Proceedings of the Seventeenth International Offshore and Polar Engineering Conference, 11-19.

Yoo, J., et al. 2008. *Development of X80/X100 Linepipe Steels with High Strain Aging Resistance.* Proceedings of the Seventeenth International Offshore and Polar Engineering Conference, 21-26.

Zhang, F., et al. 2012. *Strain Demand In Areas Of Mine Subsidence.* Proceedings of the 2012 9th International Pipeline Conference. Calgary, Alberta: Canada.

Zhang, F., et al. 2012. *Integrity of Pipeline in Area of Mine Subsidence.* Proceedings of the 2012 9th International Pipeline Conference. Calgary, Alberta: Canada.

Zhang, J., et al. 2010. *Experimental Study on Low Cycle Fatigue Behaviours Of Wrinkled Pipes*. Proceedings of the 8th International Pipeline Conference. Calgary, Alberta: Canada.

VITA

Mark D. Lower is a native of St. Louis, MO. He received a B.S. in Mechanical Engineering from the University of Missouri, an M.S. in Industrial Engineering from the University of Alabama at Huntsville in 2000, and is currently working toward a Ph.D. in Mechanical Engineering at the University of Tennessee.

Mark has worked at the Oak Ridge National Laboratory (ORNL) for over 20 years of diverse technical and managerial expertise as a Mechanical Engineer and Program Manager. He has been involved with several transmission pipeline projects across the United States for the Department of Transportation. He has been the Subject Matter Expert for Pressure Systems at ORNL including design, testing, risk-based inspection, fabrication, and maintenance. He is a commissioned inspector for the National Board of Boilers and Pressure Vessels. He has also been a member of accident investigation teams related to pressure safety. As part of these activities, he is responsible for specialized engineering assistance and technical support, including oversight of associated destructive and nondestructive testing.

He is an active member and officer for multiple American Society of Mechanical Engineers (ASME) committees for pressure vessels and the ASME Committee for Engineering Technology Accreditation (CETA). He currently serves as Chairman of the Department of Energy Pressure Vessel Committee. He is a registered Professional Engineer in the state of Tennessee. He is a member of the American Welding Society and a Certified Welding Inspector. He is presently serving as a Program Evaluator for the Technology Accreditation Commission (TAC) for ABET accrediting post-secondary education programs in engineering technology. He also serves as Secretary on the Board of Plumbing & Gas/Mechanical Examiners for the Town of Farragut, Tennessee.

Mark resides in Knoxville, Tennessee, with his wife, Lynda, and two daughters, Lori and Michelle.